
THE UNIVERSITY
*of* EDINBURGH

# Functional evaluation of miR-212-132 and miR-183-96-182 clusters during follicle-luteal transition in the monovular ovary

**Bushra Taher Mohammed**


Thesis submitted in fulfilment of the requirements for the degree of

**Doctor of Philosophy**

University of Edinburgh

December 2016

# Dedication

This thesis is dedicated to:

The Almighty Allah

My parent

# Table of Contents

# List of Figures

# List of Tables

# List of Abbreviations

| | |
|---|---|
| °C | Degree Celsius |
| 125I | Iodine |
| 3'UTR | 3' Untranslated region |
| AC | Adenylyl cyclase |
| ADAMTS | A disintigrin and metalloproteinase with thrombospondin motif |
| AGO | Argonoute |
| Akt | Protein kinase B |
| AMH | Anti-mullerian hormone |
| ATG7 | Autophagy related protein 7 |
| ATM | Ataxia telangiectasia mutated |
| ATP | Adenosine triphosphate |
| BMP | Bone morphogenetic proteins |
| BSA | Bovine serum albumin |
| BTC | Beta-cellulin |
| C/EBP | CCAAT/enhancer binding protein |
| CA | Corpus albicans |
| cAMP | Cyclic adenosine monophosphate |
| cdk | Cyclin-dependent kinases |
| cDNA | Complementary deoxyribonucleic acid |
| cGMP | Cyclic guanosine monophosphate |
| CH | Corpus haemorrhagicum |
| CL | Corpus luteum |

| | |
|---|---|
| cm | Centimetre |
| COC | Cumulus-oocyte-complex |
| cpm | Counts per minute |
| CREB1 | cAMP response element binding1 |
| CV | Coefficient of variation |
| CYP11A1 | Cytochrome P450, family 11, subfamily A, polypeptide 1 |
| CYP17A1 | Cytochrome P450, family 17, subfamily A, polypeptide 1 |
| CYP19A1 | Cytochrome P450, family 19, subfamily A, polypeptide 1 / aromatase |
| DGCR8 | Digeorge Syndrome Critical Region-8 |
| DIG | Digoxigenin |
| DNA | Deoxyribonucleic acid |
| dNTP | Deoxyribonucleotide |
| E2 | Oestradiol |
| eCG | Equine chorionic gonadotropin |
| ECM | Extracellular matrix |
| EGF | Epidermal growth factor |
| EGFR | Epidermal growth factor receptor |
| ERK | Extracellular regulated kinase |
| FACS | Fluorescence-activated cell sorting |
| FF | Follicular fluid |
| FGF | Fibroblast growth factor |
| FOXO1 | Forkhead box O |
| FSH | Follicle stimulating hormone |

| | |
|---|---|
| FSHR | Follicle stimulating hormone receptor |
| G protein | GTP-binding protein |
| g | g-force |
| GC | Granulosa cell compartment |
| GDF | Growth and differentiation factor |
| GDF-9 | Growth differentiation factor-9 |
| GDNF | Glial cell-derived neutrotropic factor |
| GH | Growth hormone |
| GnRH | Gonadotrophin releasing hormone |
| GO | Gene ontology |
| GPCR | G protein-coupled receptor |
| GTP | Guanosine triphosphate |
| hCG | Human chorionic gonadotropin |
| hLGCs | Human luteinised granulosa cells |
| HSD17B | 17- β-hydroxysteroid dehydrogenase |
| HSD3B | 3β-hydroxysteroid dehydrogenase |
| IFGR | Insulin-like growth factor receptor |
| IGF | Insulin-like growth factor |
| IGF1 | Insulin-like growth factor 1 |
| IGFBP | Insulin-like growth factor binding protein |
| IGFBP | Insulin-like growth factor binding protein |
| INHA | Inhibin A |
| IPA | Ingenuity pathway analysis |

| | |
|---|---|
| ISH | In situ hybridisation |
| ITS | Insulin, transferrin and sodium selenite |
| IU | International units |
| kDa | Kilodalton |
| kg | Kilogram |
| LC | Luteal cell |
| LH | Luteinizing hormone |
| LHCGR/LHR | Luteinising hormone receptor |
| LIF | Leukemia inhibitory factor |
| MAPK | Mitogen activated protein kinase |
| mg | Milligram |
| MGC | Mural granulosa cells |
| MHz | Megahertz |
| min | Minutes |
| miRNA | Micro ribonucleic acid (microRNA) |
| miR- | Micro ribonucleic acid (microRNA) |
| ml | Millilitre |
| mm | Milimeter |
| mM | Millimolar |
| MMP | Matrix metalloproteinase |
| mmu | Mus musculus (mouse) |
| MPF | Maturation Promoting Factor |
| MRE | MicroRNA recognition element |

| | |
|---|---|
| mRNA | Messenger ribonucleic acid |
| n | Statistical sample size |
| ng | Nanogram |
| NGS | Next generation sequencing |
| nM | Nanomolar |
| NRIP | Novel nuclear receptor interaction protein |
| NRS | Normal rabbit serum |
| NTC | No template control |
| OD | Optical density |
| P4 | Progesterone |
| P450scc | Cytochrome P450side chain cleavage |
| PA | Plasminogen activator |
| PAPP-A | Pregnancy-associated plasma protein-A |
| PBMC | Peripheral blood mononuclear cells |
| PBS | Phosphate buffered saline |
| PBS | Phosphate-buffered saline |
| PBSG | Phosphate-buffered saline with 0.1% swine skin gelatine |
| PCR | Polymerase chain reaction |
| PFA | Paraformaldehyde |
| PG | Prostaglandin |
| pg | Pictogram |
| PGE | Prostaglandin E |
| PGF | Prostaglandin F |

| | |
|---|---|
| PGR | Progesterone receptor |
| PGS2 | Prostaglandin synthase 2 |
| PI3K | Phosphoinositide 3-kinase |
| PKA | Protein kinase A |
| PKC | Protein kinase C |
| PLC | Phospholipase C |
| pre-miRNA | Precursor micro ribonucleic acid |
| pri-miRNA | Primary micro ribonucleic acid |
| PTEN | Phosphatase and tensis homologue |
| PTGS2 | Prostaglandin G/H synthase 2 |
| PTX | Pertussis toxin |
| qPCR | Quantitative polymerase chain reaction |
| RBMS1 | Ribonucleic acid binding motif single stranded interacting protein 1 |
| RIA | Radioimmunoassay |
| RISC | Ribonucleoprorein complex |
| RNA | Pol II RNA polymerase II |
| RNA | Ribonucleic acid |
| RNAsIn | RNase Inhibitor |
| rno | Rattus norvegicus (rat) |
| RT | Room temperature |
| rtPCR | Reverse transcription polymerase chain reaction |
| SF1 | Steroidogenic factor 1 |
| SPRED1 | Sprouty-related EVH1 domain containing protein 1 |

| | |
|---|---|
| StAR | Steroidogenic Acute Regulatory Protein |
| TBS | Tris buffered saline |
| TC | Theca cell compartment |
| TGF | Transforming growth factor |
| TGFBR2 | Transforming growth factor β recptor 2 |
| TRBP | TAR RNA-binding protein |
| UTR | Untranslated region |
| V | Volt |
| VEGF | Vascular endothelial growth factor |
| VEGFA | Vascular endothelial growth factor A |
| VEGFR | Vascular endothelial growth factor receptor |
| YY1 | Ying Yang 1 |
| µg | Microgram |
| µl | Microlitre |
| µM | Micromolar |

# Declaration of Originality

I hereby declare that the work presented in this thesis and the thesis itself have been composed and originated by myself, unless otherwise specified.

Bushra Taher Mohammed

December 2016

# Acknowledgements

Foremost, I am very grateful to the Almighty Allah, for having brought me to this beautiful and peaceful place to achieve my dream.

There are several people who have supported me during my PhD. First, I would like to express my sincere gratitude to my supervisor Dr. Xavier Donadeu for the continuous support of my Ph.D. study, for his patience, motivation, enthusiasm, and immense knowledge. His guidance helped me in all the time of research and writing of this thesis. Many thanks to him for kindly driving me to the Bridge of Alan. Stirling abattoir and Royal Infirmary of Edinburgh for collection of bovine ovaries and human follicular fluid, respectively.

I would also like to thank my second supervisor Dr. Colin Duncan who helped guiding me through the project and provided me with the human follicular fluid samples covered in this thesis. Further, I would like to thank the rest of my thesis committee: Prof. Helen Sang and Dr. Finn Grey, for their encouragement, insightful comments, and hard questions.

I would like to thank my colleagues and friends at Royal (Dick) School of Veterinary Studies / Roslin Institute. I thoroughly enjoyed my time here and I was lucky to get an opportunity to work in Roslin Institute. I would like to thank everybody who helped me, my special thanks go to Bob Fleming, who were an endless source of knowledge. I would like to thank Sadanand D Sontakke for kindly sharing microarray and qPCR results presented in this thesis. I also thank Tara Sheldrake and Cristina Esteves for helping me with FACS. Further, I would like to thank Jason Ioannidis and William Ho for their timely help at several occasions. I would like to thank my colleagues in Prof. Cheryl Ashworth group (Claire Stenhouse, Selene Jarrett and Charis Hogg) for their suggestion and stimulating discussion. I owe much to Prof. Ian Mason at the Queen's Medical Research Institute for kindly providing me with an antibody covered in this thesis. I would like to extend my thanks to my friends in Glasgow and Nottingham universities.

Back in Kurdistan region of Iraq, I am extremely thankful to Dr. Lokman Taib Omer, Dean of the College of Veterinary Medicine. University of Duhok, for kindly permitting me for Ph.D. study. I would like to extend my sincere gratitude towards Dr. Jabbar Basha Ali and Dr. Ali Mekail Ali for their constant motivations and supports. I would like to express my special thanks to my friend Sowaila Mekail for her kind support. Also, it's my pleasure to acknowledge generous help provided by my colleagues at University of Duhok. A special thanks to my family. Words cannot express how grateful I am to my mother, father, brothers, and sister for all the sacrifices that you have made on my behalf. Your prayer for me was what sustained me thus far.

I would like to thank the Ministry of Higher Education and Scientific Research of the Kurdistan Regional Government (KRG)/ Iraq for nominating me for the Scholarship and providing the financial support for this study. The supportive funding from my supervisor Dr. Xavier Donadeu and the Churches International Student Network (CISN) Hardship Fund is also noted.

# Research Publication

Sadanand D Sontakke, **Bushra T Mohammed,** Alan S McNeilly and F Xavier Donadeu: Characterization of microRNAs differentially expressed during bovine follicle development. Reproduction (2014) 148 271–283.

# Conference Abstracts

**Bushra Mohammed**, Sadanand D. Sontakke, W. Colin Duncan and Francesc X. Donadeu (2014). Functional evaluation of miRNAs during bovine ovarian follicular/luteal development. World Congress of Reproductive Biology, Edinburgh, UK (Oral Presentation).

**Bushra T Mohammed**, W Colin Duncan and Francesc X Donadeu (2015). Functional evaluation of miRNAs during the ovarian follicular/luteal transition. Conference of the Society of Reproduction and Fertility (SRF), Oxford, UK (Poster).

**Bushra T Mohammed**, W. Colin Duncan and Francesc X. Donadeu (2016). Functional evaluation of miRNAs during the follicle-luteal transition in the monovular ovary: Involvement of miR-132 and miR-96 in cell survival. 18th International Congress on Animal Reproduction (ICAR), Tours, France (Oral and Poster Presentation).

# Lay Summary

MicroRNAs (miRNAs) are small RNA molecules that regulate a variety of biological processes through inhibiting protein translation or causing mRNA destabilization in cells. Many studies have looked at how miRNAs are involved in ovarian follicular development but have not investigated their role during the transition between follicle and CL, a critical event for successful fertilisation and pregnancy. Several miRNAs have been shown to be differentially expressed during the follicle-luteal transition, consistent with their role in regulating this process. Previous microarray studies in the bovine ovary showed the upregulation of two clusters, miR-212-132 and miR-183-96-182, in luteal relative to follicular tissues. In this thesis, I describe studies on the role of miR-132 and miR-96 during the follicle-luteal transition. Specifically, I studied the location of these two miRNAs within the bovine CL and the effects of manipulating miRNA levels in bovine granulosa cells luteinised in vitro, bovine luteal cells and human luteinised granulosa cells. I found that miR-132 and miR-96 were not restricted to a single luteal cell type but were expressed in a variety of cells within the CL. In addition, I showed that, both in bovine luteal cells and human luteinised granulosa cells, miR-96 targets FOXO1, a transcription factor that induces cell death, thus ensuring luteal cell survival. Moreover, both miR-132 and miR-96 promoted progesterone production by luteinised granulosa cells. In summary, my results demonstrate an effect of miR-132 and miR-96 in promoting luteal cell survival and steroidogenesis in a conserved manner across cattle and humans. I believe that the insights generated by this work will facilitate the development of new treatments for infertility for both humans and livestock.

# Abstract

Low fertility is a major cause of lost productivity in the cattle industry. In addition, cattle provide a convenient model to study ovarian physiology in monovular species including humans. Our previous microarray studies in the bovine ovary showed the upregulation of two clusters, miR-212-132 and miR-183-96-182, in luteal relative to follicular tissues. The studies in this thesis were aimed at establishing the functional involvement of these miRNAs during the follicle-luteal transition using a bovine model as well as human tissues.

The aim of the first study was to characterise the expression of miR-132 and miR-96 within luteal tissue using ISH and FACS. The expression of miR-132 was detected in most luteal compartments while miR-96 was not detectable using ISH. Further examination using FACS showed that miR-212-132 expression remained unchanged in sorted endothelia (CD144+) and steroidogenic (CD144-Nile Red (NR) +) cell fractions. In contrast, expression of miR-183 and miR-96 was significantly increased in CD144+ compared to CD144-NR+ fractions. To elucidate potential roles of these miRNAs in the CL, I used existing online databases to identify putative miRNA targets. I identified 3042 predicted bovine gene targets of these miRNAs as well as 174 miRNA targets that had been experimentally validated in human, mouse and/or rat. I also identified putatively targeted signalling pathways primarily involved in cell survival, proliferation and differentiation. For further investigation, I narrowed my list of targets to FOXO1 and ADCY6, the expression of which was naturally down- regulated during luteinisation.

The second study used an in vitro model of bovine granulosa cell luteinisation. Levels of miR-183-96-182 and miR-212-132 increased significantly ($P<0.05$) during the first 4 days of luteinisation in vitro. The function of miR-132 and miR-96 during luteinisation in vitro was studied. Transfection of bovine granulosa cells with specific miRNA inhibitors or mimics of miR-132 and miR-96 led, respectively, to abolished expression and a significant increase in the levels of these miRNAs ($P<0.01$) within 4 days. These changes in miRNA levels did not have any effect on transcript levels of the predicted mRNA targets, FOXO1 and ADCY6, during luteinisation. However, progesterone production by luteinising granulosa cells

decreased ($P<0.05$) on day 2 after transfection with miR-132 inhibitor. The results demonstrated that putative miRNA target genes remained unchanged during in vitro luteinisation which was not consistent with in vivo results.

The third study aimed to elucidate the effect of miRNA inhibition in bovine luteal cells in culture. The loss of miR-132 led to an increase ($P<0.05$) in FOXO1 transcript but not protein levels. In contrast, inhibition of miR-96 increased protein but not transcript levels of FOXO1. Moreover, miR-96 inhibition induced an increase in the caspase 3/7 response of luteal cells to serum deprivation indicating an anti-apoptotic effect of this miRNA on these cells.

In the fourth study, I investigated the role of miR-132 and miR-96 in human luteinised granulosa cells obtained from IVF patients. The levels of FOXO1 protein were significantly increased following depletion of miR-132 and miR-96, whereas caspase3/7 increased in response to miR-96 inhibition, regardless of whether cells had been serum deprived or not. Similarly, using Annexin V and Trypan blue staining an increase in numbers of apoptotic cells was observed in response to miR-96 inhibition. In addition, reduction of FOXO1 with the siRNA inhibited the apoptotic effect of miR-96 inhibition. Interestingly, inhibition of pooled miR-132 and miR-96 reduced progesterone secretion. However, this effect was prevented by transfecting cells with FOXO1 siRNA. These results suggest that the effects of these miRNAs on cell survival and progesterone production are mediated through targeting FOXO1.

In summary, my results identify miR-96 and miR-132 as potentially critical factors in ensuring luteal cell survival and steroidogenesis in both cattle and human.

# Chapter 1

# Introduction

# Chapter 1: Introduction

## 1.1 The Reproductive cycle

The oestrous cycle of domestic animals and the menstrual cycle of humans each comprise two distinct phases - follicular and luteal. The follicular phase occurs between the regression of CL and ovulation, after which the luteal phase begins. The oestrous cycle in the cow lasts an average of 21-22 days, including a 4–6 day-long follicular phase (which can be further subdivided into a 2-5 day-long proestrous and a 18 h-long oestrous, at the end of which ovulation occurs) and a 14–16 days-long luteal phase (that can be divided into a 2-4 day-long metoestrous, when the early CL (corpus hemorrrhagicum) forms, and a 10-14 day-long dioestrous when the CL is fully functional). Day 0 of oestrous cycle is usually considered to be the first day of oestrous or heat (reviewed in Adams, 1999, Forde et al., 2011).

In humans, the reproductive cycle is referred as the menstrual cycle due to physiological uterine bleeding (menstruation) associated with shedding of the endometrial lining. The cycle lasts 26-35 days and begins with menstrual flow that lasts for 3-6 days and occurs at the end of luteal phase as a result of a reduction in circulating steroid levels. The heaviest blood flow can be seen on Day 2. Average duration of the follicular and luteal phases is the same (14 days of an average 28-days of menstrual cycle) (reviewed in Baerwald et al., 2003, Mihm et al., 2011, Yang et al., 2013a).

Because of many similarities in reproductive physiology (Table 1.1), cattle provide a convenient research model to study human ovarian physiology. In addition, the unrestricted access to bovine ovaries at the slaughterhouse for experimental purposes makes the bovine model both practical and ethically-suited for human reproductive research.

**Table 1.1. Similarities between the reproductive physiology of the women and cow (Sjaastad et al., 2010).**

| Features | Women | Cow |
|---|---|---|
| **Pregnancy duration** | **9 months** | **9 months** |
| **Pregnancy type** | **Single** | **Single** |
| **Cycle duration** | **28** | **21** |
| **Cycle type** | **Menstrual continuous** | **Oestrous continuous** |
| **Follicular wave** | **1-2** | **2-3** |
| **Ovulation type** | **Mono-ovulatory** | **Mono-ovulatory** |

# 1.2 Folliculogenesis

Follicles are the functional unit of the ovary within which the female germ cell, the oocyte, develops and matures before being released during ovulation. Folliculogenesis involves growth and regression of follicles within the ovarian cortex. This process occurs in different stages, as described below.

## 1.2.1 Stages of follicle development

Histologically, follicles can be classified as pre-antral and antral. Pre-antral follicles include primordial, primary and secondary follicles while antral follicle are also known as tertiary follicles (Table 1.2). Primordial follicles (100,000-250,000 follicles can be found at day 90 of pregnancy in cattle and around 6-7 million can be seen at week 15 after conception in women) form within the fetal ovary, most of which will be selected for further development after birth; however, the vast majority of these follicles will undergo atresia in pre- or post-natal life without ever reaching the antral stage. The primordial follicles are quiescent and composed of a single layer of flattened squamous granulosa cells surrounding an immature oocyte arrested at the first meiotic division (Erickson, 1966, Forabosco et al., 1991, Juengel et al., 2002).

Activation of a primordial follicle leads to a primary follicle, containing a layer of cuboidal cells surrounding the enlarged oocyte. Granulosa cells then begin to proliferate and the number of cell layers increases resulting in a secondary follicle

that is defined by the presence of two or more granulosa cell layers with a distinguishable outer theca layer and an increase in the oocyte size. Further cell proliferation is associated with formation of an antrum containing follicular fluid beginning. In addition, at this stage the zona pellucida, a thick glycoprotein surrounding the oocyte, becomes fully developed. Follicles then become tertiary or antral and the granulosa cell layer segregates into two distinct populations: a small cumulus cell population, which surrounds and makes direct contact with the oocyte through gap junctions on the oocyte surface thus permitting exchange of small molecules, and the steroidogenic mural granulosa cells which form the main component of the follicular wall (reviewed in Rodgers and Irving-Rodgers, 2010). In bovine, follicular development from the primordial stage to the ovulatory stage lasts around 180 days (Lussier et al., 1987) whereas in women it takes 90 days (McGee and Hsueh, 2000).

While pre-antral follicles depend on intraovarian growth factors for growth, antral follicles are completely dependent on gonadotropins, the effects of which are modulated by intraovarian growth factors. Growth factors involved in follicular development include the insulin growth factor (IGF) and transforming growth factor (TGF) β families as well as several other growth factors produced by ovarian somatic cells or the oocyte (Campbell et al., 2012, Webb et al., 1999).

**Table 1.2 Classification of bovine ovarian follicles based on histological features, adapted from (Braw-Tal and Yossefi, 1997).**

| | Follicle type | Granulosa layer | Follicle diameter (µm) | Oocyte diameter (µm) |
|---|---|---|---|---|
|  | Primordial | 1 | 40 | 29.7 |
|  | Primary | 1-1.5 | 40-80 | 31.1 |
|  | Small secondary | 2-3 | 81-130 | 49.5 |
|  | Large secondary | 4-6 | 131-250 | 68.6 |
|  | Small antral | > 6 | 250-500 | 92.9 |
|  | Large antral | | > 500 | |

## 1.2.2 Ovarian follicular waves

Antral follicles grow in a wave-like pattern throughout an animal's reproductive life. In cows, two or three waves of follicle development occur during the oestrous cycle, heifers start their first oestrous cycle approximately at 8-12 months old. In women, one to two waves usually develop during a menstrual cycle which starts at age 11-14 years. Each wave is characterised by follicle recruitment, selection, dominance, and ovulation or atresia (Figure 1.1) (reviewed in Forde et al., 2011, Lucy, 2007, McGee and Hsueh, 2000).

Each wave commences with the recruitment, in response to a transient increase in FSH in circulation, of 3-6 follicles growing above 4 mm in diameter in cattle and 4-14 follicles growing to ≥ 5 mm in women (reviewed in Baerwald et al., 2012, Ginther et al., 2001). FSH induces inhibin and oestrogen secretion by the follicles which result in a decline in FSH levels beginning shortly after wave emergence. A few days later, once a follicle (usually the largest in the wave, occasionally the 2 or 3 largest) reaches an average of 8.5 and 7.7 mm in cows and heifers, respectively, or 10 mm in women, it will be selected and will continue to develop as dominant follicle (DF) while smaller follicles, named subordinate follicles, will cease growing and become atretic (Ginther et al., 1996, Mihm et al., 2011).

The production of high levels of oestrogen and inhibin by the dominant follicle will continue to reduce FSH concentration ensuring the demise of subordinate follicles (Campbell et al., 1996, Gutiérrez et al., 1997b). Unlike subordinate follicles, the dominant follicle continues to grow despite low FSH levels because it acquires the capacity to 1) express LH receptor in its granulosa cells and 2) produce large amounts of growth factors such as insulin-like growth factor 1 (IGF1) and oestradiol which 1) allow the dominant follicle to respond to LH in addition to FSH and 2) provide higher sensitivity to FSH and LH, respectively. The role of the IGF system in the dominant follicle can be seen during in vitro exposure of granulosa cells to IGF-1 which induces secretion of oestrogen that in turn stimulates proliferation of granulosa cells, expansion of the antrum and formation of gap junctions (Armstrong and Webb, 1997, Campbell et al., 1996).

Only the follicular wave developing during the follicular phase of an oestrous or menstrual cycle results in ovulation of the dominant follicle (ovulatory size is 12–20 mm about 11 days of the 21-day oestrous cycle in cows or around 20 mm approximately 14 days of the 28-day menstrual cycle in woman) (Fortune et al., 1990, Ginther et al., 1996, Ginther et al., 2004). Dominant follicles from waves developing during the luteal phase (1-2 waves in cattle) do not ovulate but instead undergo atresia due to negative feedback on pituitary LH pulse frequency from the high levels of progesterone produced by the CL (Figure 1.1.A).

Unlike in cattle, waves in the luteal phase in women are controversial as the human CL produces both oestradiol and inhibin A which repress FSH thus inhibiting follicle development during the luteal phase and resulting in only one wave developing during the follicular phase of the cycle (Figure 1.1.B) (reviewed in Baerwald et al., 2012).

**A**

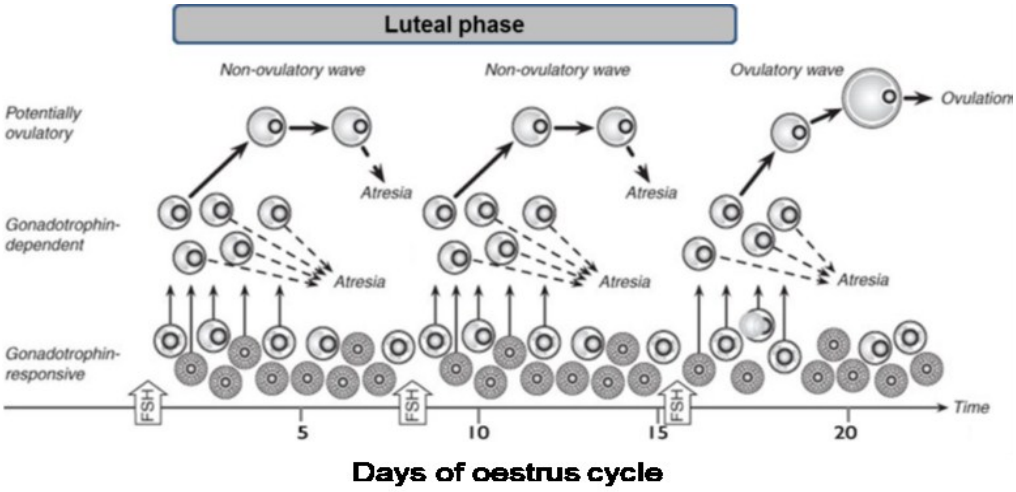


**B**

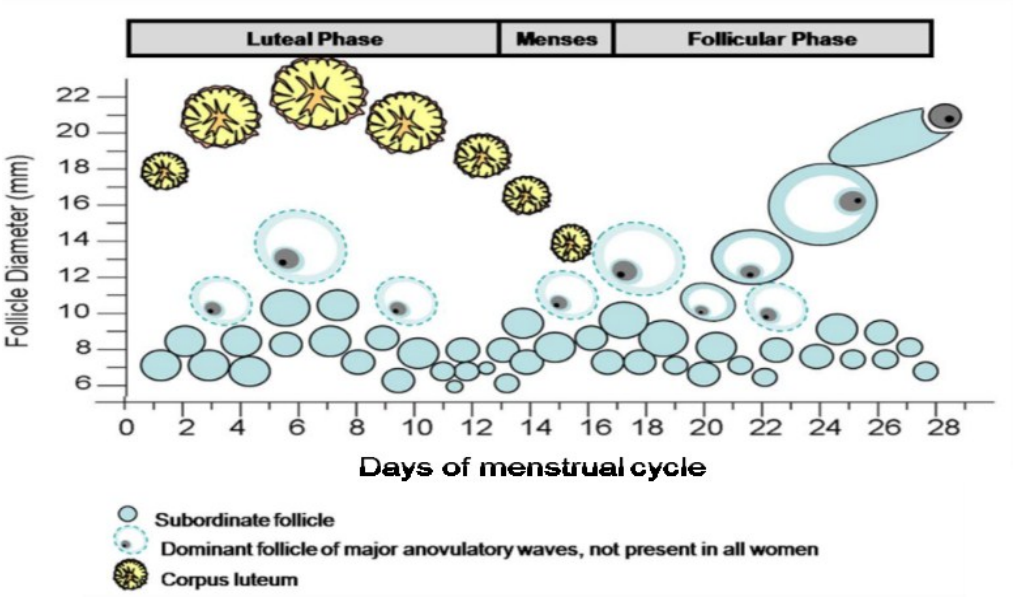


**Figure 1.1 A Schematic representation of ovarian follicular waves during reproductive cycles in the cow (A) and women (B) (reviewed in de Mello Bianchi et al., 2010, Scaramuzzi et al., 2011).**

### 1.2.3 Ovulation

In spontaneous ovulators such as cattle and humans, high levels of oestradiol produced by the dominant follicle stimulate GnRH secretion leading to an increase in LH pulsatility at the end of the follicular phase of each reproductive cycle. Distinct morphological changes occur within the ovary before ovulation including emergence of the apical part of the follicle above the ovarian surface to form a blister (the site of rupture), necrosis and shedding of cells of the surface epithelia and infiltration of leukocytes and platelets from blood capillaries (Tanaka et al., 1989). Ovulation involves three main events, completion of oocyte meiosis, cumulus expansion, rupture of follicular wall (reviewed in Richards, 2007). LH binds the LHCGR which activates several pathways leading to phosphorylation of transcription factors that are involved in ovulation and luteinisation as described in Figure 1.2. Using mice knock-outs many of these genes have been shown to be essential for ovulation and/or luteinisation including PR, COX-2, C/EBPβ and Egr-1 (Plant and Zeleznik, 2014).

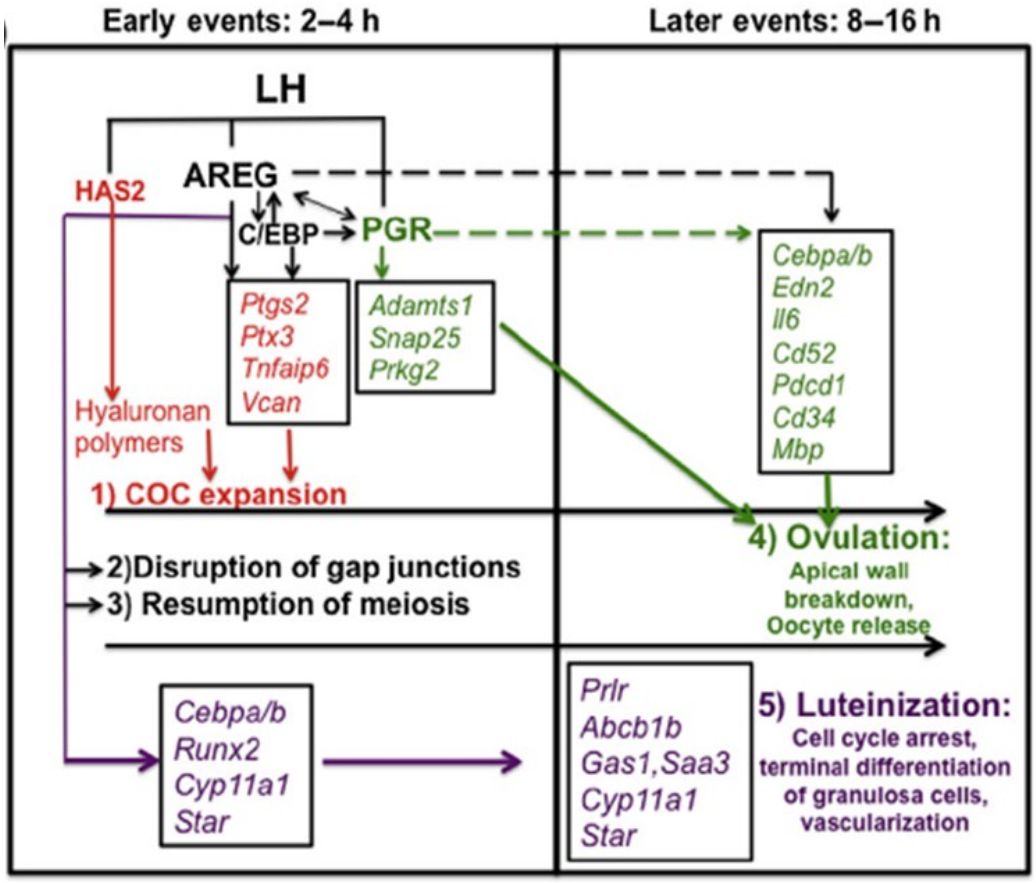


**Figure 1.2 A Schematic representation of LH activated pathways that are involved in ovulation and luteinisation. LH induces epidermal growth factors (AREG) which in turn activate C/EBP that stimulates a subset of genes that are responsible for expansion, rupture of COC and ovulation. Lastly several genes will be stimulated by LH surge including transcription factors C/EBPα/β and RUNX2, steroidogenic enzymes (CYP11A1 and StAR) and prolactin receptor (PRLR) that are associated with luteinisation (Plant and Zeleznik, 2014).**

### 1.2.3.1 Oocyte maturation

Prior to ovulation, oocytes are arrested at prophase 1 of meiosis (Mehlmann, 2005, Peters, 1969). Somatic cumulus cells produce cGMP that transfers into the oocyte through gap junctions and maintains the inhibitory effects on meiosis (Jaffe and Norris, 2010).

The LH surge prompts completion of meiosis 1 by reducing cGMP synthesis by the follicular cells and by inhibiting its diffusion through gap junctions. This enables the oocyte to progress into meiotic division in most species (Sagata, 1996).

#### 1.2.3.2 Cumulus expansion

In response to the LH surge, cumulus cells in the mature follicle produce proteoglycans and glycosaminoglycans which form a gelatinous layer around the oocyte (expansion) and permit dissociation of the COC complex from ruptured follicle as well as facilitate its transit through the oviduct (Figure 1.3) (Salustri et al., 1999). Hyaluronic acid (HA) synthase-2 (HAS2) catalyses the production of HA, a glycosaminoglycan that forms the backbone of the gelatinous layer (Weigel et al., 1997). Tumour necrosis factor-induced protein-6 (TNFAIP6; also, named TSG-6) and pentraxin3 (PTX3) are also involved in COC expansion by stabilising the ECM through binding to hyaluronan. Deletion of PTX3 and TNFAIP6 in mice led to anovulation and infertility (reviewed in Russell and Robker, 2007, Trzeciak et al., 2012). Liver receptor homolog-1 (NR5A2, LRH-1) also promotes cumulus expansion and ovulation. NR5A2 localises in the granulosa cell of ovulatory follicle and after ovulation remains in the CL. Deficient NR5A2 mice showed a decline in the expression of PGR, StAR, CYP11A1, inhibiting the progesterone synthesis and ovulation. However, no effect on formation of CL was observed (Bertolin et al., 2014). Another matrix stabilizing gene induced by LH in the periovulatory follicle is Versican (VCAN), a hyaluronan (HA) binding proteoglycan that is degraded by ADAMTS-1 (Brown et al., 2010).

#### 1.2.3.3 Rupture of follicular wall

Rupture of the follicular wall allows expulsion of the oocyte during ovulation (Figure 1.3). Several genes are involved in degradation of the multiple layers that separates the follicular antral space from the ovarian surface, such as cyclooxygenase-2 (COX-2) also known PTGS2 that induces synthesis of prostaglandins by the periovulatory follicle approximately 10 hours before ovulation in rat, cattle, and horse (Sirois et al., 2004).

Mice lacking PGs ($PGI_2$ and $PGE_2$) or its receptors showed a reduction in ovulation rate and infertility. However, it had no effect on luteinisation. Ovulation can be blocked by administration of nonsteroidal anti-inflammatory agent indomethacin, which inhibits prostaglandin synthesis (Lim et al., 1997, Sirois et al., 2004).

ADAMTS genes play an important role in the induction of protease activity that degrades the follicular tissue leading to rupture of follicular wall and removal of the cumulus oocyte complex. Expression of ADAMTS-1 decreased in the progesterone receptor knockout mice and its expression was induced by LH/hCG, showing the potential roles of this gene in ovulation (Robker et al., 2000). Regulation of ADAMTS-1 expression is mediated by PGR in rat, cow, pig, horse and primates (reviewed in Russell et al., 2015). Further findings have revealed that cathepsin L, a lysosomal cysteine protease, is highly expressed in periovulatory follicle after hCG exposure suggesting its effect on the remodelling of the extracellular matrix during ovulatory process (Robker et al., 2000). LH surge also stimulates secretion of plasminogen activators, tissue (tPA) and urokinase (uPA) by follicular cells and surrounding connective tissue. PAs have a fundamental role in activation of matrix metalloproteinase (MMPs) (Liu, 1999).

MMP family members such as collagenase (MMPs-1, -8 and -13), gelatinase (MMPs-2 and -9), stromelysins and membrane type MMPs and their associated inhibitors, tissue inhibitors of MMPs (TIMP-1 to -4) are involved in degradation of specific ECM components and remodeling at the apex of pre-ovulatory follicle. Ovulation can be blocked following administration of synthetic MMP inhibitors. ProMMPs-2 and -9 are activated by MT1-MMP and TIMP-2 and they function directly by breaking down the basement membrane of the ovulatory follicle (Dong et al., 2002, Smith et al., 1998).

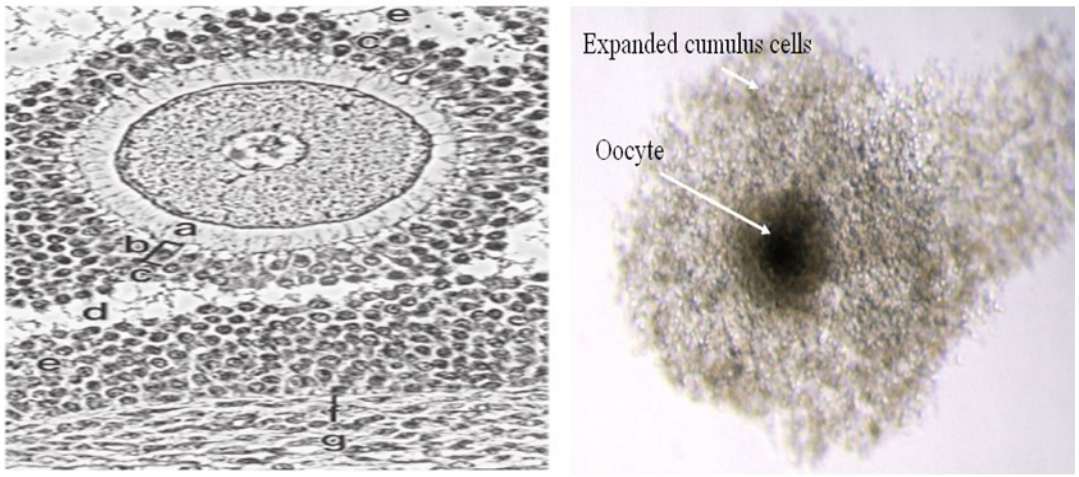


**Figure 1.3 Histological section shows before and after ovulation in the cow following LH surge,** a) zona pellucida and corona radiate (b) surround the oocyte. c) cumulus oophorus, d) antrum, e) granulosa layer lined the follicle, theca layers (f, g) (Frandson et al., 2009, Mayes, 2002).

## 1.3 Luteinisation

Luteinisation is the transformation of ruptured follicle into CL in response to the LH surge. Luteinisation involves major molecular and morphological changes including follicular cell differentiation, tissue remodelling and rapid development of vascular elements.

A common morphological event that occurs after ovulation is a significant infolding of the follicular cell layers into antrum. Moreover, specific changes in the extracellular matrix beginning before ovulation are essential for tissue remodelling leading to formation of CL. These include breakdown of basal lamina and gap junctions between granulosa and theca cells and changes in basement membrane and cell surface components. These events facilitate invasion of connective tissue, vascular elements such as proliferating endothelial cells, pericyte and some immune cells into ruptured follicle. In addition, luteinising granulosa and theca cells migrate into the centre of the forming CL in domestic species (Plant and Zeleznik, 2014).

Development of blood vessels due to proliferation of endothelial cells that form an extensive capillary network of the CL is described in section 1.3.1.2.

## 1.3.1 Histology of the corpus luteum

The CL contains a heterogeneous population of cells including steroidogenic (large and small luteal cells putatively derived from granulosa and theca cells), vascular, immune and fibroblasts (Pate and Landis Keyes, 2001). The cellular composition of the bovine CL on day 12 of the oestrous cycle is summarised in Table 1.3. In bovine corpora lutea, steroidogenic large and small luteal cells are intermingled within the luteal tissue. Luteinisation results in a 10-fold increase in granulosa cell size resulting in a high cytoplasmic-nuclear ratio (Smith et al., 1994). Indeed, the increase in tissue volume during luteal formation is accounted for by an increase in both vascularisation and hypertrophy of luteinising follicular cells.

**Table 1.3 Cell types in the bovine CL (O'Shea et al., 1989).**

| Cell types | % of cellular composition | % of total mass | Cell diameter (µm) |
|---|---|---|---|
| **Endothelial/ pericyte** | **53%** | **13.3%** | **10.8** |
| **Small luteal** | **26.7%** | **27.7%** | **> 17** |
| **Large luteal** | **3.5%** | **40%** | **> 30** |
| **Fibrocyte** | | **6.2%** | **14.8** |
| **Others** | **19.8%** | | |

In primates, steroidogenic large and small luteal cells are named granulosa-lutein and theca-lutein cells, respectively. Theca-lutein cells have the capacity to produce androgen that diffuse into granulosa-lutein layer and converted into oestrogen. Inhibin is produced by both cells but mainly the granulosa lutein cells. In contrast to domestic species and rodents, theca lutein cells do not migrate during luteal development but remain separated from granulosa-lutein cells and organise as clusters in the periphery of the CL along with vascular septa (Gaytán et al., 1999). Granulosa cells increase 2-3-fold in size during luteinisation, polyhedral granulosa-lutein cells being > 30 µm in diameter, while theca lutein cells have a diameter ≤ 20 µm (Figure 1.4). Furthermore, large granulosa-lutein cells comprise 25-35% of the total luteal volume while small theca-lutein cells make up 12- 18%. The remaining of the CL includes blood vessels (11%), connective tissue (22% to 29%), and fibroblasts (7 to 11%) (Kühnel and Kuhnel, 2003, Miranda, 2010).

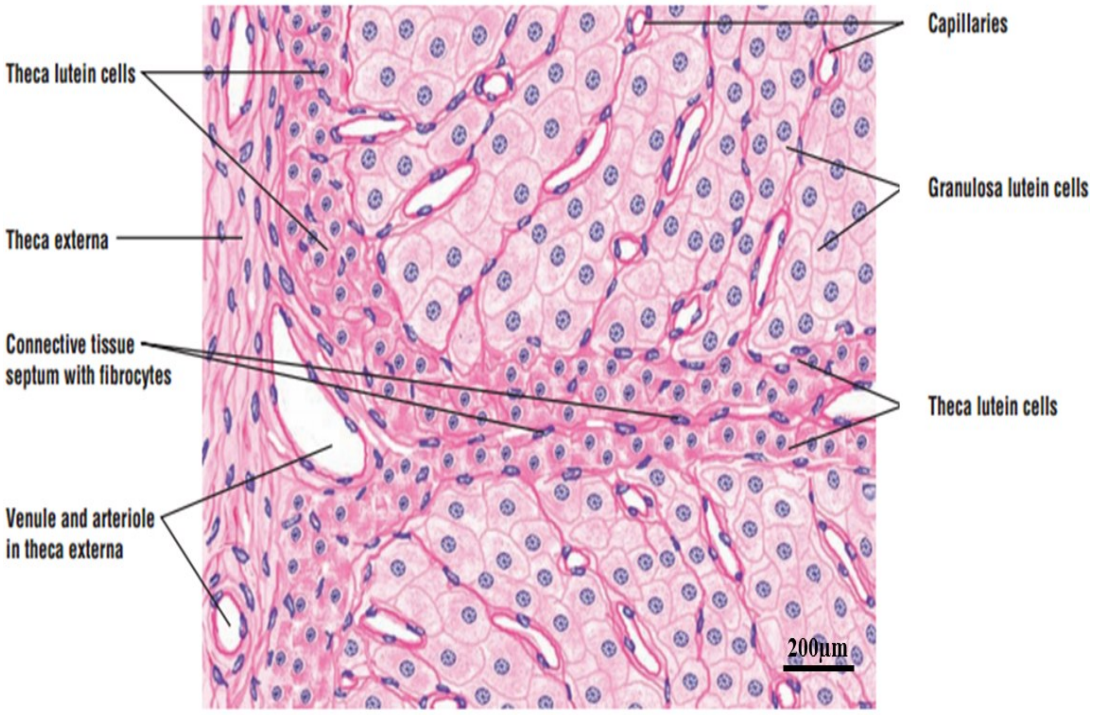


**Figure 1.4. Histological section of human CL, haematoxylin and eosin. Scale 200 µm and magnification: ×30 (Eroschenko and Di Fiore, 2013).**

#### 1.3.1.1 Steroidogenic compartment

The follicular origin of luteal steroidogenic cells in domestic animals and primates is not fully understood. It is believed that during luteinisation granulosa cells become large luteal cells and theca cells differentiate into small luteal cells. Meidan et al. (1990) showed that inducing the differentiation of bovine granulosa and theca cells with Forskolin and insulin for 9 days produced cells with characteristics of large and small luteal cells, respectively. Using monoclonal antibodies to granulosa and theca cell surface antigens in cattle, Alila and Hansel (1984) showed that the percentage of large luteal cells binding granulosa specific antibodies decreased whereas the binding to theca specific antibodies increased throughout the oestrous cycle providing evidence that small luteal cells become large luteal cells as CL develops, a conclusion which is in agreement with that of (Lei et al., 1991).

In general, large luteal cells are richer in smooth and rough endoplasmic reticulum, mitochondria and Golgi apparati than small luteal cells. Another difference between large and small luteal cells is the presence of secretory granules (0.2-4 μm in diameter) throughout the cytoplasm of large luteal cells. These secretory granules contain oxytocin in ovine and bovine while they contain relaxin in rat, pig and cow (Niswender et al., 1994, Stormshak, 2003). Furthermore, in ruminants, large luteal cells secrete around 80% of the progesterone. These cells lack LH receptors but produce PGE2 which stimulates progesterone secretion. In contrast, small luteal cells express LH receptors but are responsible for less than 20% of the total progesterone produced by the CL. Small luteal cells show a dramatic increase in progesterone production following LH treatment in sheep (reviewed in Wiltbank et al., 2012).

In human, both steroidogenic luteal cells express LHR and the difference in progesterone secretion between granulosa-lutein and theca-lutein cells is only 3-4 fold. In contrast to cattle, granulosa-lutein cells respond to hCG treatment. hCG is produced by different cell types including the gonadotrope cells of the anterior pituitary which mimic LH actions. hCG acts through the LH receptor (Choi and Smitz, 2014).

During the early luteal stage, granulosa-lutein cells secrete a greater amount of progesterone than small cells while there is no significant difference in progesterone synthesis by both cell populations during the late luteal phase after addition of hCG (Fridén et al., 1999).

Luteinisation of granulosa and theca cells is associated with exit from the cell cycle and an increase in steroidogenic capacity. A decrease in cyclin 2 levels and an induction of the cell cycle inhibitors, p21cip1 and p27kip1, were observed following LH treatment leading to granulosa cell cycle arrest in mice (Robker and Richards, 1998). Furthermore, progesterone synthesis is associated with activation of several enzymes, e.g. StAR that facilitates movement of cholesterol from the outer layer to the inner layer of mitochondria in the CL. Once the cholesterol is transferred to the inner surface of mitochondria, CYP11A1 converts cholesterol into pregnenolone and HSD3B1 converts pregnenolone into progesterone, a hormone that is essential for maintenance of pregnancy (reviewed in Pelletier et al., 2001, Stocco et al., 2007).

#### 1.3.1.2 Vascular compartment

Formation of the CL is associated with the development of blood vessels to provide a mechanism for distribution of nutrients, hormones and cholesterol, the substrate for progesterone synthesis, to the luteal cells (Davis et al., 2003, Shirasuna et al., 2012). After degradation of their adjacent basement membrane by proteolytic enzymes, endothelial cells begin migrating toward the granulosa layer to form a capillary network in the growing CL. Studies have reported that, in ruminants, endothelial cells show high rates of mitosis during early luteal phase. About 85% of endothelial cells in the early CL are proliferating, a proportion that drops to 50% as the CL ages. The CL is known to be one of the most vascularised tissues in the body (reviewed in Galv et al., 2013).

Maroni and Davis (2011) isolated bovine endothelial cells using BSL-I lectin-coated magnetic beads. Further purification was achieved by FACS using a vascular endothelial VE-cadherin (CD144) antibody, a specific endothelial cell marker. Endothelial cells are small and flat of around 10 μm in diameter, and contain central nucleus that bulge into lumen of blood capillary and few cytoplasmic organelles. Endothelial cells have a large surface area and are highly permeable, features that facilitates exchange of large molecules with other luteal cells (Meidan et al., 2005).

The density of endothelial cells is strongly associated with the size of luteal cells during different stages of luteal phases in primate. During early luteal development, the mean volume of granulosa lutein cells increased around 52% coincident with a 61% increase in the cross-sectional area of vascular compartments. This proportion decreased in both cell types during late stages of luteal phase. In the aged CL, most of steroidogenic luteal cells are closely attached to microvascular endothelial cells (Niswender et al., 1994, Wulff et al., 2001). Endothelial cells recruit support cells, namely pericytes that stabilise the forming vessels and regulate blood flow through their contractile activity. Pericytes are involved in sprouting of the blood capillaries through migrating ahead of endothelial cells (Figure 1.5) (Amselgruber et al., 1999, Redmer et al., 2001).

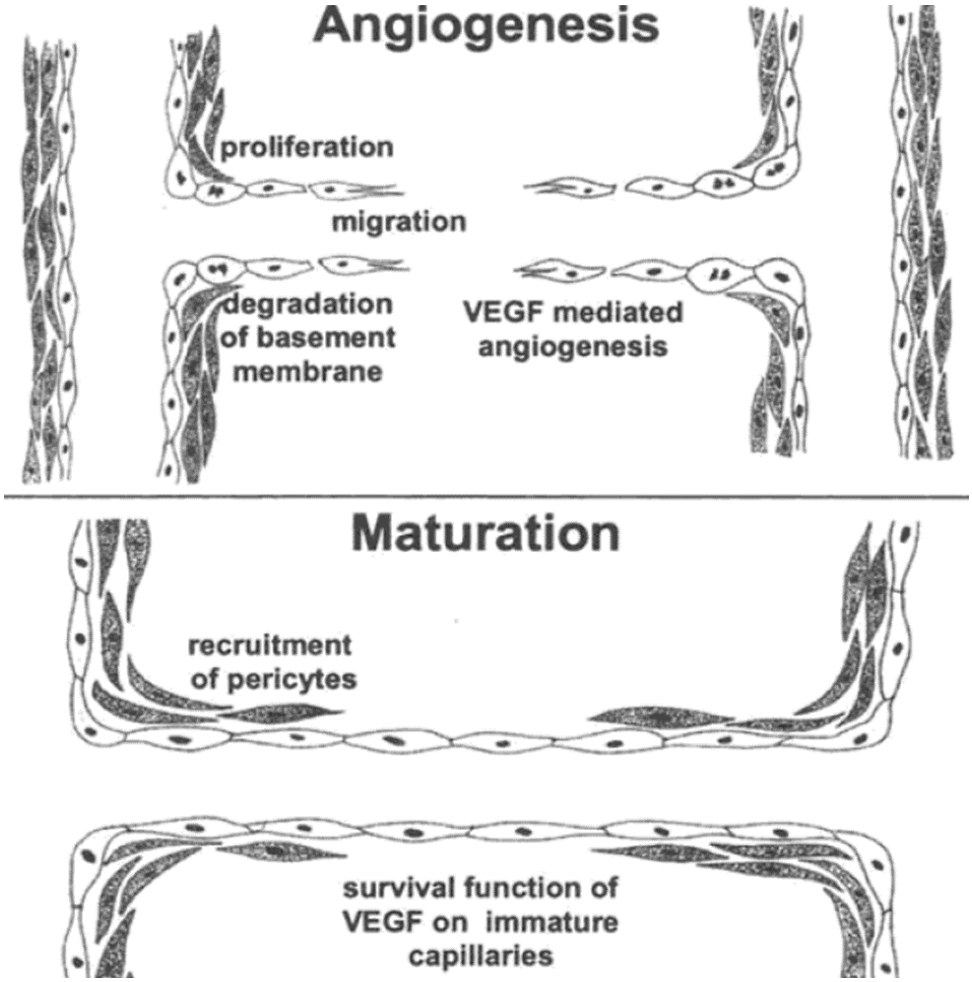


**Figure 1.5 A Schematic representation of ovarian angiogenesis. Vascular endothelial growth factor (VEGF) mediates sprout angiogenesis that involves breakdown of basement membrane, endothelial cell migration and proliferation leading to formation of a capillary network (Augustin, 2001).**

Angiogenesis in the CL is regulated by various factors including vascular endothelial growth factor (VEGF), basic fibroblast growth factor (bFGF), endocrine gland-derived VEGF (EG-VEGF) and angiopoietins (Ang-1 and Ang -2). The LH/hCG surge enhances the expression of angiogenic factors and their receptors which in turn drives endothelial cell proliferation (Doyle et al., 2010).

Pericytes produce angiogenic factors (VEGF) in response to a reduction in local oxygen concentrations. Other studies showed that VEGF is highly enriched in the steroidogenic luteal cells in addition to endothelial cells (reviewed in Duncan et al., 2009, Skarzynski et al., 2013).

### 1.3.2 Regulation of corpus luteum

There are species differences in how the CL functions. However, there are some commonalities such as the need for luteinisation, the need for progesterone and the need for luteolysis. Ovulation and luteinisation are induced by the LH surge. However, maintenance of the CL structure and function requires support also from other luteotropic factors such as PRL secreted by pituitary gland or PRL-like hormones from the uterine decidua and placenta. PRL promotes progesterone production through attenuation of 20α-hydroxysteroid dehydrogenase (20α-HSD) expression that induces degradation of progesterone and induction of other steroidogenic enzymes that involved in progesterone synthesis (CYP11A1 and HSD3B) in rat luteal cells. In addition, PRL enhances cholesterol availability and expression of many genes that are involved in steroidogenesis such as HDL, SCARB1 and SCP2 (reviewed in Stocco et al., 2007).

As already mentioned above, in primates, LH promotes secretion of progesterone by luteal cells during the mid-luteal phase. Moreover, progesterone secretion was dramatically repressed after addition of a GnRH antagonist. Such results indicate that LH is the main regulator of primate luteal function. In contrast, in ruminants, progesterone synthesis only decreases to one half in response to GnRH antagonist as the receptors for LH are located in small but not large luteal cells. Another luteotropic factor is progesterone itself which acts through specific receptor (PR) isoforms (A and B) in human and cow CLs. PR-B plays an essential role in an activation of progesterone- responsive genes while PR-A suppresses the ability of PR-B to induce transcription. However, the expression of PR is not affected by progesterone treatment (Jones et al., 1982, Roy and Greenwald, 1990).

Prostaglandin E2 (PGE2) enhances luteal cell survival factor through stimulating progesterone secretion. PGE2 binds to specific receptors and causes an increase in cAMP which in turn activates PKA pathway subsequently upregulating steroidogenic genes. Growth hormone and insulin have a significant role in the formation of the CL such as IGF-I enhance production of progesterone by luteinised granulosa and luteal cells in different species (reviewed in Plant and Zeleznik, 2014, Rekawiecki et al., 2008).

# 1.4. miRNAs and the ovary

## 1.4.1. miRNAs

MicroRNAs (miRNAs) are small non-coding RNAs with a length of 18-25 nucleotides that are responsible for post-transcriptional gene regulation through binding to target mRNAs followed by their destabilization or repression of protein translation. Many miRNAs can target the same gene and a single miRNA can regulate multiple genes (reviewed in Ha and Kim, 2014).

The classification of miRNAs can be based on their location in the genome as intergenic and intronic, most miRNAs are intronic (Lee et al., 2002). A miRNA cluster is a group of two or more miRNAs located within the same chromosome each separated by up to ten kilobases. All miRNAs within a cluster are transcribed as one long primary miRNA then cleaved into individual precursor miRNAs. miRNAs within the same cluster tend to have high sequence homology and as a result they may target the same mRNAs (Altuvia et al., 2005, Mathelier and Carbone, 2013). The genomic organization of miRNA clusters play an important role in protecting miRNAs from degradation (Siomi and Siomi, 2010).

### 1.4.1.1 miRNA biogenesis

The biogenesis of miRNAs is depicted in Figure 1.5. They are transcribed by RNA polymerase II as long primary miRNAs (pri-miRNAs, > 1 kb) containing a stem-loop (33-35 bp).

In the nucleus, pri-miRNAs will be processed by the microprocessor complex (containing nuclear RNAase III Drosha complexed with the cofactor DGCR8) to crop the stem-loop and form a hairpin-shaped precursor miRNA (pre-miRNA) approximately 60-70 nucleotides in length. This double strand RNA will be cleaved into one or two miRNAs depending on whether it is exonic or intronic (Calin et al., 2004). Intronic miRNAs can alternatively be spliced and debranched into pre-miRNAs. Pre-miRNAs are carried by Exportin 5 to the cytoplasm where further maturation occurs. Exportin 5 binds to GTP-binding nuclear protein and pre-miRNA to form transport complex that passes through the nuclear pore into cytoplasm where the complex destabilises to liberate pre-miRNA. Pre-miRNAs are then processed by RNase III endonuclease Dicer which binds to pre-miRNA at the 3’ or 5’cleavage sites leading to dicing and releasing of mature double-stranded miRNA ~ 22 nt in length. The mature miRNA duplex is loaded on to Argonaute (AGO) protein to generate RNA induced silencing complex (RISC) (Ha and Kim, 2014). miRNAs are relatively stable upon loading into RISC, then the duplex unwinds, one of the strands (passenger strand) is degraded and the other strand (guide strand) forms mature miRNA. Endonuclease C3PO plays a role in releasing passenger strand. Mismatches at the nucleotide positions 2-8 and 12-15 normally guide the unwinding of miRNA duplex (Schirle and MacRae, 2012). miRNAs contain a seed region at nucleotides 2 – 9 that binds to 3' (UTR) (untranslated region) of target mRNAs. However, recent studies suggested that miRNAs can alternatively bind 5’ UTR and protein coding sequences (Bartel, 2009).

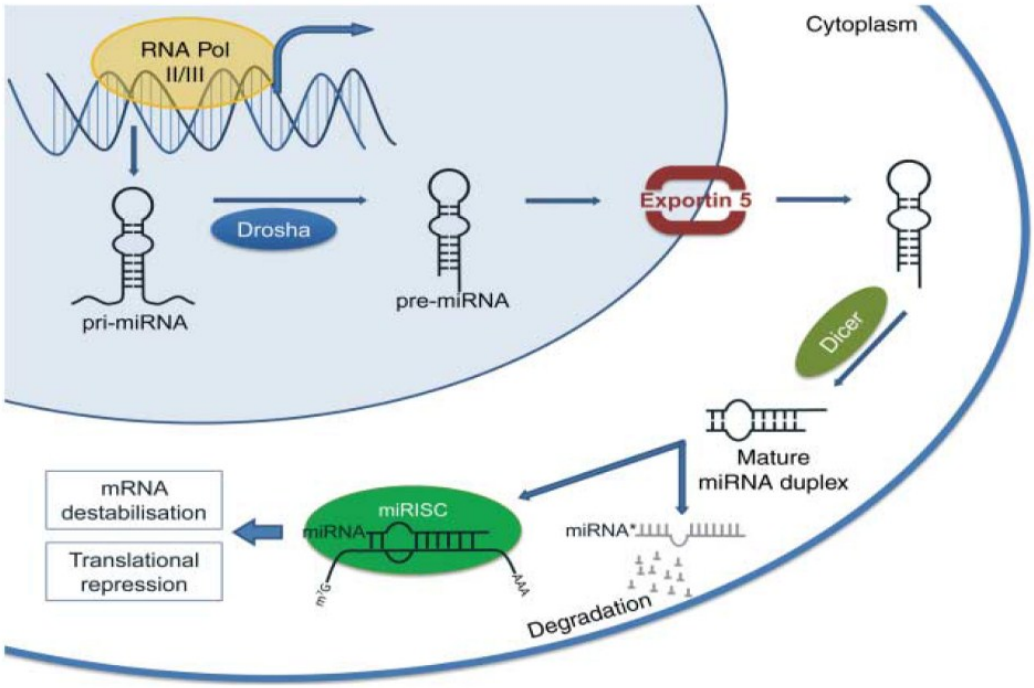


**Figure 1.6 A Schematic showing the canonical pathway of miRNA biogenesis in animal cells (Donadeu et al., 2012).**

### 1.4.1.2 Experimental approaches for studying miRNA function

miRNAs bind partially complementary gene sequences, normally in 3'UTR regions of target genes. Watson–Crick complementarity to the miRNA seed sequence is critical for target selection although complementarity to other regions of the miRNA sequence can compensate for the presence of mismatches in the seed sequence. Another important factor for target selection is free energy associated with the miRNA-target pair. In addition, many miRNA targets are conserved across species. Several algorithms to identify predicted miRNA targets are available online (Berezikov, 2011, Chi et al., 2012). The high number of predicted miRNA binding sites in human genes demonstrates the level of control of gene expression exerted by miRNAs; however, the accuracy of target prediction remains a major problem as >50% of predicted genes may actually not be actual targets (Bartel, 2009, Dongen and Enright, 2014).

Several strategies have been applied to profile miRNA expression such as RT-qPCR, high-throughput analyses (sequencing, microarray, PCR arrays) (Pritchard et al., 2012) and in situ hybridisation (Nielsen, 2012). One approach for target identification uses transfection of specific miRNA mimics or inhibitors in cells followed by microarray analysis to identify up- or down-regulated mRNA targets (Thomas et al., 2010). A more specific approach uses crosslinking, ligation, and sequencing of hybrids (CLASH) (Helwak et al., 2013, Helwak and Tollervey, 2014) or cross-linking and high-throughput analysis of cDNA (CRAC) to isolate RNA sequences bound to AGO protein (Libri et al., 2012). Identification of binding sites of cellular RNA-binding proteins (RBPs) and miRNA-containing ribonucleoprotein complexes can be performed using Photoactivatable-Ribonucleoside-Enhanced Crosslinking and Immunoprecipitation (PAR-CLIP) (Hafner et al., 2010).

## 1.4.2. Involvement of miRNAs in ovarian function

### 1.4.2.1. Ovarian miRNA populations

Small RNA populations in normal ovarian tissues have been profiled by cloning-based or next-generation sequencing in different species (Table 1.4).

**Table 1.4. Lists of most abundant miRNAs in the ovaries of different species identified using cloning-based or next-generation sequencing (modified from Donadeu et al., 2012).**

| **Human (adult)** | **Cow (neonatal/ adult)** | **Cow (fetal)** | **Cow (adult)** | **Sheep (adult)** | **Pig (adult)** | **Mouse (adult)** | **Mouse (neonatal)** |
|---|---|---|---|---|---|---|---|
| (Landgraf et al., 2007) | (Huang et al., 2011) | (Tripurani et al., 2010) | (Hossain et al., 2009) | (Hu et al., 2016, McBride et al., 2012). | (Li et al., 2011) | (Mishima et al., 2008) | (Ahn et al., 2010) |
| miR-143 | miR-143* | miR-199a | let-7b | miR-21 | miR-21 | miR-125b | miR-320 |
| miR-125b | let-7f | miR-125b | let-7c | miR-125b | miR-143-3p | miR-21 | let-7i |
| let-7b | let-7a | let-7c | miR-143* | let-7b | let-7i | miR-199a-3p | let-7d |
| let-7a | let-7c | miR-125a | miR-23b | let-7a | let-7f | miR-99a | miR-298 |
| miR-16 | miR-10b | miR-26a | let-7a | miR-16b | miR-148a-3p | miR-145 | miR-199a |
| miR-126 | let-7b | let-7b | miR-24 | miR-142-3p | let-7a | miR-351 | miR-30a |
| miR-99a | miR-26a | miR-10b | miR-27a | let-7c | let-7c | miR-214-3p | miR-140 |
| miR-26a | miR-148a | let-7a | miR-652 | miR-202 | miR-24-3p | miR-143-3p | miR-322 |
| miR-29a | miR-21 | miR-145 | miR-21 | miR-199a | miR-34c | miR-93 | miR-152 |
| let-7c | miR-140 | miR-126* | miR-126 | let-7f ovis_aries_ovary-m0033_3p | miR-29a-3p | miR-322 | miR-26a |

Using high-throughput analyses, several studies have also compared miRNA expression between healthy and atretic follicles as well as across different follicular cell compartments including granulosa and theca in domestic species (reviewed in Donadeu et al., 2012, Maalouf et al., 2016b).

miRNA populations have also been profiled in the COC of cow (Abd El Naby et al., 2013, Andrade et al., 2016, Gilchrist et al., 2016, Miles et al., 2012, Tesfaye et al., 2009, Tscherner et al., 2014), human (Assou et al., 2013, Tong et al., 2014, Xu et al., 2011b) and pig (Mahdipour et al., 2015), as well as in follicular fluid of human (Feng et al., 2015, Moreno et al., Sang et al., 2013, Santonocito et al., 2014), horse (da Silveira et al., 2012, Schauer et al., 2013) and cow (Sohel et al., 2013), and in the CL of ruminants (Ma et al., 2011, Maalouf et al., 2016a, Maalouf et al., 2014, McBride et al., 2012).

#### 1.4.2.2 The role of miRNAs during follicle growth

Studies involving knocking out Dicer, an enzyme that has a central role in the biogenesis of miRNAs, provided strong evidence that miRNAs play critical roles in folliculogenesis. In particular, conditional Dicer knockouts restricted to the reproductive system showed an increase in the number of primordial follicles due to accelerated follicle recruitment and increased follicle degeneration (Lei et al., 2010, Nagaraja et al., 2008). Later studies, mostly in vitro, have confirmed the involvement of miRNAs in dynamic regulation of follicular cell proliferation and steroidogenesis as well as whole-follicle growth, as summarised in Table 1.5.

**Table 1.5 Reported involvement of miRNAs in follicle growth and steroidogenesis.**

| miRNA | Site of expression | Reported function(s) | Target(s) | Reported changes during development | Species (reference) |
|---|---|---|---|---|---|
| miR-143 | Pre-granulosa | Inhibits proliferation of pre-granulosa cells | *(Cyclins B1, D2, E2, Cdk 4, 6)* | Increase during primordial follicle formation from 15.5 days post-coitus to 4 days post-natal | Mouse (Zhang et al., 2013a) |
| miR-145 | Neonatal Primordial follicle | Regulation of primordial follicle growth | *Tgfbr2* | Increase during initiation of primordial follicle development | Mouse (Yang et al., 2013b) |
| miR-376a | Fetal and neonatal ovaries | Enhances primordial follicle growth and blocks oocyte apoptosis | *Pcna* | n.d | Mouse (Zhang et al., 2014a) |
| miR-125b | Neonatal ovaries | Inhibits the process of primordial follicle assembly | *Acvr2a* | Decline after addition of recombinant human Activin A (rh-ActA) | Mouse (Wang et al., 2016a) |
| miR-26b | Granulosa | Pro-apoptotic | *ATM, HAS2* | Increases during follicular atresia | Pig (Lin et al., 2012, Liu et al., 2016) |
| miR-23a miR-27a | Granulosa | Promote apoptosis | *XIAP ,SMAD5* | n.d | Human (Nie et al., 2015) |

| | | | | | |
|---|---|---|---|---|---|
| let-7g | Granulosa | Pro-apoptotic | *MAP3K1* | Increases during follicular atresia | Pig (Cao et al., 2015, Zhou et al., 2015) |
| miR-34a | Granulosa | Pro-apoptotic | INHBB | n.d | Pig (Tu et al., 2014). |
| miR-145 | Granulosa | Inhibits granulosa cell proliferation | *ACVRIB* | n.d | Mouse (Yan et al., 2012) |
| miR-181a | Granulosa | Suppresses granulosa cell proliferation | *Acvr2a* | Reduced expression in ovaries of 8, 12, and 21-day old mice compared with 3-day old, and reduced expression in preantral and antral compared with primary follicles | Mouse (Zhang et al., 2013b) |
| miR-10b | Granulosa | Inhibits granulosa cell proliferation | *BDNF* | Increased in response to hCG treatment | Goat (Peng et al., 2016) |
| miR-17-92 cluster | Granulosa | Regulates granulosa cell proliferation and differentiation | *PTEN and BMPR2* | They differentially expressed in granulosa cells from subordinate and dominant follicles at day 19 of the oestrous cycle | Cow (Andreas et al., 2016) |
| miR-22 | Granulosa | Inhibits apoptosis | *SIRT1* | Increased in healthy follicles | Mouse (Xiong et al., 2016) |

| | | | | | |
|---|---|---|---|---|---|
| miR-92a | Granulosa | Inhibits apoptosis | *Smad7* | Decreased in atretic follicles | Pig (Liu et al., 2014, Quezada et al., 2012). |
| miR-125b | Granulosa | Antiapoptotic | *n.d* | Androgens enhanced miR-125b expression | Mouse (Sen et al., 2014) |
| miR-126* | Granulosa | Induced apoptosis | *FSHR* | AR and miR-126* have synergetic effects in regulation of FSHR expression | Pig (Du et al., 2016) |
| miR-224 | Granulosa | Stimulates cell proliferation, *cyp19a1*, oestradiol levels | *Smad4* | TGFβ1-induced increase in preantral follicles | Mouse (Yao et al., 2010) |
| miR-383 | Granulosa, Oocyte | Stimulates *cyp19a1*, oestradiol levels | *Rbms1* | TGFβ1-induced decrease in preantral follicles, gonadotropin-induced increase in antral follicles, decrease before ovulation | Mouse (Yin et al., 2012) |
| miR-132 | Granulosa | Increase *CYP19A1*, oestradiol levels | *Nurr1* | Increased during ovulation | Mouse (Wu et al., 2015) |
| miR-133b | Granulosa | Stimulates cell proliferation and oestradiol production | *Foxl2* | n.d. | Mouse (Dai et al., 2013) |

| | | | | | |
|---|---|---|---|---|---|
| miR-378 | Granulosa | Inhibits *CYP19A1*, oestradiol levels | *CYP19A1* | Decreased during antral follicle growth | Pig (Xu et al., 2011a) |
| miR-378 | Granulosa | Suppress follicular remodelling | *PGR* | Decrease in developing follicle | Pig (Toms et al., 2015). |
| miR-320 | Granulosa | Suppress oestradiol and promote apoptosis | *E2F2, SF1* | n.d | Mouse (Yin et al., 2014) |
| miR-125a, miR-455 | Mixture of Granulosa, adrenal, Leydig tumour | Suppress HDL uptake and steroidogenesis | *SRBI* | n.d. | Rat (Hu et al., 2012) |

### 1.4.2.3 Involvement of miRNA during oocyte maturation

Recent investigations have reported different effects of siRNA and miRNA in the mouse oocyte. Dicer and AGO2 are involved in the biogenesis of miRNA as well as siRNA while DGCR8 and Drosha are essential for regulation of miRNA biogenesis but not siRNA. Dicer1 and AGO2 conditional knockout in the mouse oocyte resulted in failure to complete meiosis due to impairment of meiotic spindle organization and abnormal chromosomal condensation, leading to a decline in ovulation rates. However, deletion of DGCR8 or Drosha had no abnormal effects on mouse follicle development and oocyte maturation (Murchison et al., 2007, Tang et al., 2007, Yuan et al., 2014). A different study by Flemr et al. (2013) showed that oocyte specific Dicer isoforms in mice has a higher tendency to cleave double strand RNAs into siRNA instead of miRNA.

These findings highlight the roles of siRNAs in oocyte maturation and suggest that miRNAs have minimal involvement in oocyte growth and COC communication (reviewed in Brachova et al., 2016).

A study with bovine oocytes showed that miR-212 regulates oocyte development through binding to 3'UTR of FIGLA, an embryonic regulatory gene (Tripurani et al., 2013). Other studies have suggested involvement of miR-196a and miR-181a in the regulation of oocyte-specific maternal genes, NOBOX and NPM2, respectively (Lingenfelter et al., 2011, Tripurani et al., 2011). Additionally, miR-133b regulated oocyte maturation through its target TAGLN2 which encodes an actin protein (Xiao et al., 2014). In vivo and in vitro findings in mouse COC have shown that miR-224 prevents cumulus expansion through targeting PTX3 (Yao et al., 2014). A different study has showed that miR-205 level was reduced in pig oocytes in response to BDNF treatment whereas overexpression of miR-205 in granulosa cells resulted in a dramatic decrease in PTX3 levels (Li et al., 2016). Overexpression of miR-378 lead to a significant reduction in the expression of genes involved in oestradiol production (CYP19A1), cumulus expansion (HAS2, PTGS2) and oocyte maturation (CX43, ADAMTS1, PGR) which in turn results in supressed cumulus expansion as well as oocyte maturation in porcine (Pan et al., 2015).

#### 1.4.2.4 The role of miRNAs during follicle-luteal transition

A small number of studies have reported the effects of specific miRNAs on follicle-luteal transition (Table 1.6). Through sequencing of sheep ovarian tissues, McBride et al. (2012) first identified miRNAs differentially expressed during the follicular-luteal transition, in particular, a decrease in levels of miR-199a-3p, miR-125b, miR-145, miR-31, and an increase in miR-21 (which the continued to increase throughout luteal growth) and miR-142-3p. In the case of miR-503, a decrease occurred in the pre-ovulatory follicle followed by an increase in the CL. Changes in the levels of some of these miRNAs could be replicated during induced follicular cell luteinisation in vitro (McBride et al., 2012).

Microarray analyses in mice identified transcriptional induction of miR-21, miR-132 and miR-212 in mural granulosa cell in response to an ovulatory dose of LH/hCG. In addition, miR-132 and miR-212 but not miR-21 increase after exposure of cultured granulosa cells to 8-Br-cAMP (Fiedler et al., 2008). In another study, and consistent with the data by McBride et al. (2012) mmu-miR-503 expression decreased in preovulatory mouse ovaries in response to hCG while up-regulation of mmu-miR-503 in primary granulosa cells resulted in down-regulation of expression of several genes (*Acvr2, Bcl2, Ccnd2, Inha, Cyp19a1, Lhcgr, Esr2, Cdkn1b*) that are involved in granulosa cell proliferation and luteinisation (Lei et al., 2010). Reported roles for miRNAs during the follicle-luteal transition are summarised in Table 1.6.

**Table 1.6 Reported roles of miRNAs during follicle-luteal transition (modified from Donadeu et al. 2012).**

| **miRNA** | **Site of expression** | **Reported function(s)** | **Target(s)** | **Reported changes during development** | **Species *(reference)*** |
|---|---|---|---|---|---|
| miR-136-3p | Granulosa | Suppresses LHR (shown in vivo) | *LHR* | Increase in ovaries during hCG-induced ovulation | Rat (Kitahara et al., 2013) |
| miR-513a-3p | Granulosa | Downregulates LHCGR (shown in vitro) | *LHCGR* | Increase in luteinised granulosa cells | Human (Troppmann et al., 2014) |
| miR-122 | Ovaries | Down regulates LHR (shown in vivo) | *LHR* | Increase in ovaries during hCG injection | Rat (Menon et al., 2015, Menon et al., 2013) |
| miR-21 | Granulosa | Anti-apoptotic | *n.d.* | Increase during hCG-induced | Mouse (Carletti et al., 2010). |
| miR-132/ | Granulosa | n.d. | *Ctbp1* | Increase | Mouse |

| | | | | |
|---|---|---|---|---|
| miR-212 | | | during hCG-induced ovulation | (Fiedler et al., 2008) |
| miR-183-96-182 cluster | Granulosa | Enhance granulosa cell proliferation | *FOXO1* n.d | Cow (Gebremedhn et al., 2016b) |

### 1.4.2.5 Involvement of miRNAs in luteal function

There is little information on the role of miRNAs in the CL. However, changes in a notable number of miRNAs were identified across different stages of luteal development in sheep, pigs and cows (reviewed in Maalouf et al., 2016b). Otsuka et al. (2008) showed that mice with hypomorphic Dicer1 allele are infertile due to impairment of CL development and function. The authors indicated that deficiency in luteal angiogenesis is associated with the significant loss of many miRNAs such as let-7b and miR-17-5p, which may be involved in regulation of antiangiogenic factor, TIMP1 (Otsuka et al., 2008). Interestingly, in the ovine CL, miR-199a-3p and miR-145 were highly expressed in corpus albicans relative to CL, whereas the expression of miR-503 was significantly reduced in corpus albicans (McBride et al., 2012). Similar studies by Maalouf et al. (2014) have identified 15 miRNAs that were differentially expressed between CLs of pregnant and non-pregnant cows, the most abundant ones being let-7 family, miR-21, miR-140, miR-199a-3p and miR-320. The same group identified miR-34a as dramatically upregulated in mid-cycle CL. Overexpression of miR-34a in vitro led to suppression of luteal cell proliferation and induced progesterone secretion through repression of Notch1 and YY1, two genes involved in tumorigenesis. YY1 and Notch1 receptor intracellular domain (N1IC) activate the c-myc proto-oncogene through binding to its promoter and induce cell proliferation. Inhibition of Notch signalling resulted in promoting apoptosis in different cells.

In the CL, blockage of Notch1 led to a significant reduction in progesterone synthesis and enhanced apoptosis (Accialini et al., 2015, Fassl et al., 2015, Maalouf et al., 2016a). Ma et al. (2011) showed that miR-378 was highly enriched in mature compared to regressing CL and suggested that miR-378 may prevent luteolysis in bovine CL through targeting Interferon gamma receptor 1(IFNGR1). In a different study, miR-126 was highly expressed in mature relative to developing or regressing bovine CL. The investigators suggested that miR-126 may mediate the regulation of Talin2 (TLN2), a cytoskeletal protein that plays a role in cell integrity and adhesion (Ma et al., 2011).

In a previous study (Sadanand Dewaji Sontakke, Thesis, 2013), large follicles (12-17 mm; N=19; classified as healthy based on follicular oestradiol concentrations and expression of LHCGR and CYP19A1 (Sontakke et al., 2014) and corpora lutea (N=9; from Days 1-4 of the oestrous cycle based on gross morphology (Ireland et al., 1980, Rodgers and Irving-Rodgers, 2010) were obtained from bovine ovary pairs collected at an abattoir. Microarray analyses using a commercial array from Exiqon Sontakke et al. (2014) were performed on the two tissue types (Figure 1.7.A) followed by qPCR validation (Figure 1.7.B). A total of 14 and 60 miRNAs were upregulated and down-regulated (>1.5-fold; FDR<0.05), respectively, in CL relative to follicles, 9 and 14 of which, respectively, were validated by qPCR. Top upregulated in the CL were 5 miRNAs (Table 1.7) located in two different clusters within the bovine genome, miR-212-132 and miR-183-96-182 (Figure 3.1). The expression of miR-183-96-182 cluster could not be detected in follicles using qPCR.

**Table 1.7 Upregulated miRNAs in bovine early CLs.**

| miRNAs | Fold change | Adj. p value |
|---|---|---|
| **hsa-miR-182-5p/bta-miR-182** | 8.80 | 0.0000 |
| **hsa-miR-96-5p/bta-miR-96** | 7.55 | 0.0000 |
| **hsa-miR-132-3p/bta-miR-132** | 7.11 | 0.0001 |
| **hsa-miR-183-5p/bta-miR-183** | 5.42 | 0.0000 |
| **hsa-miR-223-3p/bta-miR-223** | 4.79 | 0.0000 |
| **hsa-miR-378a-3p/hsa-miR-378c/hsa-miR-378d/bta-miR-378** | 3.35 | 0.0001 |
| **hsa-miR-708-5p/bta-miR-708** | 3.11 | 0.0000 |
| **bta-miR-21** | 2.67 | 0.0000 |
| **hsa-miR-155-5p/bta-miR-155** | 2.48 | 0.0001 |
| **hsa-miR-132-5p** | 3.20 | 0.0006 |
| **hsa-miR-212-3p** | 2.71 | 0.0028 |

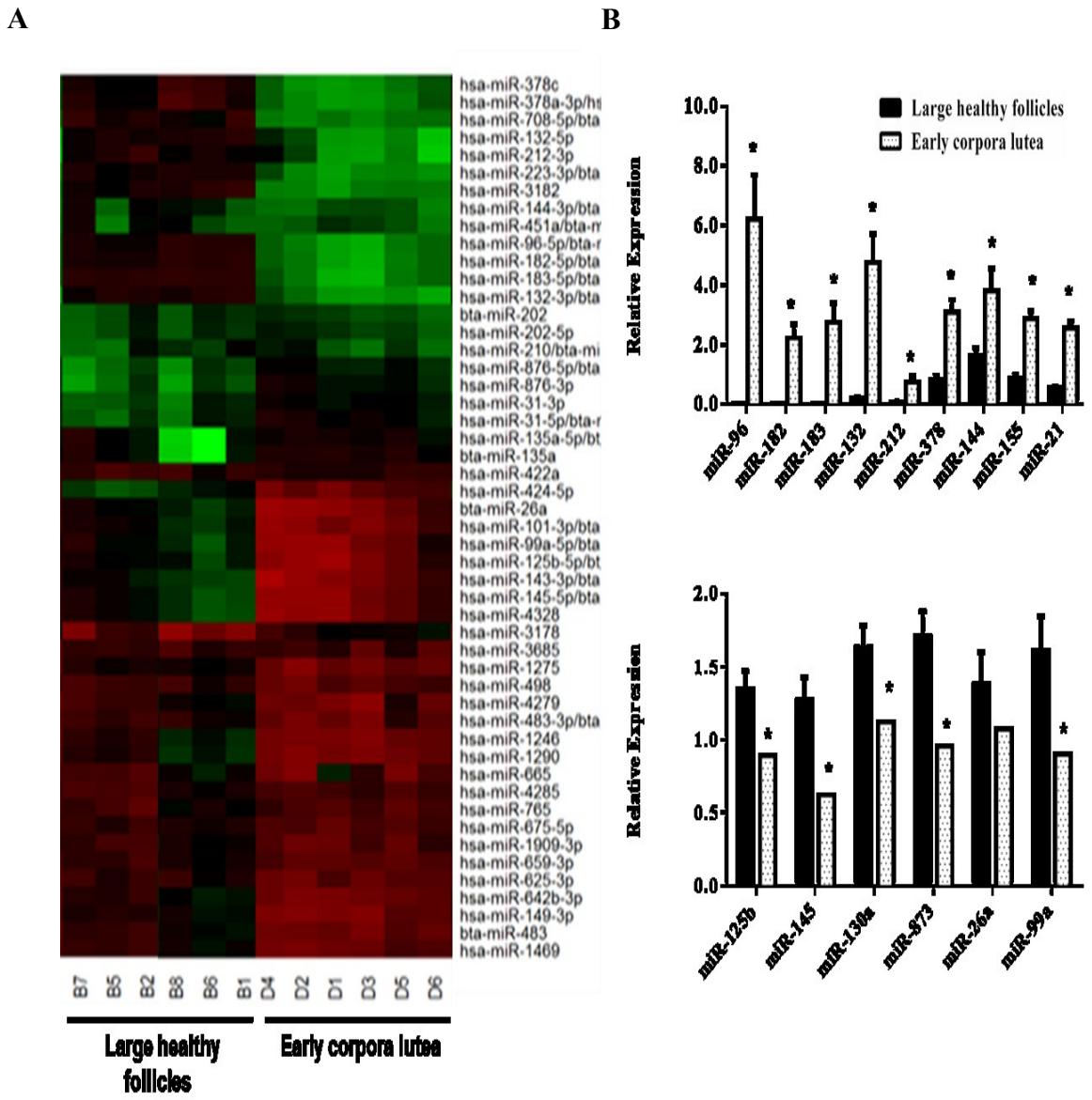


**Figure 1.7 Expression of miRNAs in bovine large healthy follicles (12–16 mm) and early corpora lutea using microarray and qPCR. A) Heat map of top 50 miRNAs with highest standard deviation in bovine large healthy follicles (12–16 mm) and early corpora lutea. Each row represents a miRNA and each column represents a sample. The colour scale illustrates the relative expression level of miRNAs. Red colour represents an expression level below the reference channel and green colour represents expression higher than the reference. B) Relative expression of selected miRNAs that, according to microarray analyses, were up-regulated and down-regulated in the early corpora lutea in relation to dominant healthy follicles, determined by RT-qPCR. Values are presented as mean (SEM) and were analysed by Student's t –test. Adapted from Sadanand Dewaji Sontakke, Thesis (2013).**

## 1.5 Rationale and Objectives

The overall aim of this thesis was to characterise the involvement of the miR-212-132 and miR-183-96-182 clusters during luteinisation. A better understanding of the molecular regulation of luteal formation will inform the development of better strategies to treat infertility in cattle and women. Luteal insufficiency resulting in insufficient progesterone production and/or short luteal lifespan has been associated with infertility and high embryo mortality rates. In cattle, a deficiency in progesterone secretion leads to early embryo loss and infertility (Lonergan and Forde, 2015). In human, luteal insufficiency is suggested to have a role in failure of implantation and abortion in the first trimester (Shah and Nagarajan, 2013).

The studies described in this thesis had the following objectives:

1. To characterise the expression of miR-132 and miR-96 within the bovine CL using in situ hybridisation and FACS, and identify predicted gene targets of these miRNAs during luteinisation.

2. To characterise the effects of inhibition or overexpression of miR-132 and miR-96 in proliferation, survival and progesterone production by bovine luteal cells.

3. To determine whether the effects of these miRNAs during luteinisation are conserved in humans.

# Chapter 2

# Materials and Methods

# Chapter 2: Materials and Methods

## 2.1 Cell isolation and culture procedures

### 2.1.1 Ovarian collection

Ovaries from forty beef heifers at various stages of the oestrous cycle were obtained from the abattoir at Bridge of Allan, Stirling, UK, and transported to Roslin Institute, university of Edinburgh, UK in PBS at 37ºC supplemented with 1% solution of antibiotics within an hour of collection. Once in the laboratory, the ovaries were rinsed with 70% Ethyl alcohol then follicles were dissected out and their diameters were measured using Vernier Calliper. Follicles with a diameter 4-8 mm were classified into healthy and atretic according to pre-established criteria (Irving-Rodgers et al., 2001, Rodgers and Irving-Rodgers, 2010). Only the healthy follicles were used which had a well-vascularised wall and transparent amber follicular fluid without debris. For luteal cell experiments, around fifteen early corpora lutea were collected from ovarian pairs deemed to originate from heifers at days 1 to 4 of the oestrous cycle based on morphological criteria outlined previously (Ireland et al., 1980). Human luteinised granulosa cells were obtained from thirty-six IVF patients treated for both female and male-related fertility diseases at the Simpson Centre for Reproductive Health of the Royal Infirmary of Edinburgh.

At the pre-determined time-points during each cell culture experiment, cells from 3-5 wells within each treatment group or control were pooled for RNA or protein extractions while medium was obtained for hormonal analysis. In this study, several methods have been used to study the role of miR-212-132 and miR-183-96-182 in both bovine and human ovarian cells (Figure 2.1).

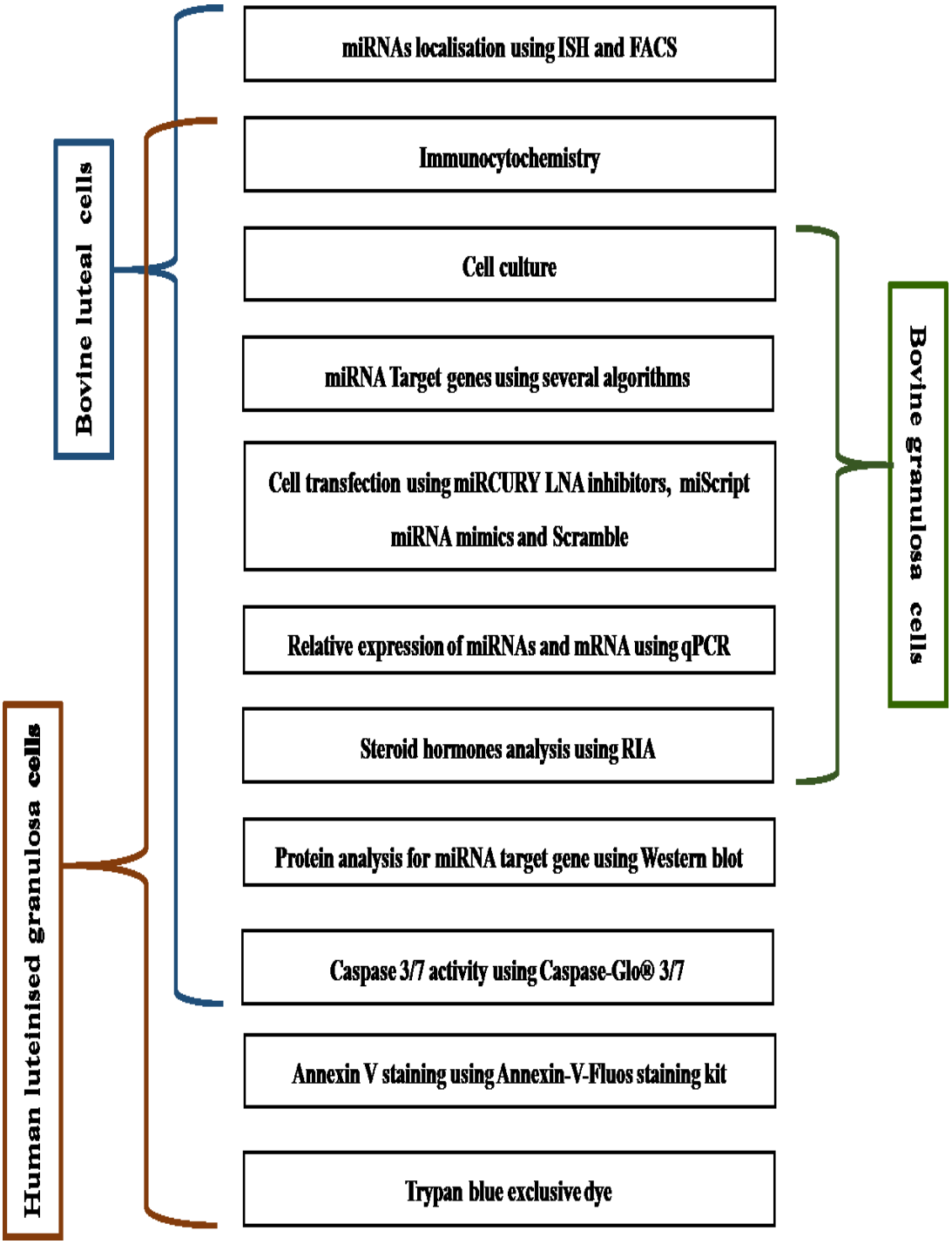


**Figure 2.1 A schematic representation of the experimental methods used in the bovine and human ovarian cells.**

## 2.1.2 Bovine granulosa cell isolation

Follicles were cut in half in a petri dish and granulosa cells (GCs) were isolated by gently rubbing the internal surface of the follicle. The GCs obtained from different heifers were pooled and harvested by centrifuging the follicular fluid at 500g for 10 min. After discarding the fluid, cell pellets were suspended in McCoy's 5a media and passed through a 70 μm cell strainer; then centrifuged at 500g for 10 minutes. Red blood cells were removed by adding 1 ml of RBC lysis buffer (8.3 gm/l $NH_4Cl$ in 0.01 M Tris-HCl buffer pH= 7.5) into cell pellet for 1 minute at RT. After centrifugation, GCs were suspended in defined McCoy's 5a media (Gutiérrez et al., 1997a). Cell number was detected using a haemocytometer and availability was identified by trypan blue exclusion, the typical viability before plating was around 35%. The pooled cells were cultured in granulosa cell culture media (appendix I) at densities of 50,000 or 500,000 cells in 96 well- or 12 well-plates in a humidified incubator at 37˚C and 5% $CO_2$. After 24 h of seeding, luteinisation was induced by treating GCs with Forskolin cocktail (Appendix I) while the control cells left untreated for 4 days and media changed every 2 days.

## 2.1.3 Bovine luteal cell isolation

Luteal cells were isolated using a modification of published protocols (Alila et al., 1988, Batista et al., 2012, Choudhary et al., 2005, Jones et al., 1992, Okuda et al., 1992, Pate and Condon, 1982, Wiles et al., 2014). Corpora lutea were weighed and washed with PBS containing 1% solution of antibiotics then minced into small pieces using a disposable scalpel. The minced tissue was placed in a 50 ml centrifuge tube (Falcon, Becton Dickinson UK Ltd) in dissociation media (Appendix I) (1 gm of tissue/10 ml of medium) and placed in a shaking incubator at 150g at 37°C for 45 min. After this the supernatant was aspirated with a Pasteur pipette while the rest of the undigested tissue was added to fresh dissociation medium and placed in a shaking incubator at 150g and 37°C for an additional 45 min. The supernatants from each incubation were pooled and passed through a 100 μm cell strainer then centrifuged at 500g for 10 min at RT.

Fresh DMEM/F-12 medium containing 0.025 mg/ml of DNase I and 0.1% BSA was added to cell pellets and placed in a shaking incubator for 10 min at 37°C. After digestion, the suspension was passed through a 70 μm cell strainer (BD Biosciences. UK). LCs were washed twice with DMEM/F-12 medium and collected by centrifugation at 500g for 5 min at RT. After discarding the supernatant, erythrocyte lysis was performed by adding 1ml of RBC lysis buffer for 1 min then the cells were washed with 10 ml DMEM/F-12 medium and centrifuged at 500g for 5 min at RT. After centrifugation, the supernatant was discarded and cells were resuspended in a suitable amount of medium. LCs were counted using a hemocytometer; cell availability was normally greater than 80%, as assessed using trypan blue exclusive dye (T8154; Sigma-Aldrich. UK). Cells were cultured in luteal cell culture media (see appendix I) for 2 days at densities of 50,000 or 500,000 cells in 96 well- or 12 well-plates in a humidified incubator at 37˚C and 5% $CO_2$.

### 2.1.4 Human luteinised granulosa cell (hLGC) isolation

The reproductive medicine subcommittee of the Lothian medical ethics committee separately approved the collection of cells from patients undergoing assisted conception. Follicular fluid aspirates from thirty six human donors undergoing in vitro fertilisation for the female and male infertility (Duncan et al., 2005) at the Simpson Centre for Reproductive Health of the Royal Infirmary of Edinburgh were provided by Dr. W.Colin Duncan. Samples were aspirated from patients 34-36 h after administration of human chorionic gonadotropin then transferred into a 50 mL centrifuge tube. After centrifugation at 500g for 10 min, the cell pellet was suspended in PBS (1% Pen/Strep+0.1%BSA). The cell suspension was placed into a 15-mL centrifuge tube and centrifuged through Ficoll Paque Plus solution (density 1.077 g/cm$^3$, GE Healthcare; 17-1440-02. UK) for 20 min at 400g at 20°C. Following centrifugation, hLGCs were collected from the middle layer and placed into a 15 mL tube containing PBS. Cell suspension was washed twice and centrifuged for 5 min at 500g at RT, as described (Chatterjee et al., 2014, Chilvers et al., 2012).

Cell viability was approximately 70%. 100 000 or 500 000 cells per well of two to three patients were cultured (appendix I) for 2 days in 24 well- or 12 well-plates in a humidified incubator at 37˚C and 5% $CO_2$.

## 2.1.5 Cell transfection

Transfections were performed using commercial reagents and pre-designed sequences (Table 2.1) as per the protocol from manufacturer. Cell culture medium was added to 1.5 ml tubes then miRNA miRCURY LNA inhibitors (Exiqon, Denmark) or chemically synthesized double-stranded oligonucleotides (miScript miRNA Mimics) or a scrambled (negative control) oligonucleotide sequence (Qiagen, UK) were added followed by Hiperfect reagent (Qiagen, UK). The mixture was briefly vortexed and left for 5 min at RT to allow the formation of transfection complexes. Transfections were done in either 96 well-plates (total culture volume, 150 µl) for later RNA extraction or 12 well plates (total culture volume 840 µl) for later protein analyses. Bovine granulosa cells were transfected with LNA inhibitors then treated with luteinisation cocktail while cells transfected with mimics left untreated. Transfection of hLGCs with FOXO1 siRNAs (siRNA ID 106653 and 106654. Life Technologies Ltd, UK) was performed as described above.

**Table 2.1 List of miRNA mimics/inhibitors and FOXO1 siRNA were used for transfection.**

| Cell type | Sequence | nM/well | Oligonucleotide sequence (5'-3') |
|---|---|---|---|
| **Bovine and human luteinised granulosa cells** | Syn-bta-miR-132 Mimic | 10 | UAACAGUCUACAGCCAUGGUCG |
| | Syn-bta-miR-96 Mimic | 10 | UUUGGCACUAGCACAUUUUUGCU |
| | hsa-miR-96-5p Inhibitor | 50 | AGCAAAAATGTGCTAGTGCCA |
| | hsa-miR-132-3p Inhibitor | 50 | ACCATGGCTGTAGACTGT |
| | Scramble | 50 | All Star negative control (Qiagen. UK) |
| | | | |

| | | | |
|---|---|---|---|
| **Human luteinised granulosa cells** | Scramble | 100 | All Star negative control (Qiagen. UK) |
| | FOXO1 siRNA | 100 | GGGUUAGUGAGCAGGUUACtt<br>GGAAAGUGAUGUAUAGUUAtt |

## 2.2 In situ hybridisation

In situ hybridisation of miRNAs on bovine ovarian frozen sections was carried out using probes (Table 2.2) with some modifications of the manufacturer protocol. Ovaries were fixed in 4% PFA overnight at 4˚C for preparation of cryosections. After overnight fixation, ovary was incubated with 30% sucrose in PBS at 4˚C and frozen in Tissue-Tek OCT reagent. Tissue sections were cut at 10µm and denatured with 5 µg/ml of proteinase K in 75 ml PBS then fixed in 4 % PFA for 10 minutes and rinsed with 0.2 % Glycine in Phosphate Buffer Saline (PBS). The tissues were incubated with freshly prepared imidazole buffer then slides were placed in a humid chamber and freshly prepared 1-ethyl-3-(3-dimethylaminopropyl) carbodiimide (EDC) were added to each slide for 1 h at RT followed by two hours of pre-hybridisation with 50% formamide and 5x SSC buffer at 25°C. Sections were then incubated overnight with Double Digoxigenin labelled LNA modified oligonucleotide probe (80 nM for miR-132 and miR-96, (negative controls 3 nM U6snRNA and 80 nM Scramble probe) (Exiqon, Vedbaek, Denmark) in hybridisation buffer. After application of probe, slides were covered with gel bond film and heated to 60°C for 5 min, then placed in humidifying chamber at 45°C. After overnight incubation, slides were washed with 4x, 2x and 0.2x SSC post hybridisation buffers for 10 min at 50°C to avoid unspecific binding and then rinsed with 1x Tris Buffer Saline (TBS). Slides were then incubated with blocking solution for 1 h at RT. Anti-digoxigenin antibody (1:200) was added to slides for 2 h at RT followed by colour development with NBT/BCIP at 4°C up to 16 h. Signal was analysed with a light microscope. Three independent analyses were performed using different ovarian sections.

**Table 2.2 List of miRCURY LNA™ Detection probes used for ISH.**

| Probe name | Product code | Probe Sequences (5`-DIG and 3`-DIG labeled) |
|---|---|---|
| **hsa-miR-132** | 38031-15 | CGACCATGGCTGTAGACTGTTA |
| **hsa-miR-96** | 38474-15 | AGCAAAAATGTGCTAGTGCCAAA |
| **mmu-miR-202-5p** | 39486-15 | AAAGAAGTATATGCATAGGAA |
| **U6 snRNA** | 99002-15 | CACGAATTTGCGTGTCATCCTT |

## 2.3 Immunochemistry

The bovine ovaries were fixed in 4% PFA overnight at 4°C followed by overnight incubation in 30% sucrose in PBS at 4°C and freezing in Tissue-Tek OCT reagent. Sections were cut at 10 µm on a cryostat then mounted on Superfrost /Plus slides and air dried before use. The slides were incubated with blocking solution for 1 h at RT then incubated with primary antibody (Table 2.3) overnight at 4°C. After washing with TBST buffer, sections were incubated with secondary for 1 h then washed three times. For bovine and human luteal cultured cells, cells were grown on coverslips and fixed in acetone: methanol (1:1) for 10 min at 4°C. Following blocking, cells were incubated with primary antibodies overnight at 4°C then washed with washing buffer and incubated with secondary antibodies (Table 2.3). Negative controls in each case consist of similar concentrations of isotypes and secondary replacing the primary antibodies. The slides were mounted with DAPI and visualized with a Leica DMLB fluorescence microscope.

## 2.4 Fluorescence-Activated Cell Sorting (FACS)

After digestion of three early corpora lutea with collagenase solution, luteal cells were separated using FACS to localize miRNAs expression. Firstly, the concentration of antibodies was optimised using flow cytometry. Cells $1\times10^6$ were used for sorting. For intracellular staining, cells were fixed in 1% PFA for 15 min at 4°C then washed with PBS buffer twice and centrifuged at 500g for 5 min. For surface staining, cells were washed with FACS buffer and centrifuged at 500g for 5 min. After discarding the supernatant, cell pellets were blocked with FACS Buffer for 15 min at 4°C. Afterward, cells were incubated with primary antibodies for 1 h at 4°C in the dark, followed by incubation with secondary antibody for 1 h at 4°C (Table 2.3). To distinguish steroidogenic luteal cells, cells were stained with Nile red (N3013; Sigma-Aldrich. UK) (1 µg/ml) in PBS for 15 min at 4°C. Cells were resuspended in FACS buffer and sorted by BD FACS Aria IIIu (Becton, Dickinson and Company, UK). Dead cells were excluded using DAPI then single cells were gated for analysis., 50000 cells per sample stained with Nile Red or CD144 were gated as positive or -negative fractions. Samples stained with secondary antibody or without primary antibody were used as controls. Data analysis was carried out using Flow J software.

**Table 2.3 Antibodies used for immunochemistry and FACS.**

| Antibody | Catalogue no./Supplier | Species | Dilution |
|---|---|---|---|
| HSB3β1 | Gift from Prof J.I. Mason | Rabbit | 1:500 |
| FOXO1 | #2880 / Cell Signalling | Rabbit | 1:20 |
| CD144 | AHP628Z/ AbD Serotec | Rabbit | 1:100 |
| CD45 | MCA832F/AbD Serotec | Mouse | 1:10 |
| IgG1 (Isotype) | MCA928F/AbD Serotec | Mouse | 1:10 |
| IgG Isotype | NBP2-24893/Novus biologicals | Rabbit | 1:100; 1:500 |

| | | | |
|---|---|---|---|
| Alexa Fluor 568 | A10042/ Invitrogen | Rabbit | 1:300 |
| Alexa Flour 405 | ab175654/Abcam | Rabbit | 1:300 |
| DAPI | D1306/ Thermo Fisher | | 1:1000 |

## 2.5 miRNA target prediction and functional annotation

Identification of the miRNA target genes was performed using TargetScan for bovine species. Other bioinformatic software such as mirTarBase and TarBase (Table 2.4) were detected human, rat and mouse homologs. Functional analysis of target genes was imported to DIANA- mirPath v.3 software (Vlachos et al., 2015) followed by using functional annotation clustering which were detected several clusters at highest stringency rate, only clusters that had (p- value of 0.05) were chosen for further analysis.

**Table 2.4 List of software programs and statistical packages.**

| **Programs (software) and statistical packages** | ***Source*** | ***Access date*** |
|---|---|---|
| ***BLAST cow sequences*** | http://www.ncbi.nlm.nih.gov/genome/seq/BlastGen/ | 2012-2016 |
| ***Entrez Gene*** | www.ncbi.nlm.nih.gov/entrez/query.fcgi?db=gene | 2012-2016 |
| ***Gene Ontology*** | http://www.geneontology.org | 2014 |
| ***miRBase release 21.0*** | www.mirbase.org | 2012-2016 |
| ***miRTarBase version 4.5,6*** | http://mirtarbase.mbc.nctu.edu.tw/ | 2014-2016 |

| | | |
|---|---|---|
| ***DIANA-TarBase v7.0*** | http://diana.imis.athena-innovation.gr/DianaTools/index.php?r=tarbase/index | 2015-2016 |
| ***mirPath v.3*** | http://snf-515788.vm.okeanos.grnet.gr/ | 2015-2016 |
| ***Primer BLAST*** | http://www.ncbi.nlm.nih.gov/tools/primer-blast/ | 2012-2016 |
| ***Ingenuity Pathway Analysis*** | http://www.ingenuity.com/products/ipa | 2014-2016 |
| ***Ovarian Kaleidoscope Database*** | http://ovary.stanford.edu/ | 2013-2016 |
| ***TargetScan (Release 6.2, 7)*** | www.targetscan.org | 2015-2016 |
| ***miRecord*** | http://mirecords.biolead.org/ | 2014 |
| ***miRSearch V3.0*** | https://www.exiqon.com/mirsearch | 2014 |
| ***FlowJo.10.0.8r1*** | http://www.flowjo.com/ | 2015-2016 |
| ***GraphPad prism v6*** | GraphPad software, Inc. | 2015- 2016 |
| ***Minitab 16, 17*** | https://www.minitab.com/en-us/ | 2014-2016 |

# 2.6 Quantification of miRNA and mRNA levels

## 2.6.1 RNA isolation

Total RNA was isolated from cultured ovarian cells using TRIzol® Reagent (15596-026; Life Technologies. UK) following the manufacturer´s instructions. After removing culture medium, Trizol reagent was added to each well and the cells were collected by scraping with a pipette tip into a 1.5 ml low binding tube. The cells were homogenised by briefly vortexing then chloroform (25668; FLUKA. UK) was added

and the mixture was shaken for 30 seconds, followed by centrifugation at 12,000g for 15 min at 4°C to separate the mixture into aqueous and organic phases.

After this, the upper aqueous phase containing RNA was aspirated and placed into new tube. Precipitation of RNA was carried out by adding absolute Ethanol and briefly pipetted up and down then the mixture left at RT for 10 min. Following centrifugation at 12,000g for 10 min at 4°C, the supernatant was discarded and cell pellet was washed with 75% Ethanol prepared with DEPC water (D5758; Sigma-Aldrich. UK) then spun at 7,500g at 4°C for 5 min. The supernatant was discarded and the pellet was left to air dry for 10 min. Finally, a 20µl of RNAse free water were added to RNA pellet, incubated at 50°C for 10 min and stored at -80°C until further use.

### 2.6.2 RNA quantification using RiboGreen assay

The concentration of RNA was determined by Quant-iT™ RiboGreen® RNA kit (R11490; Invitrogen. UK) using the low-range assay in a 200 µL total volume in the 96-well format (Costar. UK) as recommended by manufacturer. Each sample was quantified twice. A sensitive fluorescent dye binds to RNA and emits at the range 500-525 nm. Buffers and reagent were prepared on the day of the experiment. TE (10 mM Tris-HCl, 1 mM EDTA, pH 7.5) in DEPC water was used to dilute Quant-iT™ RiboGreen® reagent and ribosomal RNA standards. RNA samples were added followed by Quant-iT™ RiboGreen® reagent to all wells and incubated for 5 min. Finally, the fluorescence was measured by Wallac 1420 and the data were calculated by logit-log standard values. The rRNA standard curve ranged between 0.2-10 ng/ml.

### 2.6.3 Reverse transcription (RT)

Synthesis of the cDNA was performed using miScript II RT Kit (218161; QIAGEN Ltd. UK) according to manufacturer's instructions. A total of 100 ng of RNA was reverse transcribed in a 10 µl reaction. Master mix containing 2 µl of HiFlex buffer, 1 µl of nucleic acid mix (dNTPs, rATP, oligo-dT primers, and an internal synthetic RNA control (miRNA reverse transcription control [miRTC]), 1µl of Reverse Transcriptase (RT), RNAse free water and final amount of RNA were mixed and then briefly spun.

In addition, no Reverse Transcriptase and no RNA template controls were used to detect DNA contamination. The PCR tubes were incubated in a programmable Thermocycler (Biometra T-Gradient Thermocycler, UK) at 37°C for 60 min followed by an RT inactivation step at 95°C for 5 min and cooling at 4°C before storage at – 20°C.

### 2.6.4 Quantitative PCR (qPCR) analyses of miRNAs

miRNA levels were quantified using miScript SYBR Green PCR Kit (218073; QIAGEN Ltd. UK) following the manufacturer´s recommendations. A working solution of cDNA was prepared by diluting 1:40 in RNase free water and a standard curve was prepared from a sample pool. One µl of cDNA was added to 9 µl master mix containing 5 µl of SYBR Green, 1 µl Universal Primer (x10), 1 µl miRNA specific Primer Assay (Table 2.5) and 2 µl PCR grade water. The real time PCR analysis for each sample was carried out in duplicates using Mx3005P real time PCR system (Stratagene, La Jolla, CA) following a standard qPCR protocol: Activation of HotStarTaq DNA Polymerase for 15 min at 95°C followed by 40 cycles of denaturation for 15 seconds at 94°C then annealing for 30 seconds at 55 °C and extension for 30 seconds at 70°C, with fluorescence data collection (Figure 2.2). miRNA expression was normalised by dividing the corresponding value by the value of snoRNA U6B.

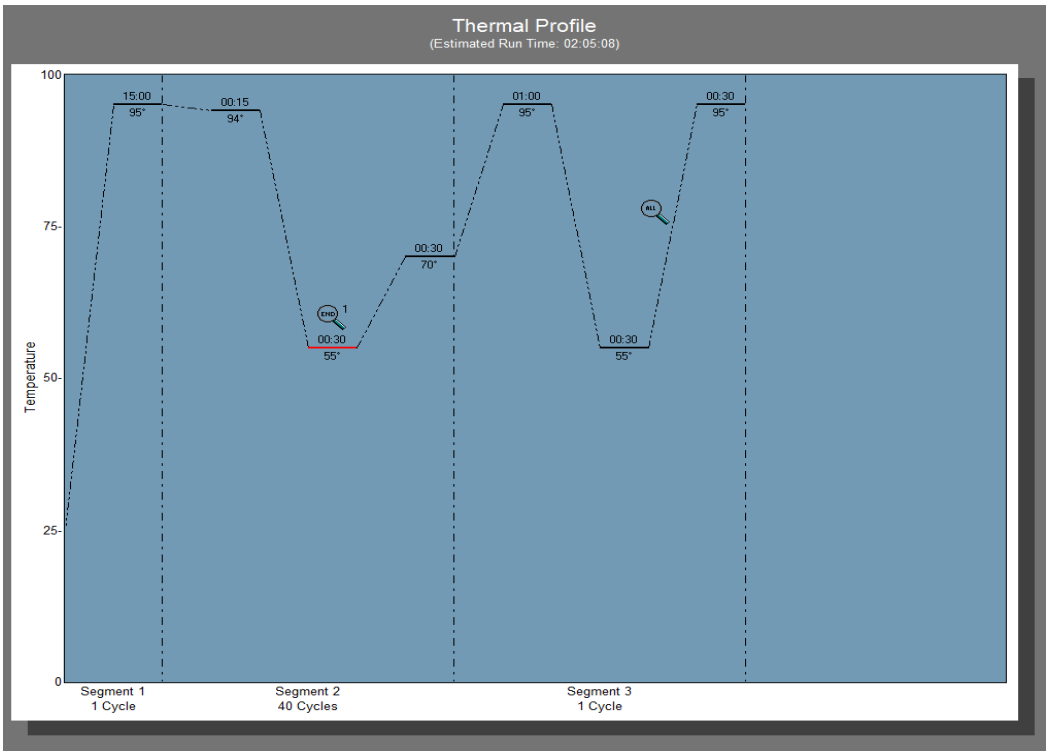


**Figure 2.2 Thermal Profile Setup for qPCR of miRNAs.**

**Table 2.5 Qiagen miscript primer assays used for quantification of miRNAs.**

| miRNA | Product code | miRNA sequence (5'-3') |
|---|---|---|
| **hsa-miR-378a-3p** | MS00006909 | ACUGGACUUGGAGUCAGAAGG |
| **hsa-miR-202-5p** | MS00009044 | UUCCUAUGCAUAUACUUCUUUG |
| **bta-miR-21-5p** | MS00044758 | UAGCUUAUCAGACUGAUGUUGA |
| **bta-miR-126-3p** | MS00050211 | CGUACCGUGAGUAAUAAUGCG |
| **hsa- miR-142-5p** | MS00006671 | CAUAAAGUAGAAAGCACUACU |
| **bta-miR-222** | MS00051058 | AGCUACAUCUGGCUACUGGGU |
| **hsa-miR-155-5p** | MS00031486 | UUAAUGCUAAUCGUGAUAGGGGU |
| **bta-miR-199a-5p** | MS00050869 | CCCAGUGUUCAGACUACCUGUU |
| **hsa-miR-132 -3p** | MS00003458 | UAACAGUCUACAGCCAUGGUCG |
| **hsa-miR-212 -3p** | MS00003815 | UAACAGUCUCCAGUCACGGCC |

| | | |
|---|---|---|
| **hsa-miR-182-5p/bta-miR-182** | MS00008855 | UUUGGCAAUGGUAGAACUCACACU |
| **hsa-miR-183-5p/bta-miR-183** | MS00031507 | UAUGGCACUGGUAGAAUUCACUG |
| **hsa-miR-96-5p/bta-miR-96** | MS00003360 | UUUGGCACUAGCACAUUUUUGCU |
| **RNU6** | MS00033740 | CGCTTCGGCAGCACATATACTA |

## 2.6.5 QPCR analyses of mRNAs

Expression of mRNA transcripts was measured with SensiFAST$^{TM}$ SYBR Lo-ROX Kit (BIO-94005; Bioline Reagents Ltd, UK) on the MX3005P real-time PCR system (Stratagene, La Jolla, CA. USA) following the protocol of manufacturer. Validation of the primers was based on dissociation curve analysis to verify single product of the expected size. A standard curve was used to determine PCR efficiency (> 85%) and the reaction's linear range.

PCR assays were performed in a total volume of 10 µl, containing 2 µl of cDNA template (1:16 for each test specific gene (Table 2.6) and 1:100 for reference genes (*18S*), 5µl of SYBR® Green, 0.4 µl of gene-specific forward and reverse primers (final concentration 0.4 µM) and RNase-free water. Thermal profile was as follows: Activation for 2 min at 95°C, followed by 40 cycles of denaturation for 5 seconds at 95°C, annealing for 11 seconds at 60°C and extension for 5 seconds at 72°C, with fluorescence data collection (Figure 2.3). Levels of all transcripts were normalised to levels of *18S*.

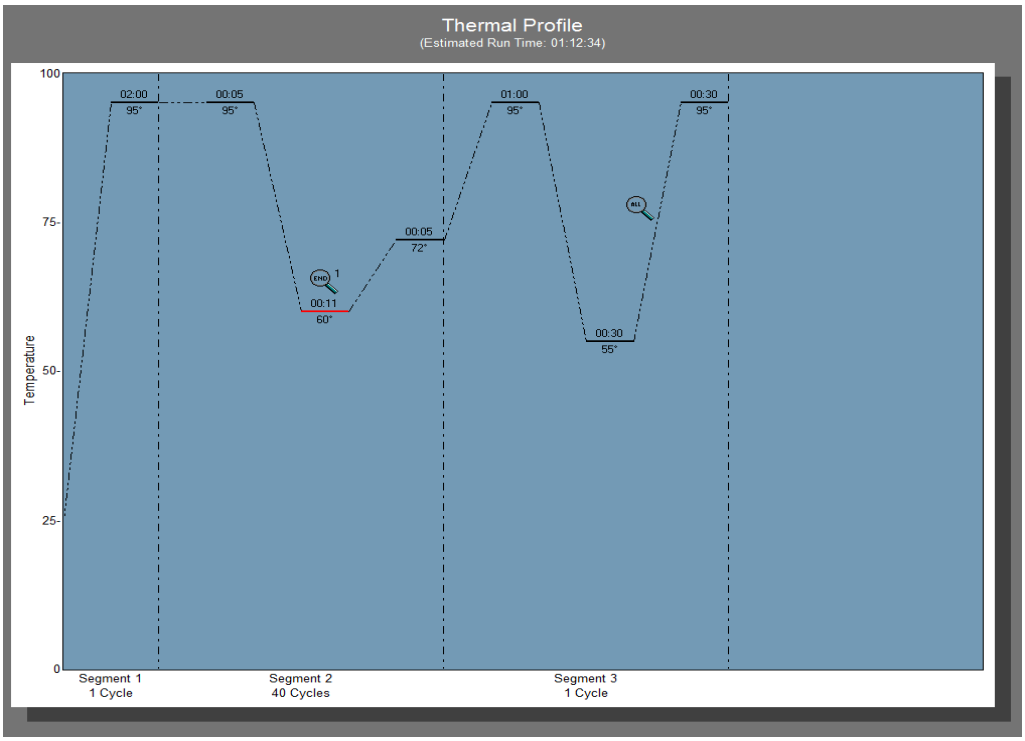


**Figure 2.3 Thermal Profile Setup for qPCR of mRNAs.**

**Table 2.6 Primer pair sequences used for qPCR.**

| Genes | | Sequence (5'-3') | Predicted product size |
|---|---|---|---|
| **18S** | FW | GCTGGCACCAGACTTG | 209 |
| | RV | GGGGAATCAGGGTTCG | |
| **Bovine-FOXO3** | FW | TATGAGTGGATGGTGCGCTG | 96 |
| | RV | TGACAGGTTGTGCCGGATAG | |
| **Bovine- CDKN1A** | FW | GGA GAC CGT GGT TGG GAG A | 89 |
| | RV | CTC AGA CAT GGC ACC TGT GG | |
| **Bovine- FOXO1** | FW | AGTGGATGGTCAAGAGCGTG | 155 |
| | RV | GAGCATCCACCAGGAGCTTT | |
| **Bovine- ADCY6** | FW | CTGGGGCTCGTTTATCTGGT | 157 |
| | RV | TGTATTTGAGTGCCACCCTCC | |

| | | | |
|---|---|---|---|
| **Bovine- HBEGF** | FW | GGAGGAGCGTGGGAAAAGAA | 168 |
| | RV | TGGCACCTCTCTCCGTGATA | |
| **Bovine- CASP3** | FW | GAGGCAGACTTCTTGTACGCA | 101 |
| | RV | AGCATCTCACAAAGAGCCTGG | |
| **Bovine- ECT2** | FW | TCGACATGTAGCCAACACCAT | 193 |
| | RV | TCGGAGAGCTCTTTTTGGAGT | |
| **Bovine- CYP27A1** | FW | GTTGGTGCAAGGCTACGTTC | 95 |
| | RV | TCTGAGGCCCTACTCGGTTT | |
| **Bovine- FRS2** | FW | GCCTCCGACGCTATGGTTAT | 107 |
| | RV | TTCTTCTGCACGAGCACACT | |
| **Bovine- ACVR1** | FW | TTGGGCCTTTGGACTTGTCT | 107 |
| | RV | TTGGGTCATTGGGAACCACA | |
| **Bovine- MMP9** | FW | CCATTAGCACGCACGACATC | 125 |
| | RV | GAAGGTCACGTAGCCCACAT | |
| **Bovine- RASA1** | FW | GAACTGCGGACGCTCAGTAA | 184 |
| | RV | ACTGATGTGATTTACCATTTTGGG | |
| **Bovine- HSD3B1** | FW | GCGTTTCTCAGTGCTCAGATTT | 195 |
| | RV | TCAGCTTGATCTTGCTCTGGA | |
| **Bovine- CD144** | FW | ACAGGGACACCTTCACCATC | 85 |
| | RV | ATGCGTTCATAGTCCAGGGG | |
| **Bovine-StAR** | FW | TGCCGGAAGCTCCTACAGAC | 184 |
| | RV | GTCGCTGTAGAGAGGGTCTTC | |
| | | | |

| | | | |
|---|---|---|---|
| **Human-ADCY6** | FW | ATGACCTACTGCTTGGCGTC | 120 |
| | RV | ACACCAGCAGAATCACAGGG | |
| **Human-FOXO1** | FW | TCTACGAGTGGATGGTCAAGAG | 114 |
| | RV | TGAACTTGCTGTGTAGGGACAG | |
| **Human GAPDH** | FW | GTTCGACAGTCAGCCGCATC | 172 |
| | RV | TGAAGGGGTCATTGATGGCA | |

## 2.7 Western blotting

After transfection, total protein from ovarian cells was extracted by adding sample buffer at 60ºC to each culture plate well then cells were scraped off with a pipette tip and the extracts combined and stored at -80. Samples were heated for 5 min at 95ºC then separated on 12% SDS-PAGE gel (Appendix I) with Colorplus prestained protein marker (P7711S; Bio-Rad. UK) as loading ladder and run in 1x running buffer on Mini Trans-Blot® Cell (Bio-Rad. UK) at 150 volts for 90 min. The separated proteins were transferred to a 0.2µM Nitrocellulose membrane (10600004; GE healthcare. UK) using Trans-Blot® SD Semi-Dry Transfer Cell (BioRAD. UK) at 15 volt for 60 min in transfer buffer. The membrane was washed with TBST for 5 min and incubated in the blocking solution for 1 h at RT on a rocker. After washing, the blot was incubated with FOXO1 antibody diluted at 1:500 (#2880; Cell Signalling. USA) and β-Tubulin antibody (as control) diluted at 1:1000 (#2146; Cell Signalling. USA) overnight at 4°C on a rocker. After probing with primary antibody, the membrane was washed twice with TBST for 5 min each then incubated with IRDye®680RD Donkey anti-rabbit IgG antibody (926-68073; LI-COR. UK)

in 1:10000 at RT for 1 h, followed by several washes with TBST for 5 min each. β-Tubulin was used as internal control. Visualisation and quantification of the bands was carried out using LI-COR Odyssey infrared imaging scanner and Image Studio Lite 5.0, respectively.

## 2.8 Monitoring cell proliferation

Measurement of Cell-Electrode Impedance was carried out using the xCELLigence Real-Time Cell Analysis (RTCA) system 96 well-E-Plate (ACEA Biosciences. USA) according to manufacturer protocol. Firstly, 100 µL of prepared Mc Coy´ s medium was added to each well to obtain baseline background readings. Granulosa cells in 100 µl volume were added and mixed with reciprocal shaking. The E-Plates were placed on the device station (in the 37°C $CO_2$ incubator). The cells were allowed to settle to the bottom of the wells (approx 30 min) before starting the reading. Cells were left to grow overnight then transfections were performed as described in section 2.1.5. The cell impedance was monitored every 30 min and converted to cell index (CI) values by computing method.

## 2.9 Apoptosis assays

### 2.9.1 Caspase activity Assay

Caspase activity was detected using Caspase-Glo 3/7 assays (G8091; Promega. UK) following the manufacturer´s recommendations. Bovine and human ovarian cells were plated in 96-well plates at density of $2x10^4$ per well and transfected one day later (section 2.1.5). After a further 24 h, cells were deprived of serum for 12 h then apoptosis activity was assayed by adding Caspase-Glo 3/7 reagent to each well at a ratio 1:1, and the content of the well was gently mixed and incubated at RT for 2 h. Plates were read in a luminometer (Synergy BioTek micro plate reader. UK). Background signal was obtained from wells containing culture medium only and subtracted from test sample values. Measurements were performed in triplicate.

### 2.9.2 Annexin V staining

Cell death was also evaluated using Annexin-V-Fluos staining kit (11858777001; Roche. UK) following the manufacturer´s instructions. Annexin-V binds to phosphatidyl serine in the outer membrane of apoptotic cells and propidium iodide (PI) stains the DNA of the necrotic cells. The hLGCs were grown on coverslips for 24 h post transfection (section 2.1.5). After removing medium, Annexin-V and PI were added and incubated for 15 min at RT in the dark. Samples were analysed with a Leica DMLB fluorescence microscope.

### 2.9.3 Trypan blue staining

Trypan blue was used to determine the viability of the hLGCs after transfection with miRNA inhibitors as described in section 2.1.5. The experiments were repeated three times.

## 2.10 Quantification of steroid hormones levels in culture media

### 2.10.1 Progesterone

Concentration of progesterone was detected directly from bovine and human cultured media using Coat-A-Count radioimmunoassay kit (Siemens Healthcare Diagnostics Inc. USA) following manufacturer´s instructions. Media samples from bovine non-luteinised and FSK-treated granulosa were diluted 1:100 in PBSG and 1:2000, respectively and human luteinised granulosa cells samples were diluted 1:2000 while samples from bovine luteal cells were diluted 1:100 in PBSG. 100 µl of sample was added to polypropylene tubes coated with antibody then 1 ml of $^{125}$I Progesterone was added to each tube and vortexed. Following incubation for 4 h at RT, the tubes were decanted thoroughly, except total count tubes, then counted for 60 seconds on a gamma counter. The results were calculated using logit-log of calibration curve of known standard ranges (0.1- 40 ng/ml). The assay sensitivity and coefficient of variance (CV) were 0.01 ng/ml and 4.32%, respectively.

### 2.10.2 Oestradiol

Oestradiol levels in the hLGCs were measured by DIAsource E2-RIA-CT kit (DIAsource ImmunoAssays S.A, Belgium). Cultured media from human luteinised granulosa cells was diluted 1:1 in PBSG. Fifty microlitres of each standard and sample were dispensed in duplicates into antibody-coated tubes. Five hundred µl of $^{125}$I labelled E2 were added and mixed before incubation for 4 h at RT. Then tubes were decanted and washed with 1x wash solution (TRIS-HCl) except total count tubes, then counted for 60 seconds on a gamma counter. The results were calculated using logit-log of calibration curve of known standard ranges (9-3900 pg/ml). The assay sensitivity and coefficient of variance (CV) were 1.5 pg/ml and 2.64% respectively.

## 2.11 Statistical analyses

Results from all experiments were analysed using one-way or two-way ANOVA followed by Tukey's multiple comparison tests in Minitab17 statistical software. Normality was determined using Kolmogorov-Smirnoff test ($P<0.05$) and non-normal data or data with unequal variance were log-transformed prior to statistical analysis. Three to six biological replicates were analysed in all experiments.

# Chapter 3

# Results

# Chapter 3: Results

## 3.1 Characterisation of miR-212-132 and miR-183-96-182 clusters

Following on results of preliminary microarray analyses from our laboratory showing upregulation of miR-212-132 and miR-183-96-182 in the CL, the aims were examining the sequences and genomic location of these two miRNA clusters. After that, proceeded to the identification of computationally-predicted and experimentally-validated miRNA target genes. Finally, before studying the biological function of these miRNAs, ISH and FACS were used to identify which luteal cell types expressed miR-96 and miR-132 using:

### 3.1.1 miRNA sequences and genomic organisation

Firstly, miRBase v21 was utilised to identify the primary and mature sequences of miR-212-132 and miR-183-96-182 (Figure 3.1.A.B). The bovine miR-132 sequence identified by microarray (bta-miR-132) is homologous to hsa-miR-132-3p. The hsa-miR-132-5p sequence was also identified (with less abundance; Table 1.7) although it is not registered as a bovine sequence in miRBase v21. For miR-212, the sequence identified by microarray corresponds to hsa-miR-212-3p, which is not present for bovine in miRBase. The miRNAs (miR-212-3p and miR-132-3p) share the same primary transcript and their mature sequences have same 'seed' region (nucleotide positions 2-8; Figure 3.1.B), as result of which they may target the same mRNAs, although with variable affinities due to differences on their 3' ends. The three miR-183-96-182 cluster miRNAs identified by microarray are homologous to the human -5p sequences. While miR-96 has the same seed region as miR-182, miR-183 has a single nucleotide different in its seed sequence (Figure 3.1.B). The Ensembl algorithm shows that miR-212-132 and miR-183-96-182 clusters that are intergenic and highly conserved across species including human and cows (Figure 3.1.C).

**A** **Stem-loop primary miRNA (pri-miRNA)**

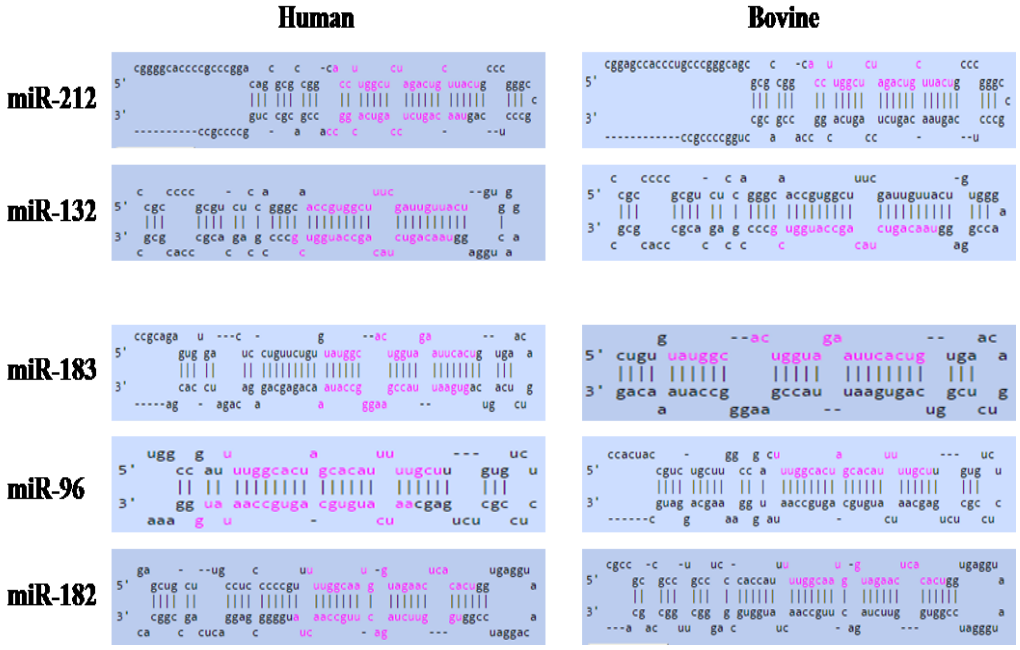


**B**

**miR-183-96-182 cluster**

**miR-183**: 5'-UAUGGCACUGGUAGAAUUCACU -3' UAUGGCACUGGUAGAAUUCACU 22

**miR-96**: 5'-UUUGGCACUAGCACAUUUUUGCU -3' UUUGGCACUAGCACAUUUUUGCU 23

**miR-182**: 5'-UUUGGCAAUGGUAGAACUCACACU -3' UUUGGCAAUGGUAGAACUCACACU 24

**miR-212-132 cluster**

**miR-212**: 5'-UAACAGUCUCCAGUCACGGCC -3' 21 ACCUUGGCUCUAGACUGCUUACU 23

**miR-132**: 5'-UAACAGUCUACAGCCAUGGUCG -3' 22 UAACAGUCUACAGCCAUGGUCG 22

**C**

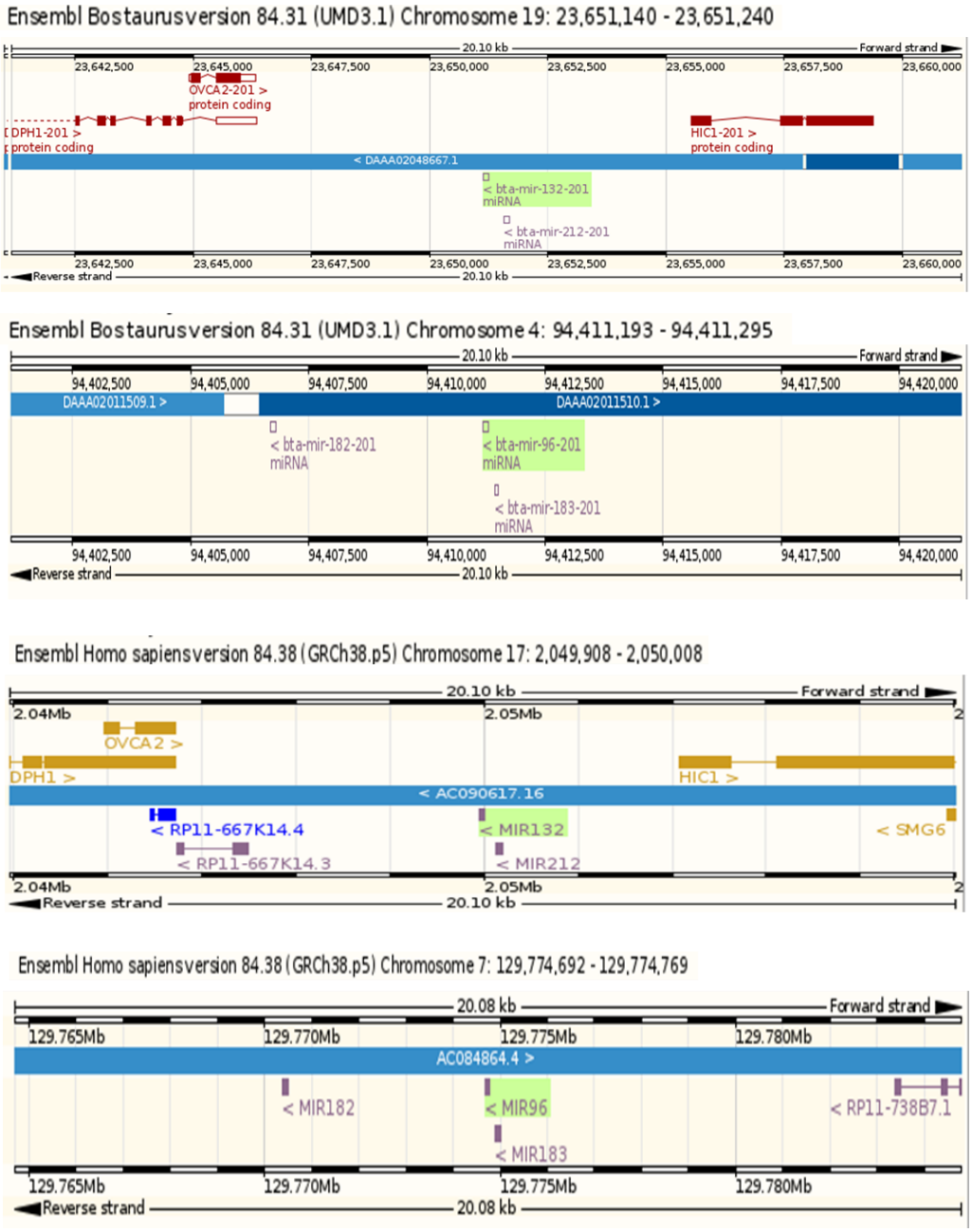


**Figure 3.1 miR-212-132 and miR-183-96-182 sequences and genomic organisation. A) The stem-loop sequences of primary miR-212, miR-132, miR-183, miR-96, miR-182. The region which will become mature miRNA is shaded in pink. B) Mature sequences of miR-212-132 and miR-183-96-182 clusters in human (hsa) and bovine (bta) sourced from miRBase (v21). Nucleotide differences between the two species are showed in red. C) Genomic organisation of miR-132 and miR-96 clusters in Bovine and Human (sourced from Ensembl (v84.31)).**

## 3.1.2 Identification of gene and cell function targets of the miR-212-132 and miR-183-96-182 clusters

### 3.1.2.1 Target prediction

To gain insight into potential functions of the two miRNA clusters during luteinisation, different algorithms were used to identify gene targets of these miRNAs. TargetScan 6.2 and 7.0 provide predicted biological targets of miRNAs based on the presence of sequences in a 3'UTR that are complementary to 8mer, 7mer and 6mer sequences within the seed region of a miRNA. Moreover, TargetScan groups miRNAs that have similar seed sequences into families, different from the families named in miRBase 21. Because computational miRNA target prediction can yield a high number of false positives and false negatives (Agarwal et al., 2015, Nam et al., 2014), predicted targets were chosen with conserved sites, which provides increased confidence. I obtained a total of 3042 predicted targets of miR-212-132-3p and miR-183-96-182-5p, of which 27 bovine genes were simultaneous targets of at least 4 of these miRNAs (Table 3.1). Experimental validation is eventually essential to confirm miRNA-target interactions predicted computationally. The miRTarBase 6.2 and TarBase 7.0 databases provide lists of experimentally validated miRNA: target interactions (MTIs) for different species excluding cows. Targets are listed based on validation methods that provide direct (reporter assay, western blot and qPCR) or indirect (Microarray, NGS, pSILAC and other) evidence of MTIs. Both databases are comprehensive, manually curated and provide published references. A total of 174 directly validated (strong evidence) gene targets in human, mouse and rat were identified, 27 of which were common to ≥ 2 of the miRNAs in the two clusters (Table 3.2).

**Table 3.1 List of top up-regulated miRNAs during the follicle-luteal transition in the cow and their predicted targets obtained from Targetscan 6.2 and 7.0 (only genes targeted by ≥4 miRNAs are shown).**

| Gene symbol | Gene name | miR-212 | miR-132 | miR-183 | miR-96 | miR-182 |
|---|---|---|---|---|---|---|
| ACVR2B | activin A receptor, type IIB | ■ | ■ | ■ | ■ | |
| AGO2 | argonaute RISC catalytic component 2 | | ■ | ■ | ■ | ■ |
| AZIN1 | antizyme inhibitor 1 | | ■ | ■ | ■ | ■ |
| BACH2 | BTB and CNC homology 1, basic leucine zipper transcription factor 2 | ■ | | ■ | ■ | ■ |
| BNC2 | basonuclin 2 | ■ | ■ | ■ | ■ | ■ |
| CELF2 | CUGBP, Elav-like family member 2 | | ■ | ■ | ■ | ■ |
| CELSR3 | cadherin, EGF LAG seven-pass G-type receptor 3 | | ■ | ■ | ■ | ■ |
| CTDSP1 | CTD (carboxy-terminal domain, RNA polymerase II, polypeptide A) small phosphatase 1 | ■ | | ■ | ■ | ■ |
| DAAM1 | dishevelled associated activator of morphogenesis 1 | | ■ | ■ | ■ | ■ |
| DAB1 | Dab, reelin signal transducer, homolog 1 (Drosophila) | | ■ | ■ | ■ | ■ |
| DGCR2 | DiGeorge syndrome critical region gene 2 | ■ | | ■ | ■ | ■ |
| DOCK4 | dedicator of cytokinesis 4 | ■ | ■ | ■ | ■ | ■ |
| EI24 | etoposide induced 2.4 | ■ | | ■ | ■ | ■ |
| FOXO1 | forkhead box O1 | | ■ | ■ | ■ | ■ |
| GABPB2 | GA binding protein transcription factor, beta subunit 2 | ■ | ■ | ■ | ■ | |
| GAN | Gigaxonin | ■ | | ■ | ■ | ■ |
| GMFB | glia maturation factor, beta | | ■ | ■ | ■ | ■ |
| HBEGF | heparin-binding EGF-like growth factor | | ■ | ■ | ■ | ■ |
| KAT7 | K(lysine) acetyltransferase 7 | ■ | ■ | | ■ | ■ |
| MECOM | MDS1 and EVI1 complex locus | | ■ | ■ | ■ | ■ |
| | | | ■ | ■ | ■ | ■ |

| | | | | | | |
|---|---|---|---|---|---|---|
| PAIP2 | poly(A) binding protein interacting protein 2 | | | | | |
| QKI | QKI, KH domain containing, RNA binding | | | | | |
| RDX | Radixin | | | | | |
| SCN3A | sodium channel, voltage-gated, type III, alpha subunit | | | | | |
| SLC8A1 | solute carrier family 8 (sodium/calcium exchanger), member 1 | | | | | |
| TCF7L2 | transcription factor 7-like 2 (T-cell specific, HMG-box) | | | | | |
| TMEM178B | transmembrane protein 178B | | | | | |

**Table 3.2 List of experimentally validated targets of ≥2 miRNAs (sourced from miRTarBase 6.2 and TarBase 7).**

| Gene symbol | Gene name | miR-212 | miR-132 | miR-183 | miR-96 | miR-182 |
|---|---|---|---|---|---|---|
| Ache | acetylcholinesterase | | | | | |
| ADCY6 | adenylate cyclase 6 | | | | | |
| BDNF | brain-derived neurotrophic factor | | | | | |
| BRCA1 | breast cancer 1 | | | | | |
| CCNA2 | cyclin A2 | | | | | |
| CCNB1 | Cyclin B1 | | | | | |
| CDH1 | Cadherin-1 | | | | | |
| CDKN1A | Cyclin-dependent kinase inhibitor 1A (p21, Cip1) | | | | | |
| Clic5 | chloride intracellular channel 5 | | | | | |
| Cy2e1 | cytochrome P450, family 2, subfamily e, polypeptide 1 | | | | | |
| Ep300 | E1A binding protein p300 | | | | | |
| FOXO1 | forkhead box O1 | | | | | |
| | | | | | | |

| | | | | | | |
|---|---|---|---|---|---|---|
| FOXO3 | Forkhead box O3 | | | | | |
| GSK3B | Glycogen synthase kinase 3 beta | | | | | |
| IRAK4 | Interleukin-1 receptor-associated kinase 4 | | | | | |
| MECP2 | Methyl CpG binding protein 2 | | | | | |
| MITF | Microphthalmia-associated transcription factor | | | | | |
| Mmp9 | Matrix metallopeptidase 9 | | | | | |
| PDCD4 | Programmed cell death 4 | | | | | |
| Pten | phosphatase and tensin homolog | | | | | |
| Rasa1 | RAS p21 protein activator (GTPase activating protein) 1 | | | | | |
| RB1 | Retinoblastoma 1 | | | | | |
| RECK | Reversion-inducing-cysteine-rich protein with kazal motifs | | | | | |
| SMAD4 | SMAD family member 4 | | | | | |
| SNAI2 | Snail family zinc finger 2 | | | | | |
| ZEB1 | Zinc finger E-box binding homeobox 1 | | | | | |
| ZEB2 | Zinc finger E-box binding homeobox 2 | | | | | |

### 3.1.2.2 Gene ontology analysis

DIANA-miRPath v3.0 was used for subsequent gene ontology and pathway analysis of experimentally validated miRNA targets. DIANA-miRPath v3.0 integrates Kyoto Encyclopedia of Genes and Genomes (KEGG) pathways as well as GO and GOSlim annotations, allowing functional and biological process of miRNAs and miRNA combinations using all datasets. Gene and miRNA annotations originate from Ensembl and miRBase, respectively (Vlachos et al., 2015). Using categories and pathways union options I identified all the pathways significantly targeted by miR-212, miR-132, miR-183, miR-96 and miR-182.

Conservative statistics were used (DAVID's EASE score), the Fisher's ExactTest, EASE score and False Discovery Rate to rank gene subsets by significance and to control error rate due to multiple comparisons.

Biological and molecular pathways enriched among miRNA targets as shown in Figure 3.2.A.B. Among these, FoxO signalling pathway is common to miR-182, miR-96 and miR-132 (p-value = 0.001, 0.004, 0.045, respectively) (Figure 3.2.B). Figure 3.3 shows the genes (highlighted in red) which are involved in FoxO signalling. FOXO transcription factors are involved in multiple cell functions including differentiation, proliferation, metabolism and survival (Zhang et al., 2016).

**A**

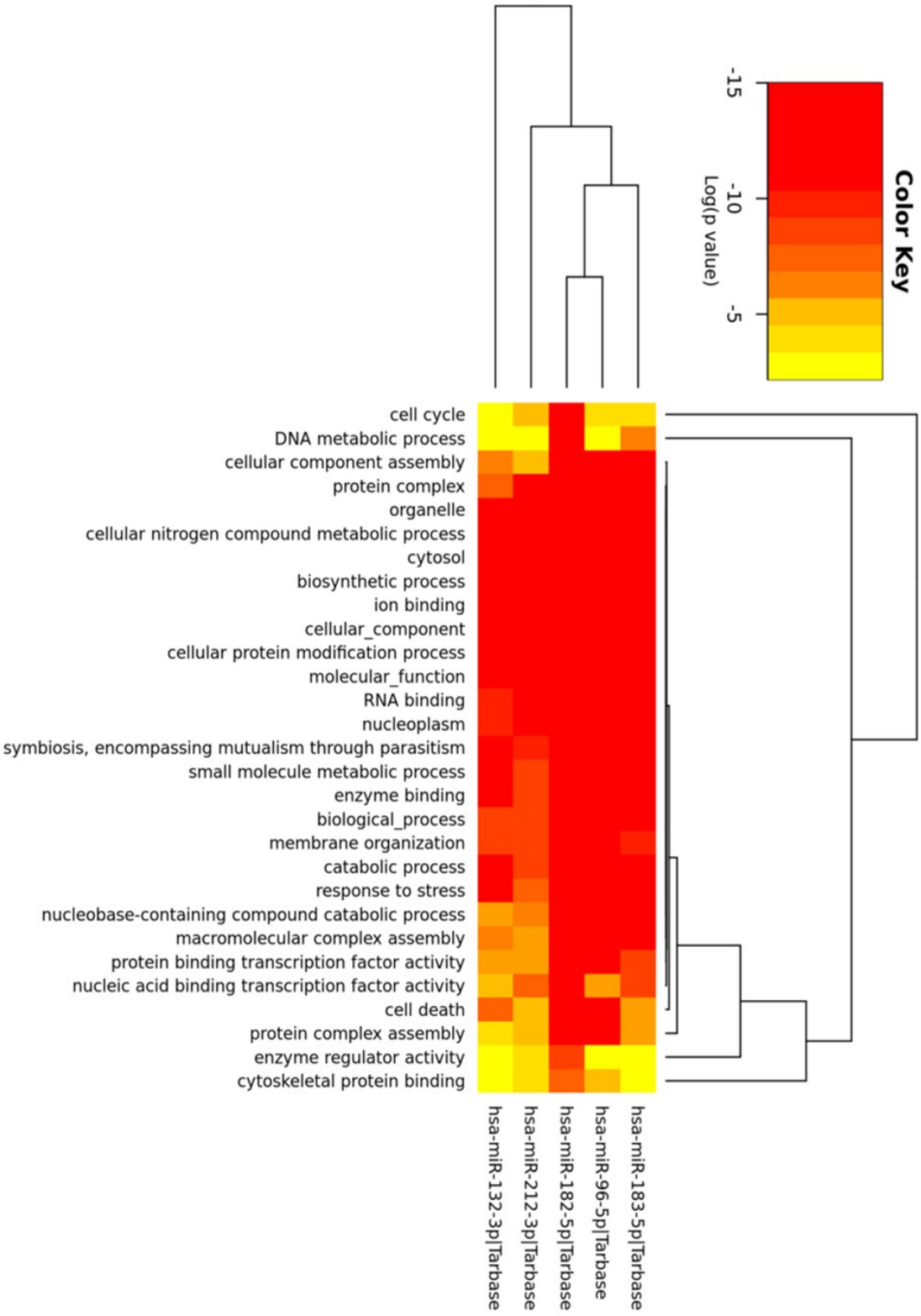
Color Key
Log(p value)
-15
-10
-5
cell cycle
DNA metabolic process
cellular component assembly
protein complex
organelle
cellular nitrogen compound metabolic process
cytosol
biosynthetic process
ion binding
cellular_component
cellular protein modification process
molecular_function
RNA binding
nucleoplasm
symbiosis, encompassing mutualism through parasitism
small molecule metabolic process
enzyme binding
biological_process
membrane organization
catabolic process
response to stress
nucleobase-containing compound catabolic process
macromolecular complex assembly
protein binding transcription factor activity
nucleic acid binding transcription factor activity
cell death
protein complex assembly
enzyme regulator activity
cytoskeletal protein binding
hsa-miR-132-3p|Tarbase
hsa-miR-212-3p|Tarbase
hsa-miR-182-5p|Tarbase
hsa-miR-96-5p|Tarbase
hsa-miR-183-5p|Tarbase

**B**

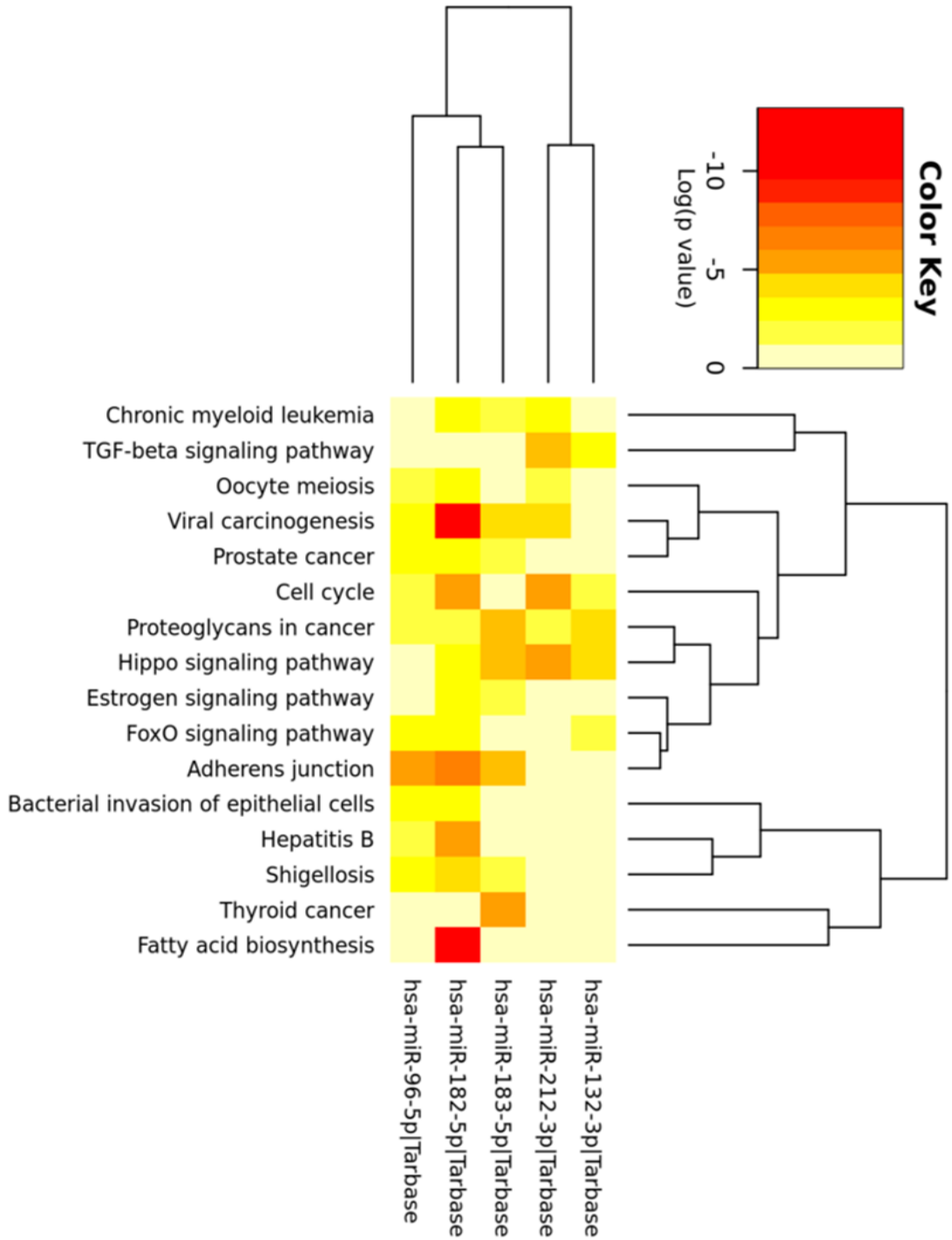


**Figure 3.2 GOSlim categories and KEGG pathways enriched among miRNA targets. A) The heat map depicts the level of enrichment in GO categories among targets of miR-212-132 and miR-183-96-182 clusters. B) Heat map of KEGG pathways targeted by the two miRNA clusters. Heat map was created directly from the DIANA-miRPath v3.0 interface in Homo sapiens.**

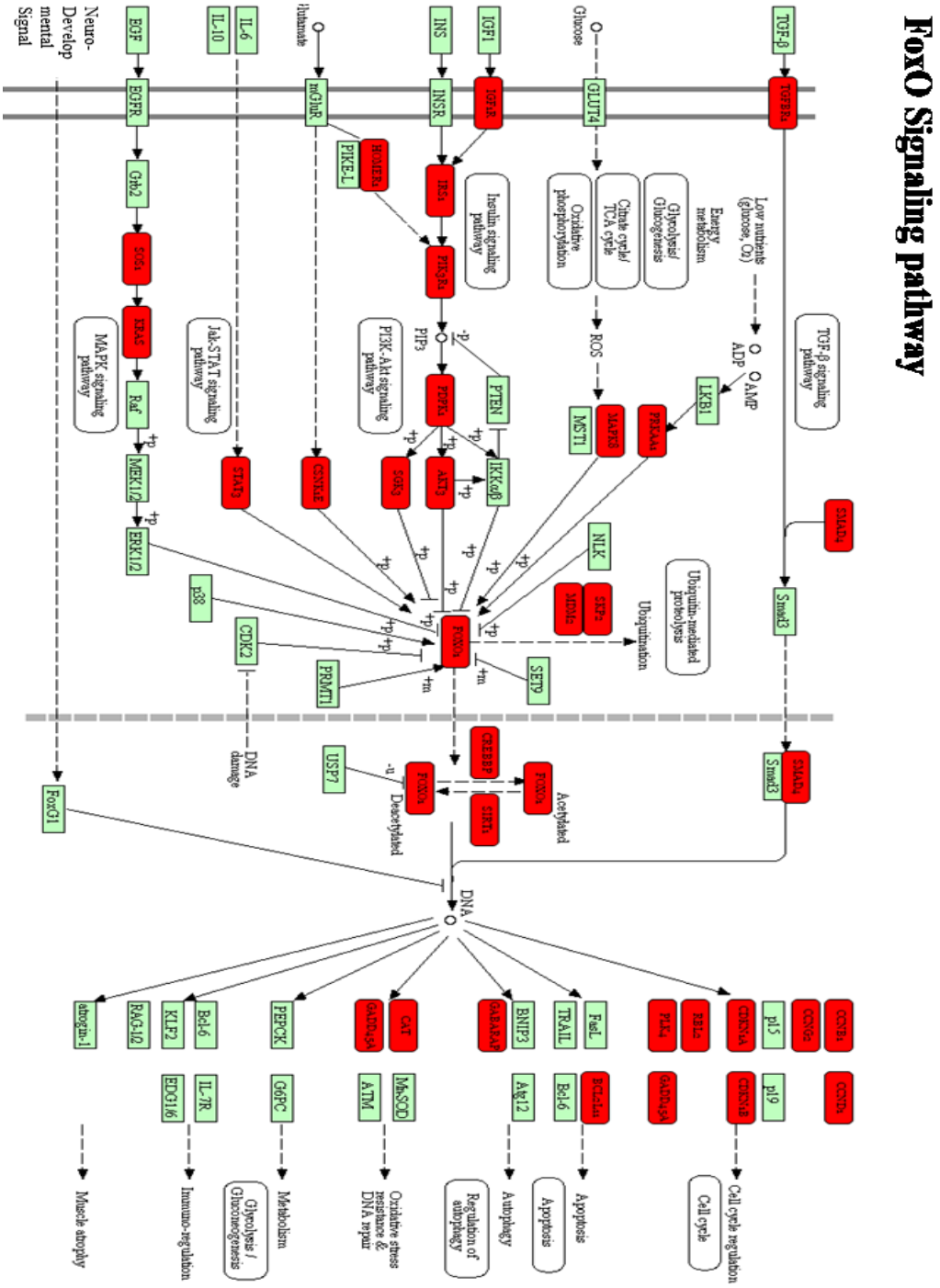


**Figure 3.3 FoxO signalling pathway. Genes that are targets of the miR-212-132 and miR-183-96-182 clusters are highlighted in red (adapted from Diana-mirpath v3.0/pathways).**

### 3.1.2.3 Expression of miRNA target genes during the follicle-luteal transition

Genes targeted by the miR-212-132 and/or miR-183-96-182 would be expected to decrease in expression during luteinisation. To identify candidate gene targets, qPCR analysis was carried out in large steroidogenically active follicles and early corpora lutea from bovine ovaries collected at an abattoir. As expected, CYP19A1 expression was significantly reduced in CL while HSD3β1 was increased in CL as shown in (Figure 3.4.A). A subset of genes was selected among the lists of predicted (HBEGF and ECT2) and validated target genes (FOXO1, ADCY6, MMP9 and CDKN1A) based on their putative involvement in luteinisation (Ovarian Kaleidoscope Database and Genecard**)** (Figure 3.4.B). FOXO1 and ADCY6, two genes that play potential roles in folliculogenesis and luteinisation in mammalian ovaries (Castilho et al., 2014, Liu et al., 2009) were significantly downregulated in early CL relative to large steroidogenically active follicles, consistent with these being targets of miR-132 and/or miR-96 cluster miRNAs.

Figure 3.5.A.B shows the sequences on the 3′-UTR of bovine FOXO1 and ADCY6 that are predicted to be targeted by miR-132 and miR-96 cluster miRNAs.

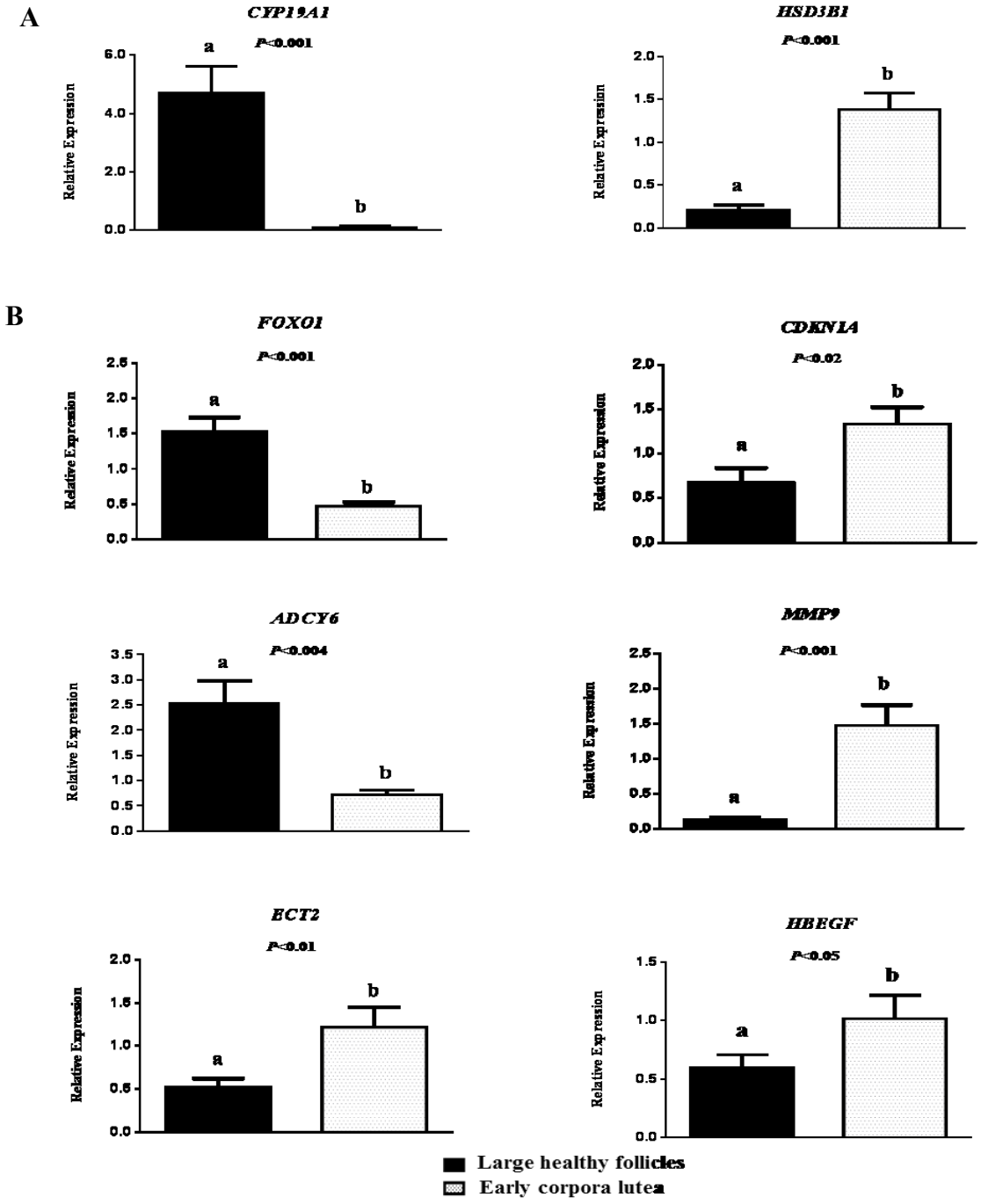


**Figure 3.4 RT-qPCR analysis of early corpora lutea (N= 9) and dominant healthy follicles (12-17 mm diameter; N= 12). A) Expression of the markers of luteinisation, CYP19A1 and HSD3B1. B) Expression profiles of predicted (HBEGF and ECT2) and validated target genes (FOXO1, ADCY6, MMP9 and CDKN1A). Values are presented as mean (± SEM) and were analysed by Student's *t* –test (P< 0.05 and are represented by different letters (a-b).**

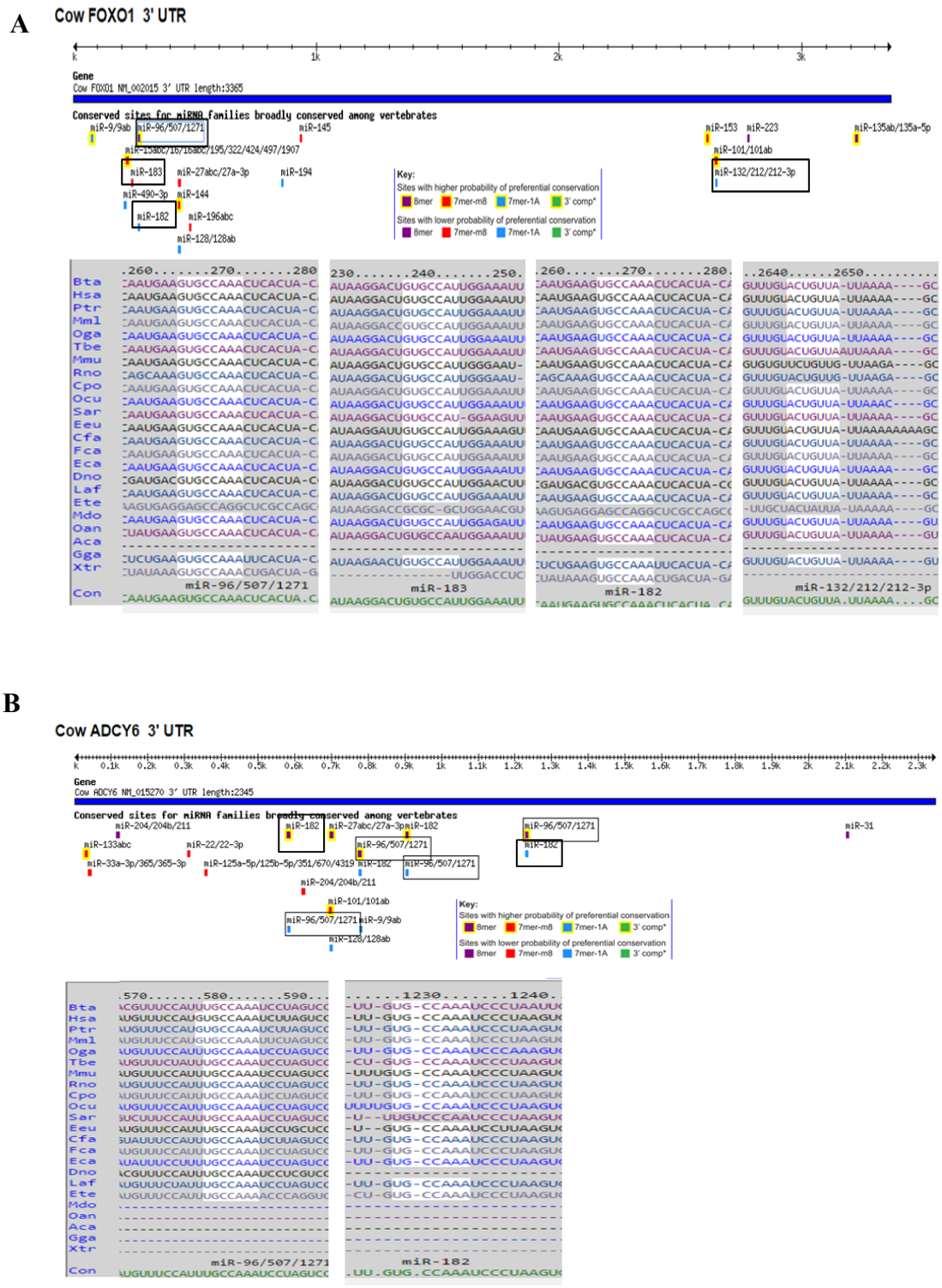


**Figure 3.5 Predicted miRNA binding sites (white) in the 3′-UTR of bovine FOXO1 (A) and ADCY6 (B) obtained from TargetScan 6.2.**

## 3.1.3 Localisation of miR-132 and miR-96 within the bovine CL

### 3.1.3.1 In situ hybridisation

To determine expression of miR-132 and miR-96 in the luteal tissue, ISH was carried out using double Digoxigenin labelled LNA (Locked Nucleic Acid) antisense oligonucleotides (single strand oligonucleotides complementary to endogenous miRNAs). Firstly, the procedure was optimised (Sontakke et al., 2014), afterward I set out to use probes against miR-132 and miR-96 in bovine luteal sections. Firstly, paraffin embedded ovarian section was used but the signal was weak therefore I used frozen luteal section and EDC fixative reagent in order to improve the retention of nucleic acid probes. A homogeneous miR-132 signal was obtained throughout each luteal section (Figure. 3.6. A) while miR-96 probe provided, no signal suggesting expression was very low or the probe was not suitable. RnU6 had again a strong nuclear localisation whereas the negative control gave no signal (Figure. 3.6. B.C).

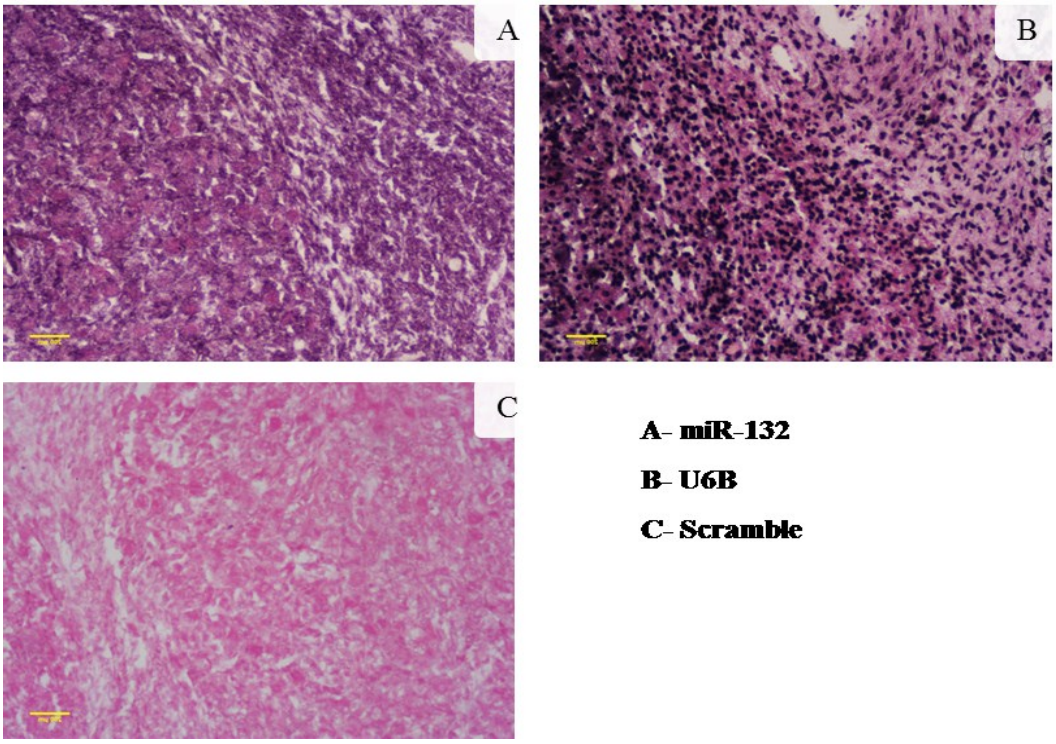


**Figure 3.6 Identification of miR-132 using ISH in frozen bovine ovarian sections. Scale 200 µm and magnification: ×20.**

### 3.1.3.2 Fluorescence-Activated Cell Sorting (FACS) and qPCR

Given that miR-96 could not be detected by ISH, a different approach was attempted using FACS. This also provided the means to confirm the results of ISH in relation to miR-132. Cells from bovine CL were isolated and processed as indicated in section 2.1.3. First I tried to identify antibodies that could be used to distinguish different luteal cell types. Immunofluorescence (IF) and flow cytometry (FC) of cultured luteal cells were used to test antibodies for CD144 (endothelia), CD146 (pericyte), CD45 (leukocyte) and HSD3B1 (steroidogenic luteal cells). Antibodies for CD45, CD146 did not work. However, HSD3B1 was detected in steroidogenic luteal cells by IF (Figure 3.7.B. left panel) although the antibody did not work in FC. Luteal endothelial cells were detected by both IF (Figure 3.7.A, left panel) and FC. Given that the HSD3B1 antibody did not work for FC. Therefore, Nile Red (NR) was used, a dye which binds lipids, as a marker for steroidogenic luteal cells. Concentrations of 1, 5 and 10 µg/ml NR (diluted in PBS) were tried for 15 min follow by RNA extraction and qPCR for 18S. Samples stained with 5 and 10 µg/ml showed no detectable expression of 18S using qPCR, therefore, 1µg/ml of NR was used to stain luteal cells for IF and FACS. Furthermore, immunohistochemistry analysis of unfixed (Figure 3.7.C) and fixed cultured luteal cells (Figure 3.7.C) revealed that most steroidogenic luteal cells contained numerous lipid globules as detected by NR staining.

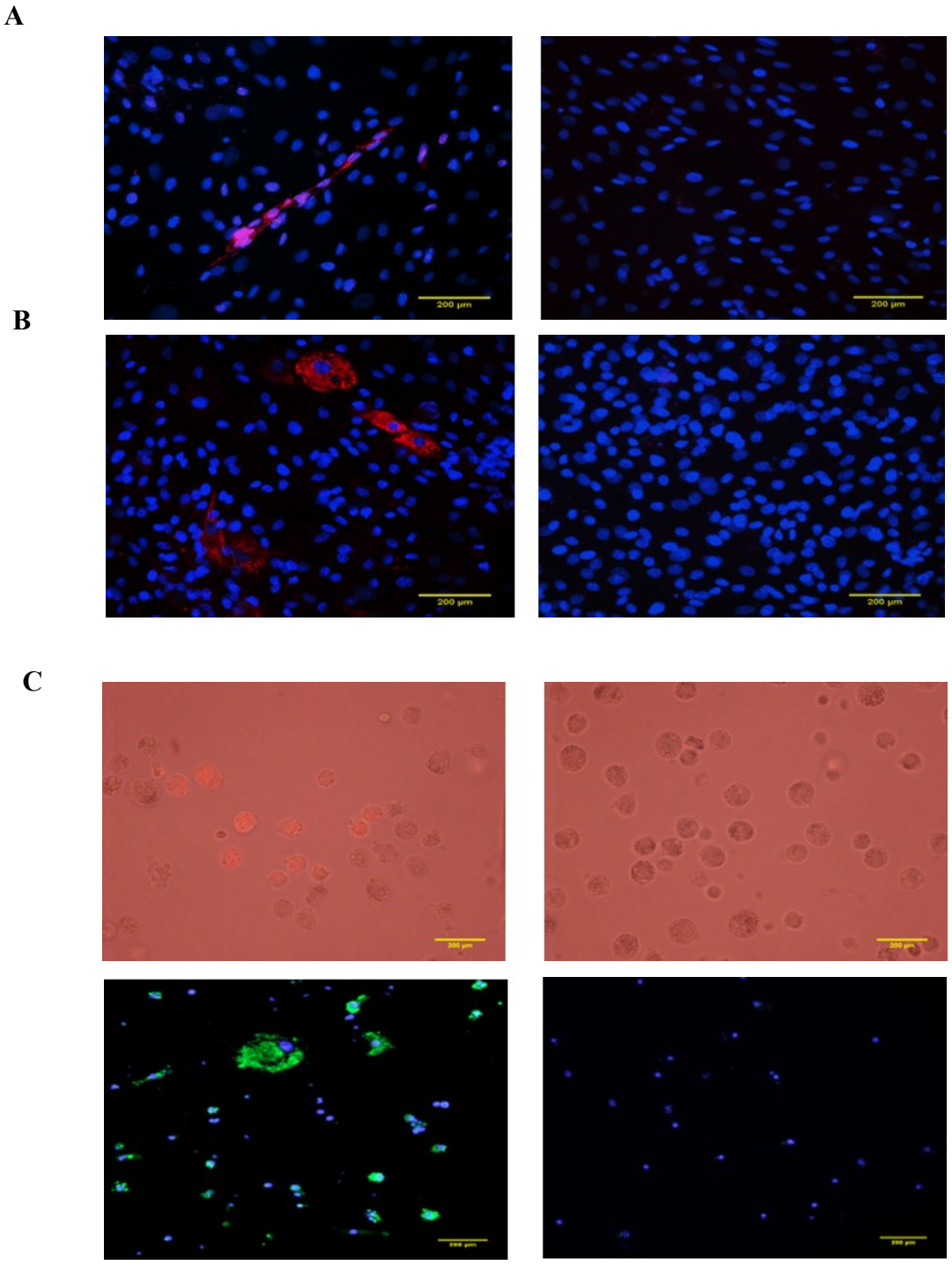


**Figure 3.7 Immunocytochemical detection of CD144, HSD3B1 and NR in cultured bovine luteal cells. Staining for A) CD144 (left panel) and negative control (right panel) and B) HSD3B1 (left panel) and negative control (right panel). Detection of lipid droplets in unfixed (C, upper row) and fixed (C, lower row) cells showed by Nile-Red staining (left panels); non-stained controls are shown in right panels. Scale 200 µm and magnification: ×20.**

FACS was performed on dispersed luteal cells stained with a combination of CD144 antibody and the lipid dye (Nile Red). DAPI was used to exclude dead cells. Single cells were then gated to be subsequently analysed. Figure 3.8.A. shows a dot plot (left) and respective histogram (right) with positive shift of fluorescence for single staining with CD144 (CD144 primary antibody + secondary AF405, in red), while results for negative controls of secondary antibody (AF405, in orange) and primary CD144 alone (in blue) were similar to unstained cells and therefore negative. NR results (figure 3.8.B) also showed positive sift of fluorescence. Figure 3.8.C shows a representative plot used to sort the endothelial cell fraction, CD144+, and the NR+ cells were obtained from CD144 negative fraction, as depicted in the figure. Two wavelengths, 586 and 582 nm were used to distinguish the steroidogenic luteal cells that stained intensely with NR dye. The fraction of cells identified in the figure as NR+ was used for subsequent analysis.

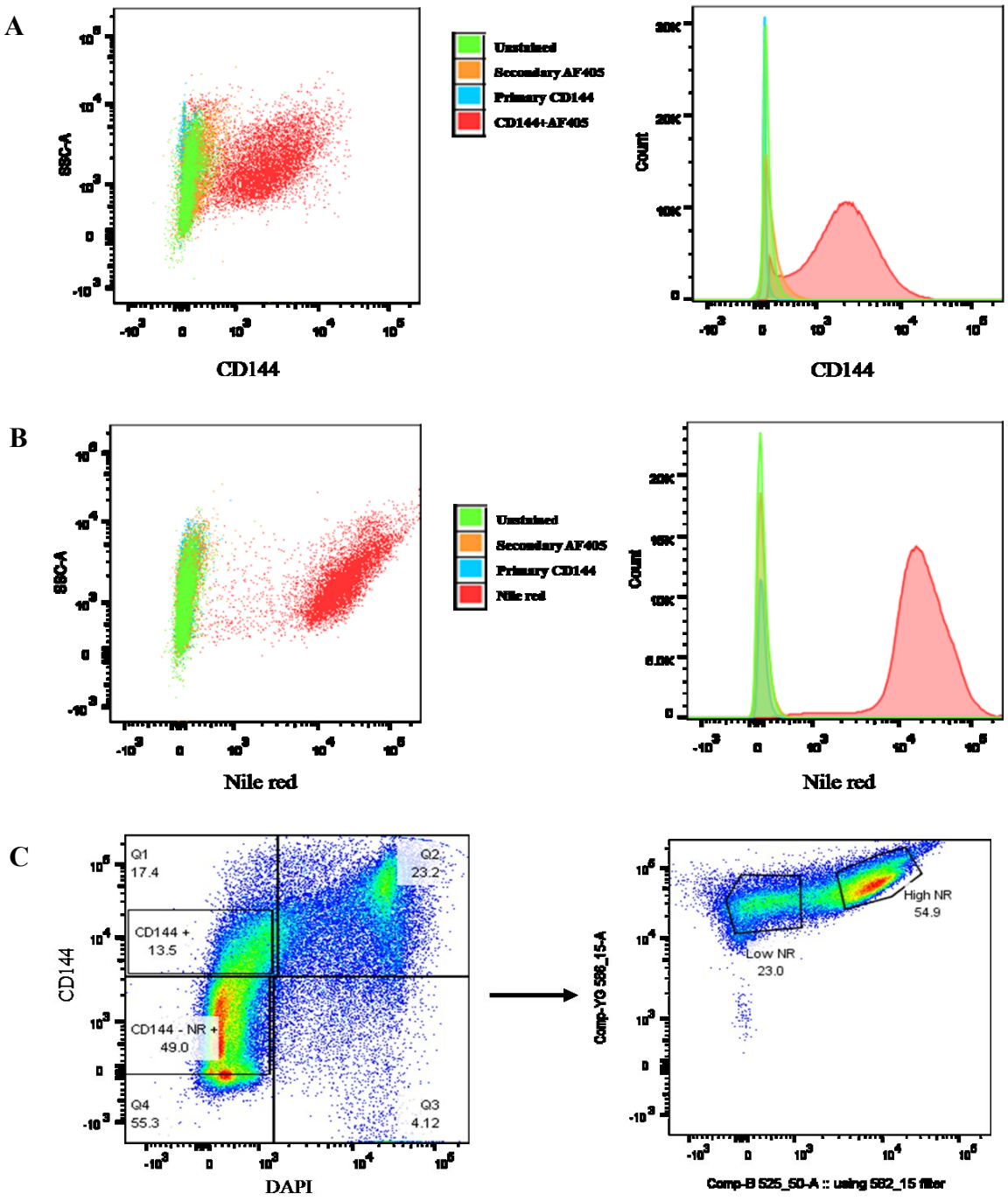


**Figure 3.8 Fluorescence-Activated Cell Sorting analysis of luteal steroidogenic and endothelial cells in bovine CL (n=3 experiments). (A.B) Dot and histogram plots of single-cell to validate CD144 and NR. Cells were incubated with the controls (unstained, primary and secondary antibodies) to determine the gating parameters for sorting. (C). A FACS pseudo-color dot plot showing live cells are first gated, followed by CD144 gating to sort positive endothelial cells then negative CD144 sorted into Nile Red-positive.**

The identity of the sorted cell fractions was confirmed by qPCR of CD144 and HSD3B1 followed by determination of the relative expression of miR-212-132 and miR183-96-182 clusters in these fractions. Results showed that CD144+ fraction cells predominately expressed CD144 but not HSD3B1. Moreover, HSD3B1 expression was higher in Nile red fraction cells compared to CD144+ fraction cells (Figure 3.9.A).

Moreover, miR-126, a marker of endothelial cells was enriched in the CD144+ fraction further confirming this fraction contained mostly endothelial cells (Figure 3.9.B). miR-212-132 and miR-183-96-182 levels were then quantified in both cell fractions. miR-132 was expressed at similar levels in CD144 and NR fractions, consistent with ISH data. miR-212 expression was also similar in the two cell fractions, as expected. In contrast, both miR-96 and miR-183 were expressed at higher levels in CD144 positive cells (Figure 3.9.B).

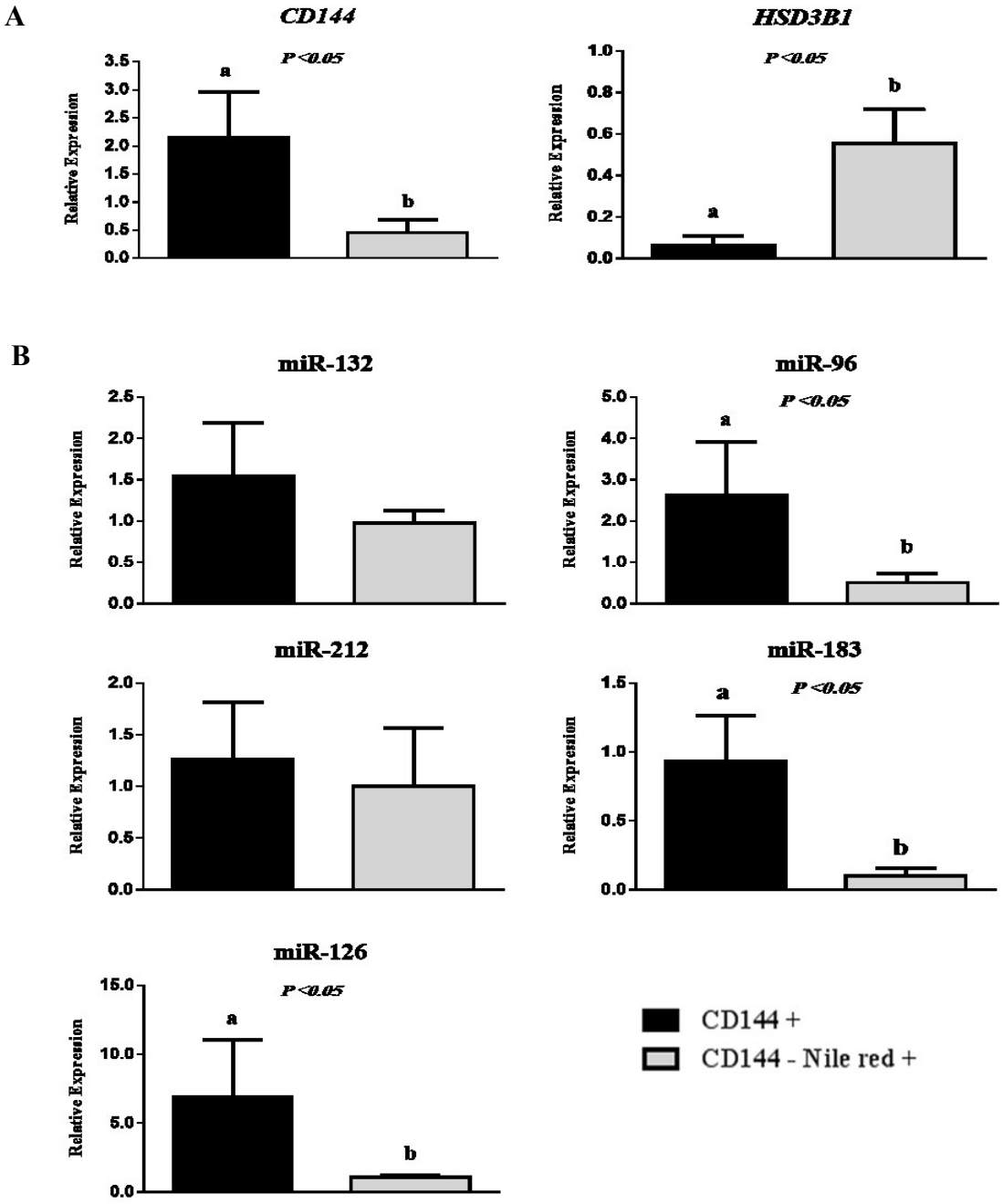


**Figure 3.9 Relative expression of mRNAs and miRNAs in luteal cell fractions obtained from FACS (n=3 experiments). Relative levels of A) CD144 and HSD3B1 and B) miRNAs in FACS fractions. Values are presented as mean (□ SEM) and were analysed by Student's t –test (P< 0.05) and are represented by different letters (a-b). Within each experiment gene expression values were normalised to the value in unsorted cells (taken as 1).**

## 3.2 Functional analysis of miRNAs in bovine luteinising granulosa cells

Results from ISH and FACS indicated that miR-132 and miR-96 were expressed in several cell types in CL including steroidogenic cells. Therefore, an in vitro granulosa cell model was firstly used to investigate the effects of these miRNAs during luteinisation.

### 3.2.1 Validation of an in vitro model of bovine granulosa cell luteinisation

Luteinisation in vitro was induced by treating bovine granulosa cell with Forkolin, FCS and Insulin (luteinisation cocktail) to mimic the effects of the LH surge (section 2.1.2). In addition to morphological changes (granulosa cells start to attach and increased in cell size) that are consistent with luteinisation (Meidan et al., 1990) (Figure 3.10.A), differentiating cells showed a significant increase in the expression of HSD3ß1 and progesterone production (markers of luteinisation) on day 2 and 4, as expected (Figure 3.10.B). Moreover, induced luteinisation was associated with a significant up regulation of miR-132, miR-212, miR-96 and miR-183 (miR-182 could not be detected using qPCR) (Figure 3.11), thus replicating changes observed between ex-vivo dominant follicles and early luteal tissues and providing a suitable model to study the roles of these miRNAs (Figure 1.7).

**A**

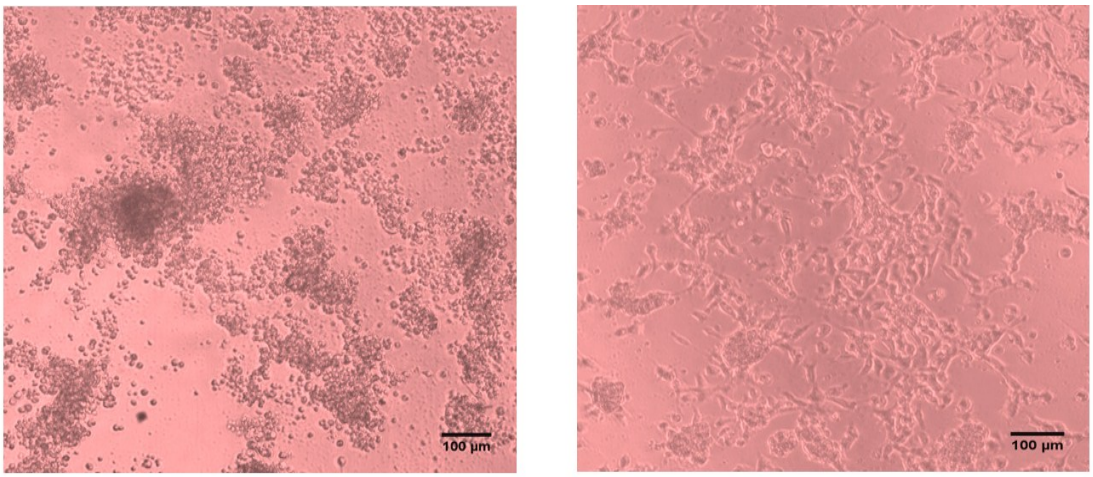


**B**

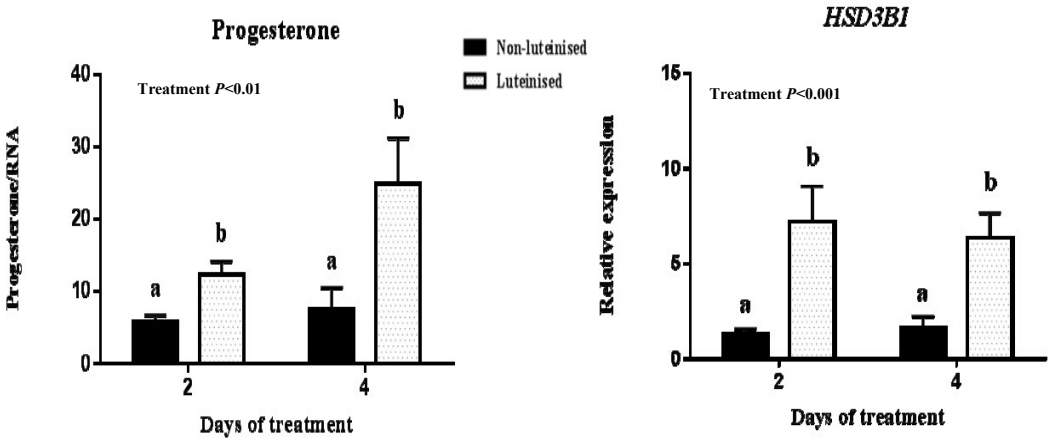


**Figure 3.10 A) Photographs showing in vitro luteinisation of bovine granulosa cells. Granulosa cells from 4-8 mm follicles were cultured for 4 days in a modified McCoy's medium supplemented with forskolin, insulin and FCS or left untreated. Scale 100 µm and magnification: ×10. B) Quantification of progesterone production and HSD3ß1 expression revealed a significant increase during luteinisation (n=4 experiments). Values are presented as mean (± SEM). Differences in mean values were identified using two way ANOVA followed by Tukey's test and are shown by different letters (a-b).**

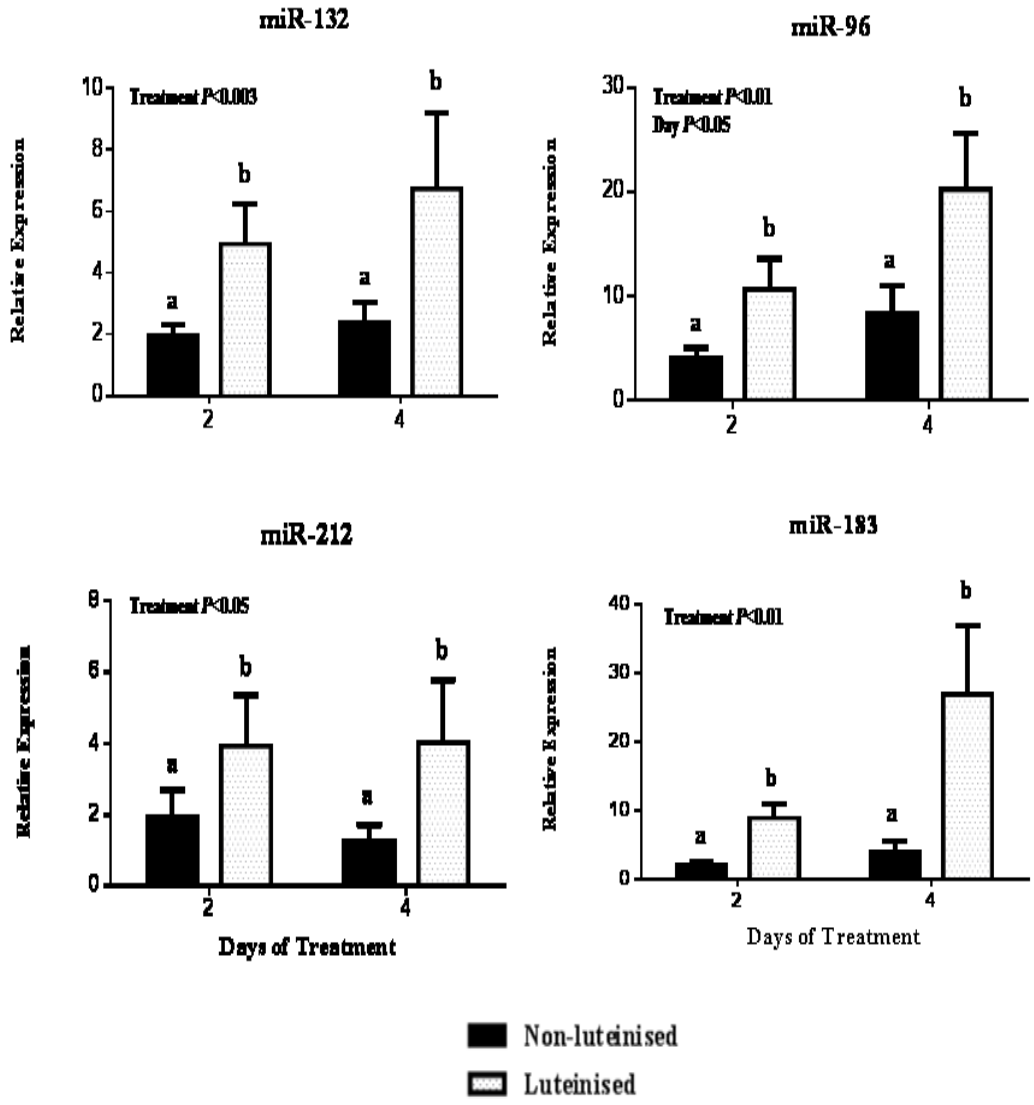


**Figure 3.11 qPCR analysis of miR-212-132 and miR-183-96 clusters during luteinisation in vitro. Expression of all miRNAs was up-regulated in luteinised relative to non-luteinised cells (n=4 experiments). Values are presented as mean (± SEM). Differences in mean values were identified using one way ANOVA followed by Tukey's test and are shown by different letters (a-b).**

### 3.2.2 Manipulation of miRNA levels *in vitro*

To focus on the functional evaluation of miR-132 and miR-96 specifically as these were the most highly expressed miRNAs within each cluster. I first evaluated the effect of their down in cultured granulosa cells using Locked Nucleic Acid (LNA) inhibitors (antisense oligonucleotides complementary to endogenous miRNAs). LNAs are a class of nucleic acid analogs in which the ribose ring is 'locked' with a methylene bridge connecting the 2'-O atom with the 4'-C atom. This modification provides increased sensitivity and specificity, and resistance to enzymatic degradation (Exiqon. Denmark). In addition, mimics (double stranded synthetic miRNAs) (Qiagen. UK) were used to up regulate the levels of miRNAs. Dosages used were based on manufacturer's recommendations and results of previous studies in the laboratory (section 2.1.5). Cells transfected with LNAs were then treated with luteinisation cocktail while cells transfected with mimics remained untreated. As revealed by qPCR analysis, LNAs dramatically lowered the concentrations of each target miRNA on day 2 and 4 after transfection (Figure 3.12.A).

In contrast, transfection of cultured granulosa cells with miR-132 and miR-96 mimics (10nM) resulted in a significant increase in the levels of these miRNAs, as expected (Figure 3.12.B). Moreover, transfection with LNA or mimic specific for miR-132 decreased or increased, respectively, the levels of miR-132 but did not affect miR-96 levels. Similarly, transfection with LNA or mimic specific for miR-96 decreased or increased, respectively, the levels of miR-96 but did not affect miR-132 levels (Figure 3.12.A and B). In addition, there were no effects of LNA or mimics on the levels of mIR-212 and miR-183, except for a reduction in the levels of miR-212 in response to miR-132 LNA (Figure 3.12.A). Interestingly miR-182 could not be detected in cultured granulosa cells using qPCR.

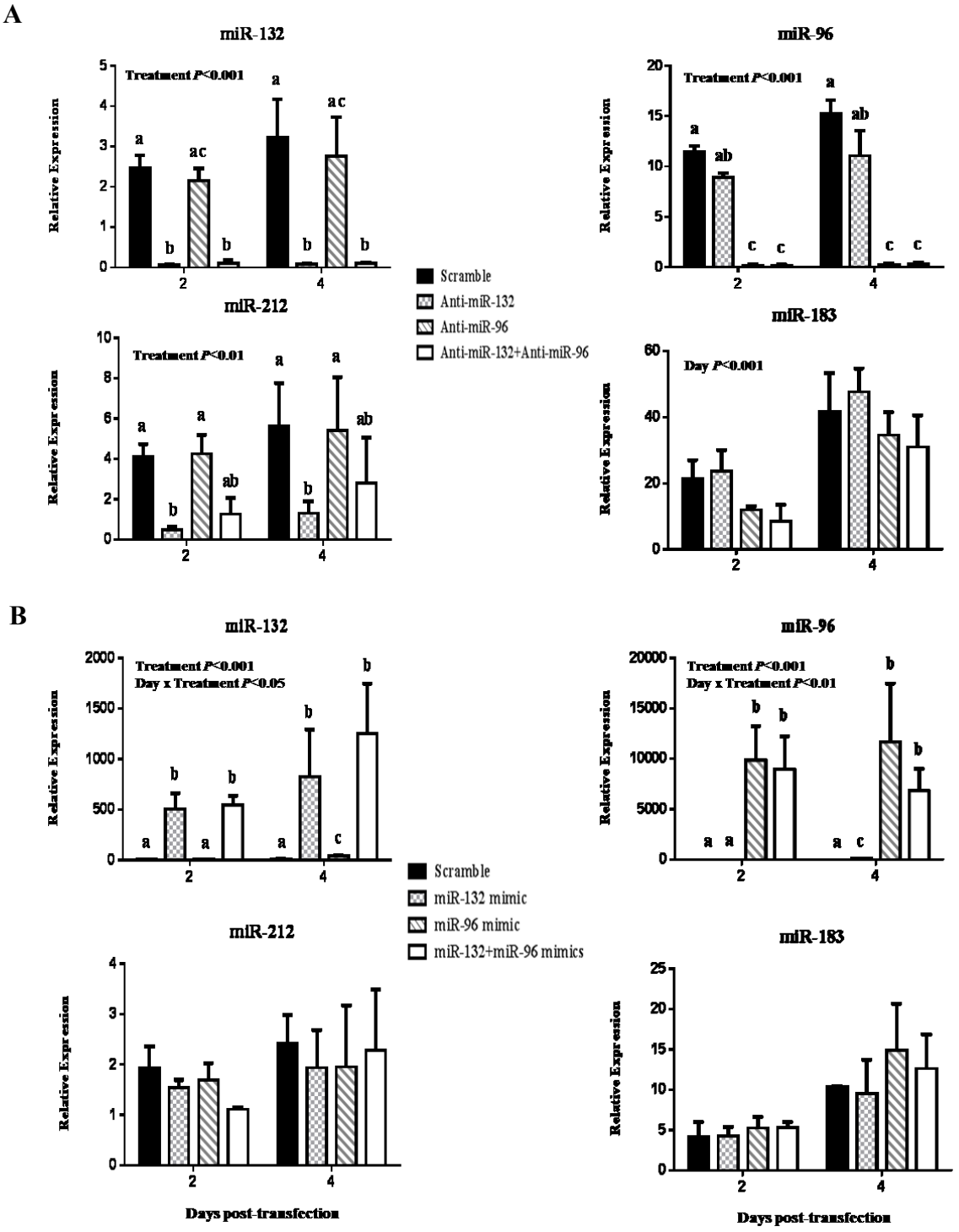


**Figure 3.12 Changes in the expression of miRNAs in the cultured granulosa cells after transfection with specific LNAs (A) and mimics (B) (n=4 experiments). Values are presented as mean (± SEM) and were analysed using two-way ANOVA and Tukey's test. Significant differences are represented by different letters (a-c).**

#### 3.2.2.1 Effects of miRNA over-expression and inhibition on target gene expression in bovine granulosa cells

Unexpectedly, inhibition of miR-132 and miR-96 in luteinising granulosa cells or overexpression of the two miRNAs in undifferentiated cells did not influence mRNA levels of the predicted target genes FOXO1 and ADCY6 (Figure 3.13.A). In fact, the expression of the two genes did not change in non-transfected cells during luteinisation (Figure 3.13.B), which was not consistent with the decrease in mRNA levels of FOXO1 and ADCY6 in corpora lutea relative to large steroidogenically active follicles (Fig 3.4.B).

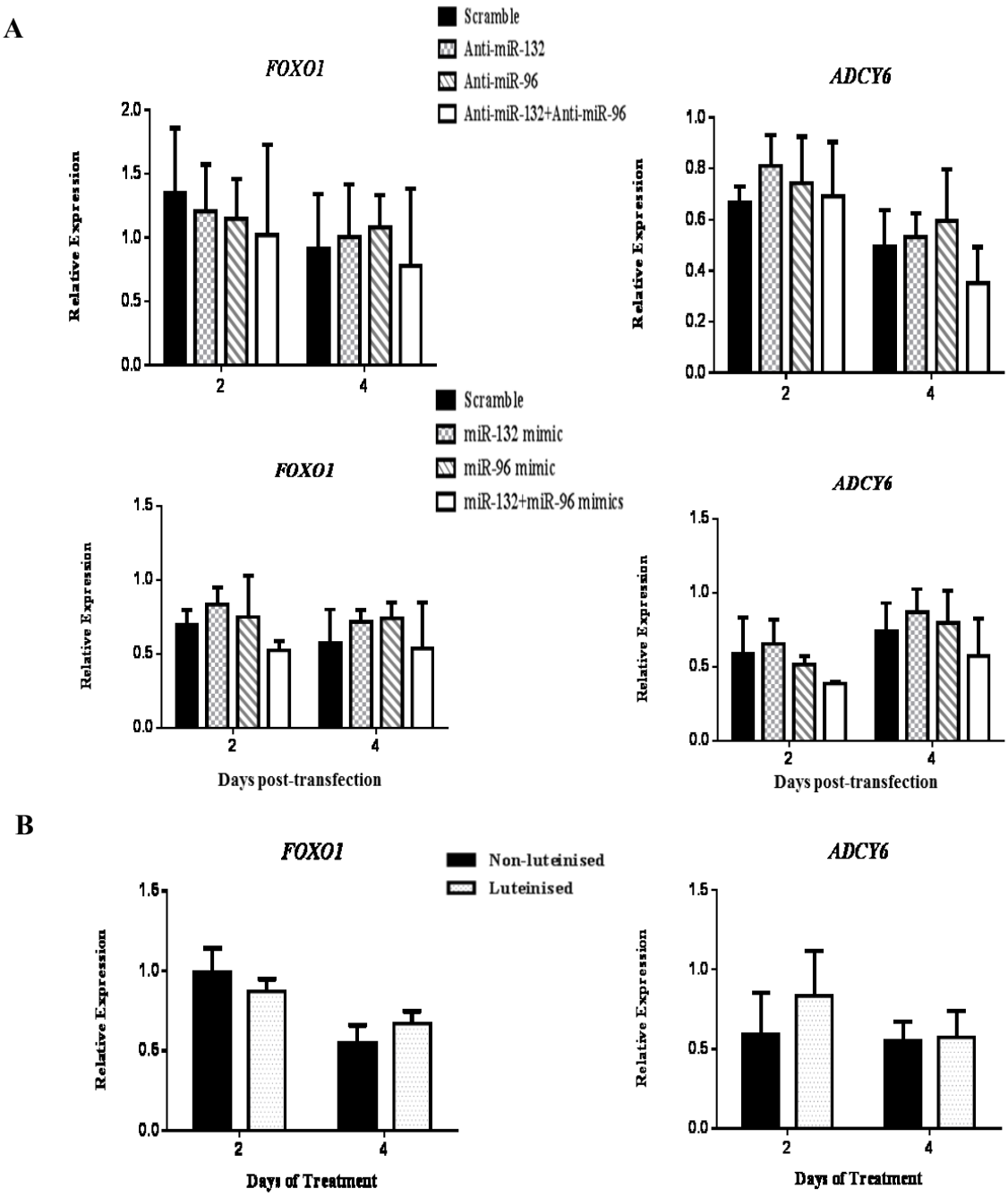


**Figure 3.13 A) Effects of inhibition and over-expression of miR-132 and miR-96 on mRNA levels of the predicted targets, FOXO1 and ADCY6. B) Expression of FOXO1 and ADCY6 during luteinisation in vitro (n=4 experiments). Values are presented as mean (± SEM).**

### 3.2.2.2 Effect of inhibition or overexpression of miR-132 and miR-96 on cell growth

Cell growth responses were analysed using xCELLigence System. This system uses electrodes to mesure electrical impedance as an indicator of cell contact with a culture vessel surface; these changes can be related to cell numbers (the more cells in the vessel the greater the surface of vessel occupied by cells) or cell morphology (large fibroblast-like cells will generate higher impedance than small round cells). Cultured granulosa cells started to differentiate and change their morphology and the cell impedence gradually increased 48 h after luteinisation was induced. In contrast, impedence values in non-luteinised granulosa cells droped as the cells rounded up or aggregated as shown in Figure 3.14.A. There was no significant decrease or increase in cell index after transfection with LNA inhibitors or mimics compared to control groups, indicating miRNA inhbiiton or overexpression did not affect cell numbers or cell morphology (Figure 3.14.B).

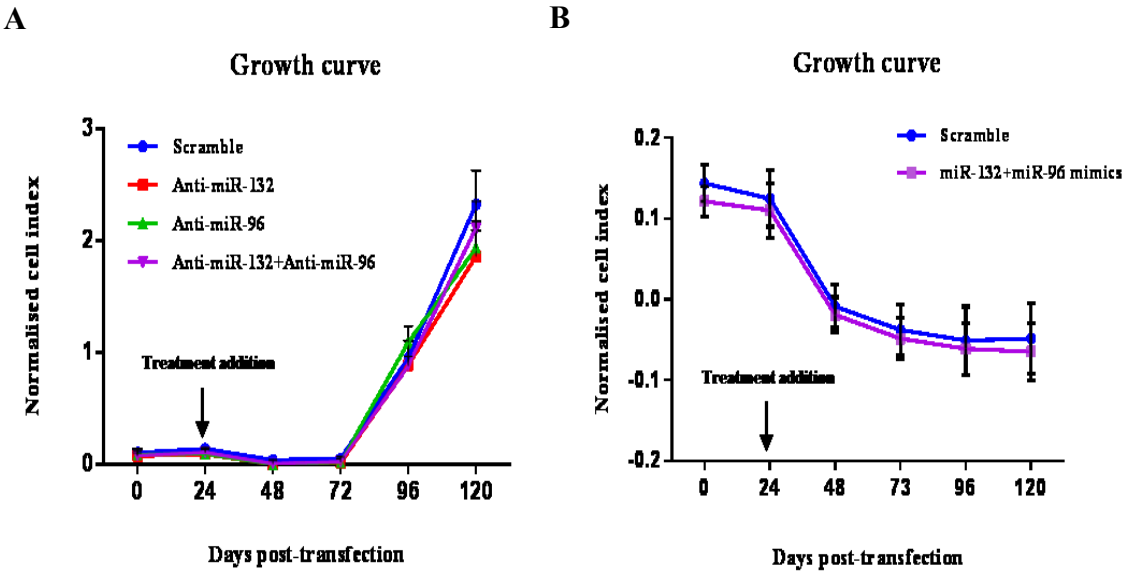


**Figure 3.14 Representative graph comparing the rate of cell growth of cultured granulosa cells when incubated with LNA inhibitors and mimics (*n*=3 experiments).**

### 3.2.2.3 Progesterone production in response to inhibition or overexpression of miR-132 and miR-96

The effect of manipulating the levels of miR-132 and miR-96 on progesterone production was measured by RIA. Progesterone levels in spent media decreased 2 days after transfection of cultured granulosa cells with miR-132 inhibitor (Figure 3.15.A). An increase in progesterone levels in response to transfection with mimics was observed on day 4 but was significant (P<0.03) only when all mimic-transfected groups were combined (Figure 3.15.B).

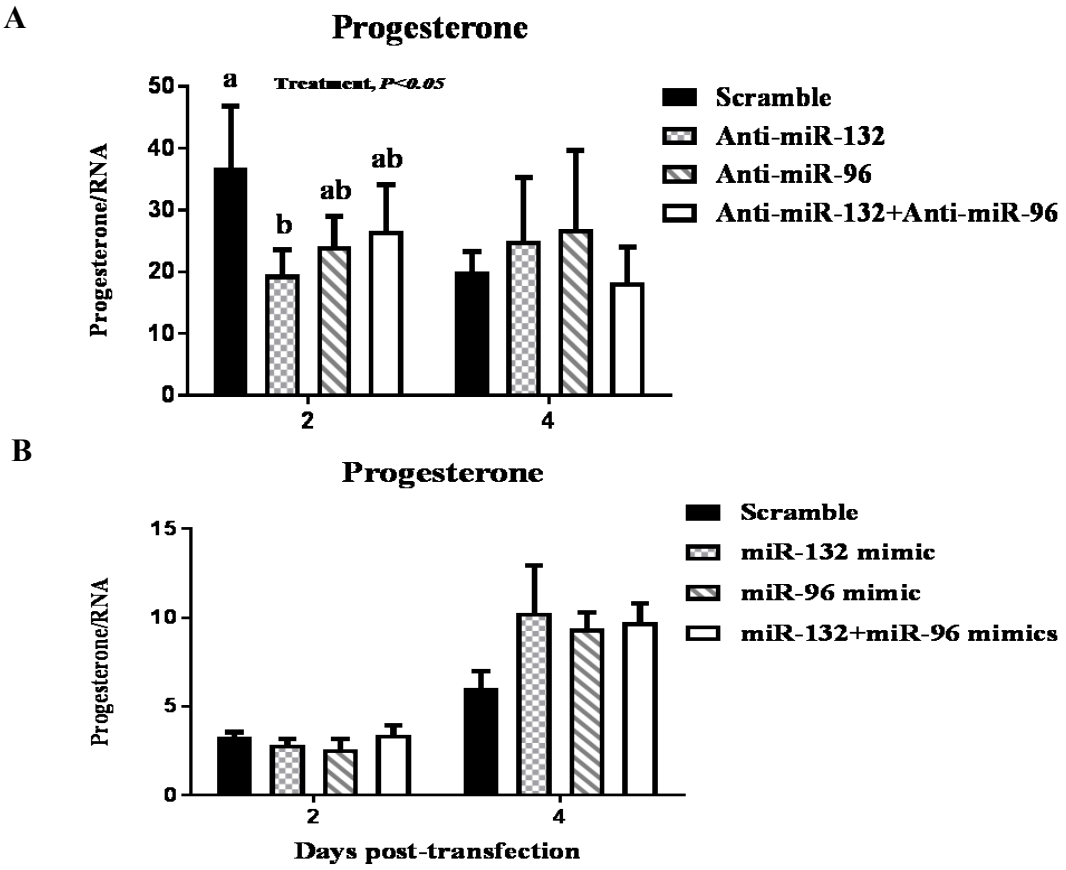


**Figure 3.15 Mean (± SEM) progesterone concentrations after transfection of bovine granulosa cells with LNAs or mimics (n=4 experiments). Data were normalised to RNA level and to the corresponding value on the day of treatment (Day 0). Values are presented as mean (± SEM) and were analysed using one-way ANOVA and Tukey's test. Significant differences are represented by different letters (a-b).**

## 3.3 Functional analysis of miRNAs in bovine luteal cells

Since the in vitro luteinisation model failed to replicate changes in miRNA target expression occurring in vivo, I decided to instead use luteal cells to examine the functions of miR-132 and miR-96. Cultures of bovine luteal tissue contained different cell types as confirmed by IF (Figure 3.7).

### 3.3.1 Manipulation of miRNA levels *in vitro*

LNA inhibitors were utilised to knockdown the miRNA levels in cultured luteal cells. As with granulosa cells transfection with miR-132 inhibitor resulted in a significant reduction in the expression of miR132 with no significant reduction in miR-96 expression (Figure 3.16.A). Similarly, inhibition of miR-96 led to a measurable decrease in the level of the miRNA (Figure 3.16.B), as revealed by qPCR analysis, LNAs dramatically lowered the concentrations of each target miRNA on day 1 and 2 after transfection.

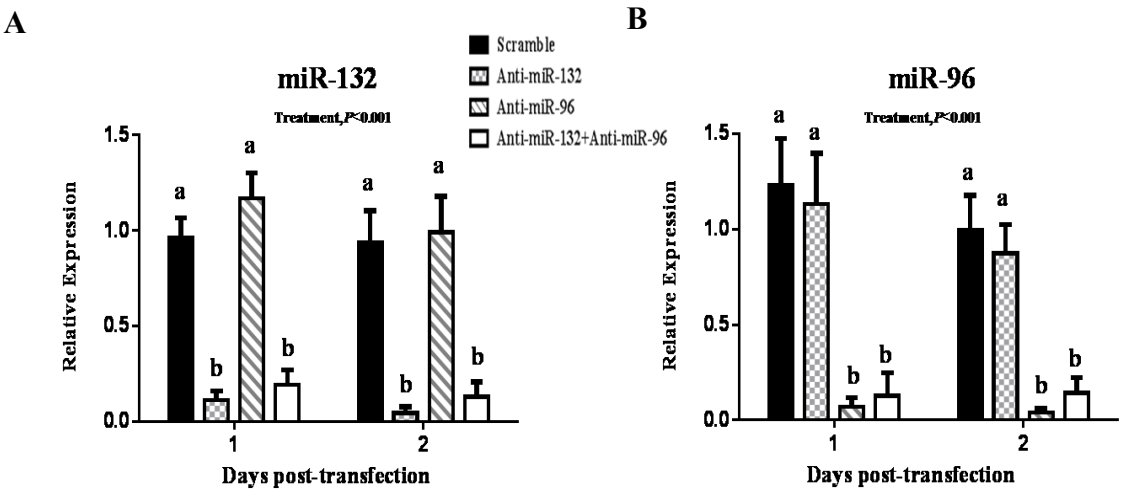


**Figure 3.16 Changes in the level of miRNAs in the cultured luteal cells after transfection with specific LNAs (n=4 experiments). Values are presented as mean (± SEM) and were analysed using two-way ANOVA and Tukey's test. Significant differences are represented by different letters (a-b).**

#### 3.3.1.1 Effects of miRNA depletion on target gene expression in bovine luteal cells

qPCR and western blot analysis were performed to monitor expression of predicted target genes (FOXO1 and ADCY6) and their protein products in response to miR-132 and miR-96 inhibition in cultured luteal cells. Inhibition of miR-132 led to an increase ($P<0.05$) in FOXO1 transcript but not protein levels. In contrast, inhibition of miR-96 increased protein but not transcript levels of FOXO1. (Figure 3.17.A.B). Unlike FOXO1, the expression of the ADCY6 was unchanged in the transfected luteal cells and I could not detect ADCY6 protein because ADCY6 antibody (SAB2100054-50UG, Sigma-Aldrich. UK) did not work for bovine luteal cells. HEKC293 were used as positive control for antibody evaluation (Figure 3.17.C).

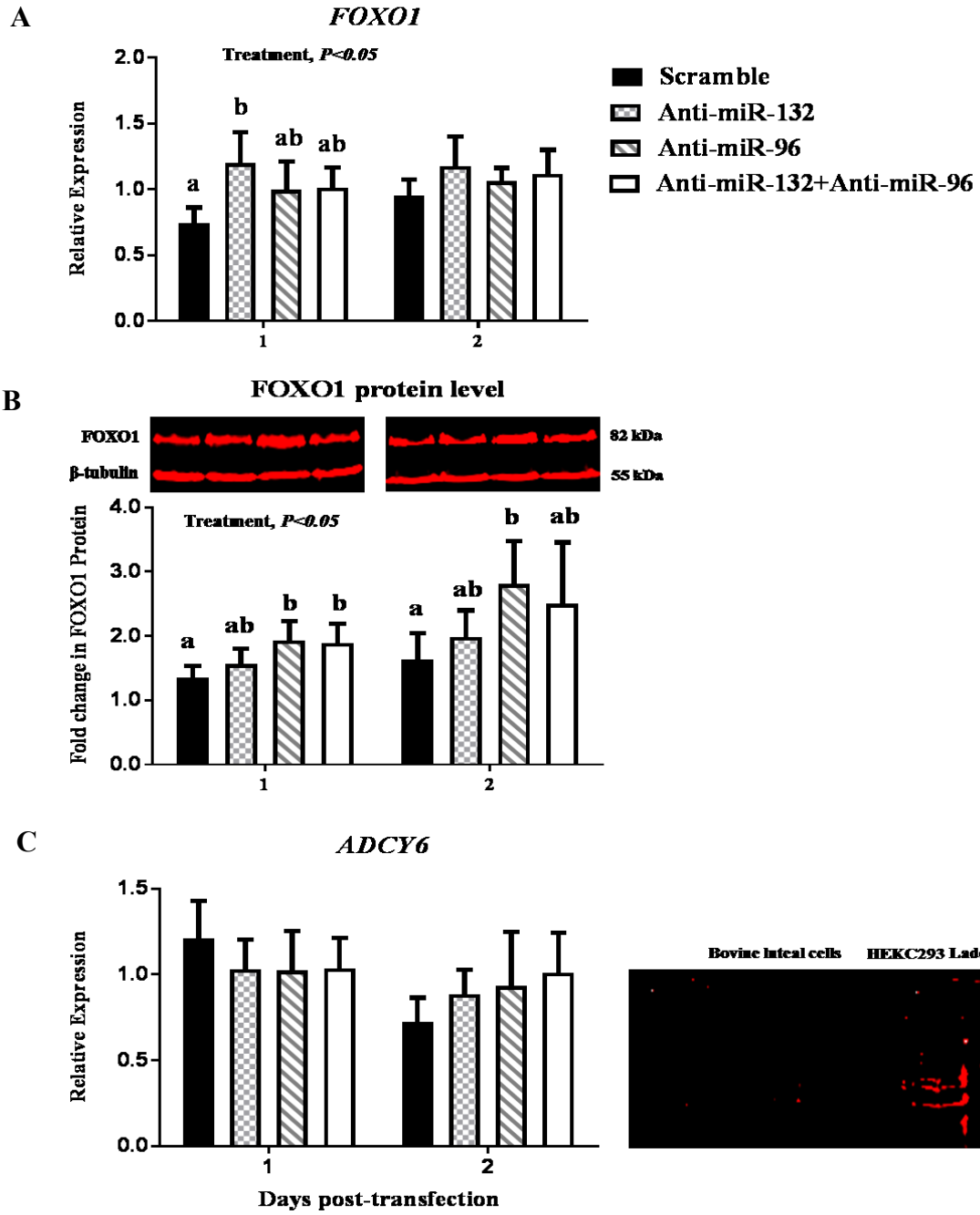


**Figure 3.17 qPCR and western blot analysis of the putative miRNAs target genes FOXO1 and ADCY6 in bovine cultured luteal cells (n=4 experiments). Levels of A) FOXO1 transcript and B) FOXO1 protein and C) ADCY6 transcript and protein. Values are presented as mean (± SEM) and were analysed using one-way ANOVA and Tukey's test. Significant differences are represented by different letters (a-b).**

### 3.3.1.2 Effect of inhibition or overexpression of miR-132 and miR-96 on cell survival

In order to assess whether reduction of miR-132 and miR-96 levels induced luteal cell apoptosis, luteal cells were transfected with miRNA inhibitors for 24h then left in serum free medium for 12 h. Afterward, cell apoptosis responses were analysed using caspase 3/7 activity assay. There was a significant increase in caspase 3/7 activity after transfection with miR-96 inhibitor compared to controls transfected with scramble oligonucleotide and deprived of serum (Figure 3.18.A). Overexpression of miRNAs had no significant effect on apoptosis (Figure 3.18.B). qPCR analysis showed that expression of Caspase 3 mRNA remained unchanged after inhibition of miRNA levels (Figure 3.18.C).

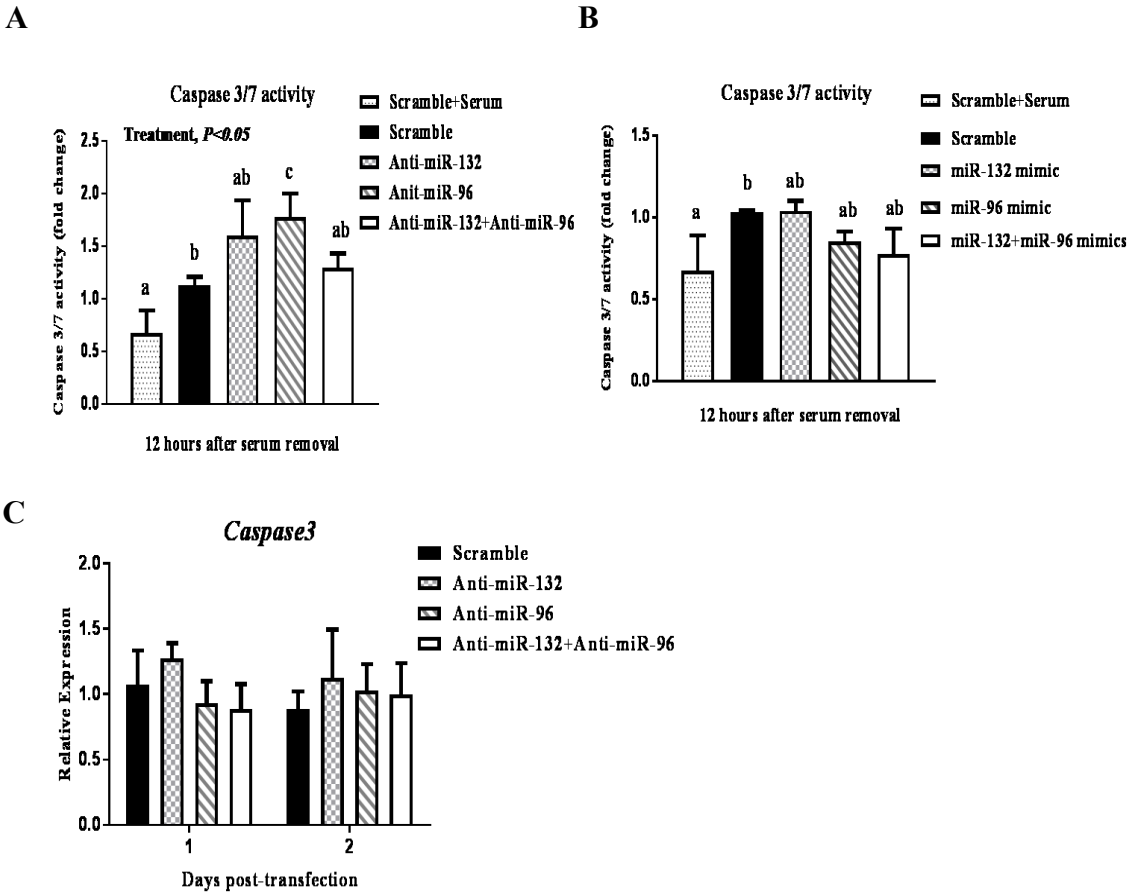


**Figure 3.18 Representative graphs comparing the rate of cell apoptosis of cultured luteal cells when incubated with A) LNA inhibitors and B) mimics (*n*=3 experiments). Cells were transfected with miRNA inhibitors for 24h then left in serum free medium for 12 h. C) qPCR analysis of Caspase 3 expression after transfection with miRNA inhibitors. Values are presented as mean (± SEM) and were analysed using one-way ANOVA and Tukey's test. Significant differences are represented by different letters (a-b).**

### 3.3.1.3 Effect of inhibition of miR-132 and miR-96 on progesterone production and expression of steroidogenic genes

The effect of depletion of miR-132 and miR-96 on progesterone secretion by luteal cells was measured by RIA. There was no significant effect on progesterone synthesis after transfection of cultured luteal cells with miR-132 and miR-96 inhibitors (Figure 3.19.A).

In addition, I investigated the effect of miR-132 and miR-96 inhibition on steroidogenic genes; RT-qPCR data showed that inhibition of miR-96 enhanced expression of CYP27A1 but not significantly. CYP27A1 an enzyme involved in cholesterol catabolism to oxysterols (Figure 3.19.B). However, there were no significant differences in the mRNA levels CYP11A1 and 3βHSD (Figure 3.19.C).

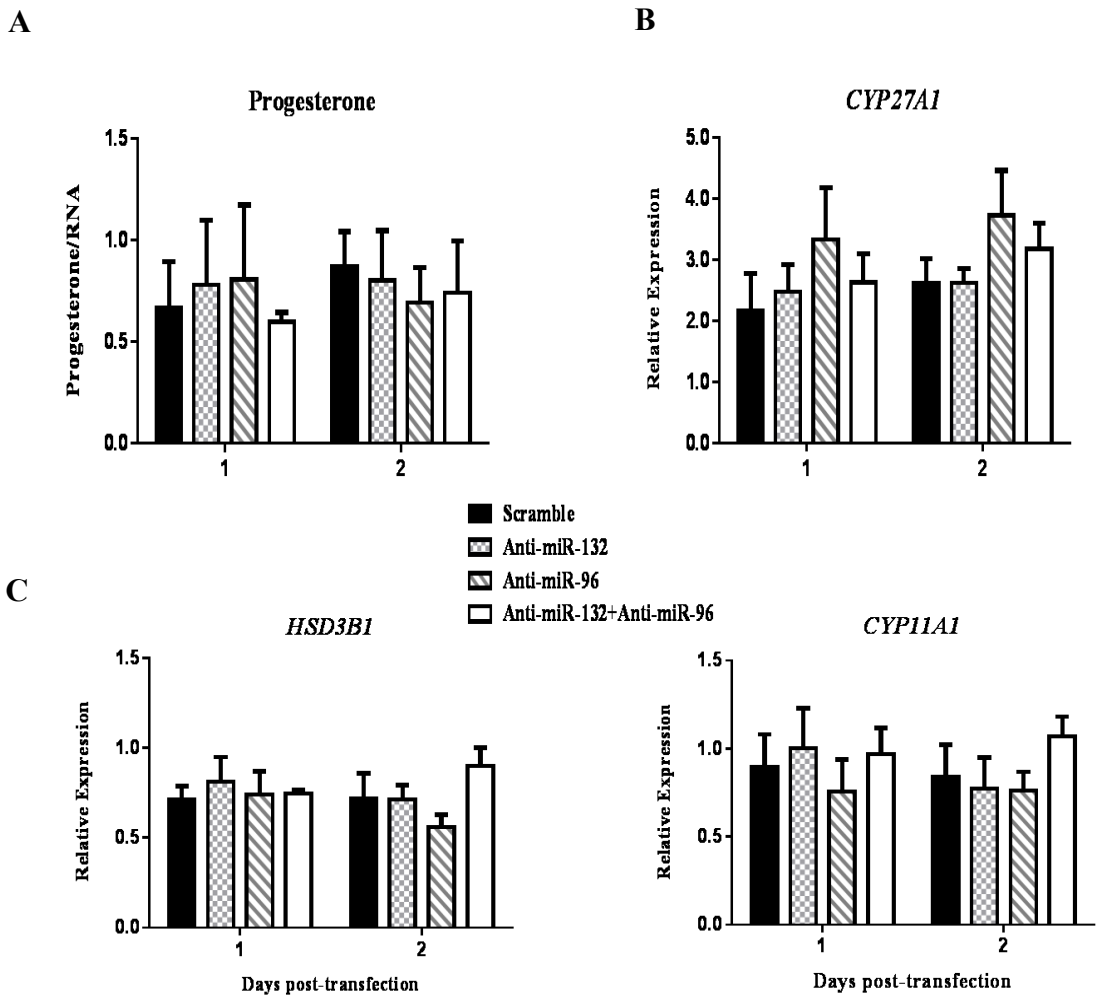


**Figure 3.19 Mean (± sem) progesterone concentrations and RT-qPCR analysis of several genes related to steroidogenesis after transfection of bovine luteal cells with LNAs (n=4 experiments). Data for progesterone were normalised to RNA level and to the corresponding value on the day of treatment (Day 0). QPCR data were normalised to *18S* and the corresponding value on the day of treatment (Day 0).**

## 3.4 Functional analysis of miRNAs in human luteinised granulosa cells

In order to address whether the effects of miR-132 and miR-96 during luteinisation are conserved in humans, this study was conducted through down-regulation of miR-132 and miR-96 in human luteinised granulosa cells (hLGCs) obtained from IVF patients.

### 3.4.1 Manipulation of miRNA levels *in vitro*

Firstly, I measured the levels of miR-132 and miR-96 in hLGCs treated with hCG in vitro (cDNA provided by Dr. Colin Duncan). As shown in Figure 3.20.A, there was a significant up-regulation of miR-132 and miR-96 expression in response to hCG which was consistent with the increase in miRNA levels observed during luteinisation of bovine granulosa cells in vitro (Figure 3.11). For testing the effects of miRNA inhibitors, hLGCs were isolated from follicular fluid using Ficoll solution and cultured for two days. The purity of isolated granulosa cells was assessed by IF (Figure 3.20.B). Inhibition of miR-132 and miR-96 expression induced the down-regulation of these miRNAs in cultured hLGCs (Figure 3.20.C).

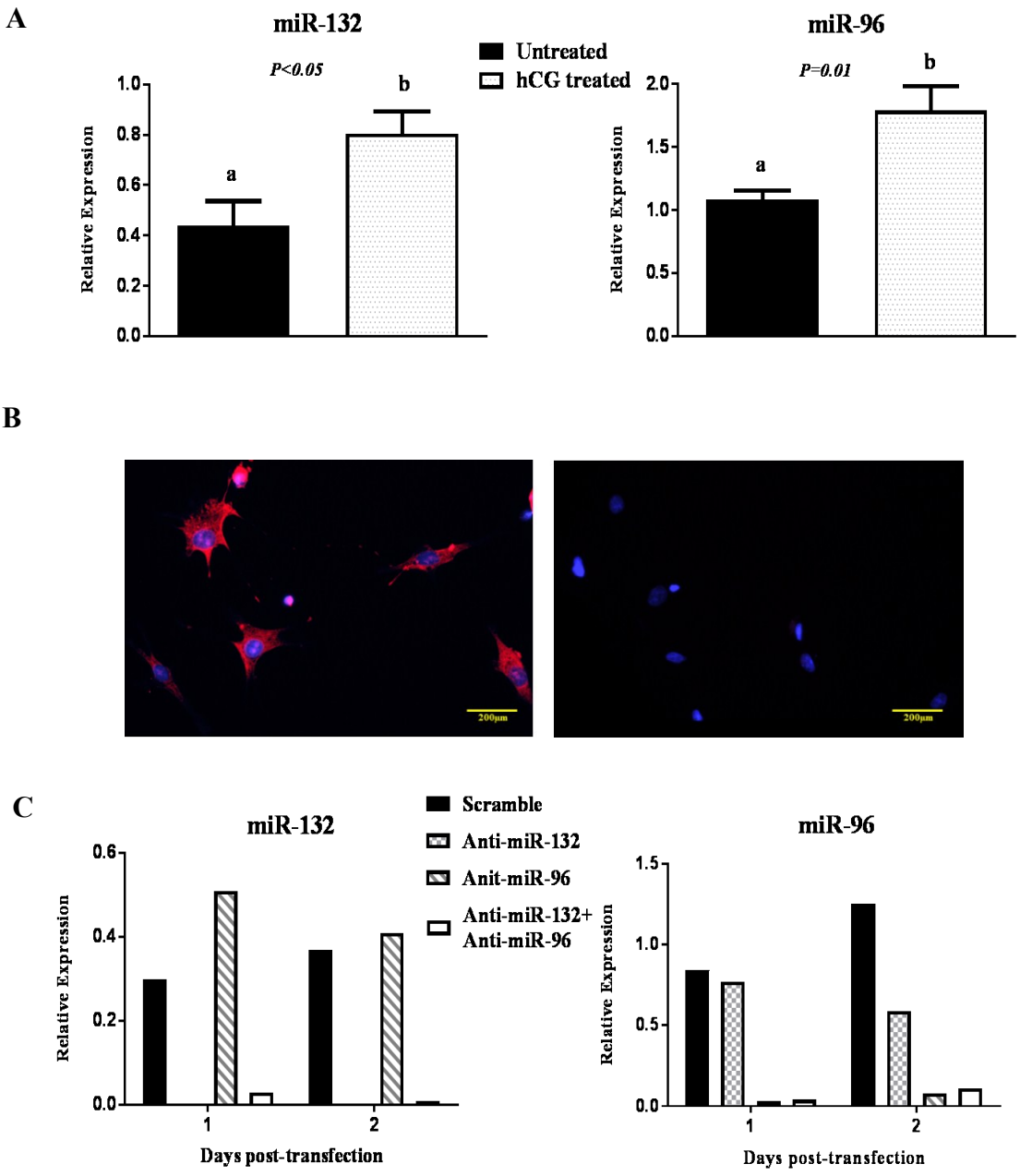


**Figure 3.20 A) miR-132 and miR-96 levels in cultured human luteinised granulosa cells treated with hCG for 6 days (n=3 experiments). B) Immunofluorescence showed the presence of HSD3B1, a marker of luteinised granulosa cells. Scale 200 µm and magnification: ×40. C) Changes in the level of miRNAs in the cultured human luteinised granulosa cells after transfection with specific LNAs (n=1 experiment). Values are presented as mean (± SEM) and were analysed using Tukey's test (P<0.05). Significant differences are represented by different letters (a-b).**

### 3.4.1.1 Effects of miRNA inhibition on target gene expression

Western blotting showed a significant increase in FOXO1 protein levels one day after transfection of hLGCs with miR-132 and miR-96 inhibitors. An increase in FOXO1 in day 2 was significant only after transfection with inhibitors for both miR-132 and miR-96 (Figure 3.21).

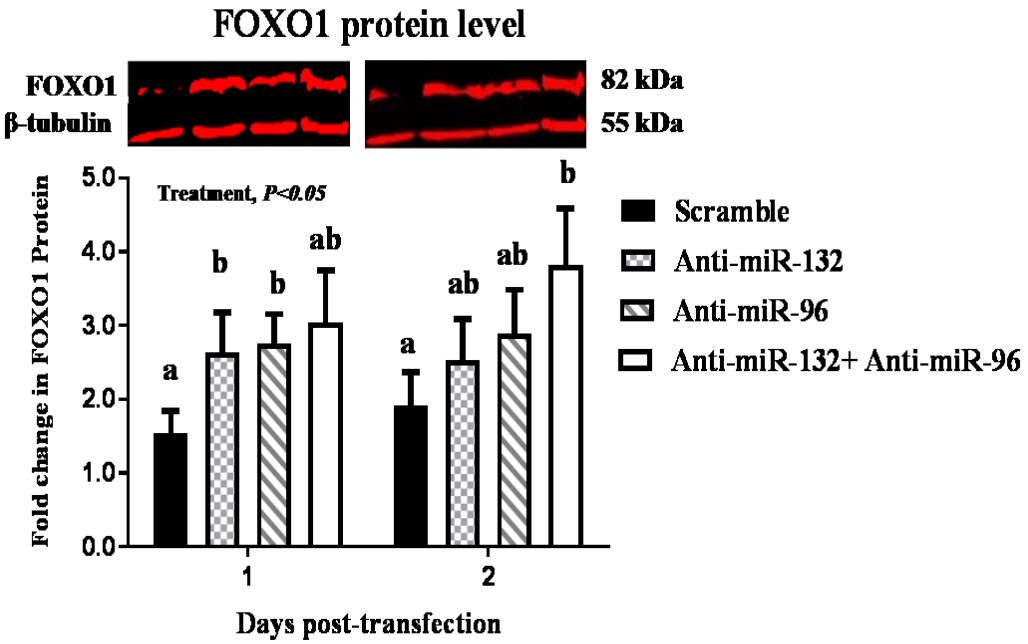


**Figure 3.21 Western blot analysis of the putative miRNAs target gene FOXO1 (n=4 experiments). Values are presented as mean (± SEM) and were analysed within Day using one-way ANOVA and Tukey's test. Significant differences are represented by different letters (a-b).**

### 3.4.1.2 Effect of inhibition or overexpression of miR-132 and miR-96 on cell apoptosis

#### 3.4.1.2.1 Caspase 3/7 activity

Analysis of human granulosa cell apoptosis following inhibition or over-expression of miR-132 and miR-96 using inhibitors and mimics, respectively, showed a significant increase in apoptosis 24h after transfection with miR-96 inhibitor,

regardless of whether cells had been previously deprived of serum (Fig. 3.22.A left panel). Moreover, granulosa cells transfected with pooled inhibitors showed significant induction of caspase 3/7 activity only in the presence of serum (Fig. 3.22.A). On the other hand, transfection of hLGCs with miR-96 mimic resulted in reduced caspase 3/7 activity 24h later but miR-132 mimic had no effect (Fig. 3.22.B right panel). No significant differences were observed after transfecting cells with mimics in the absence of serum (Fig. 3.22.B left panel).

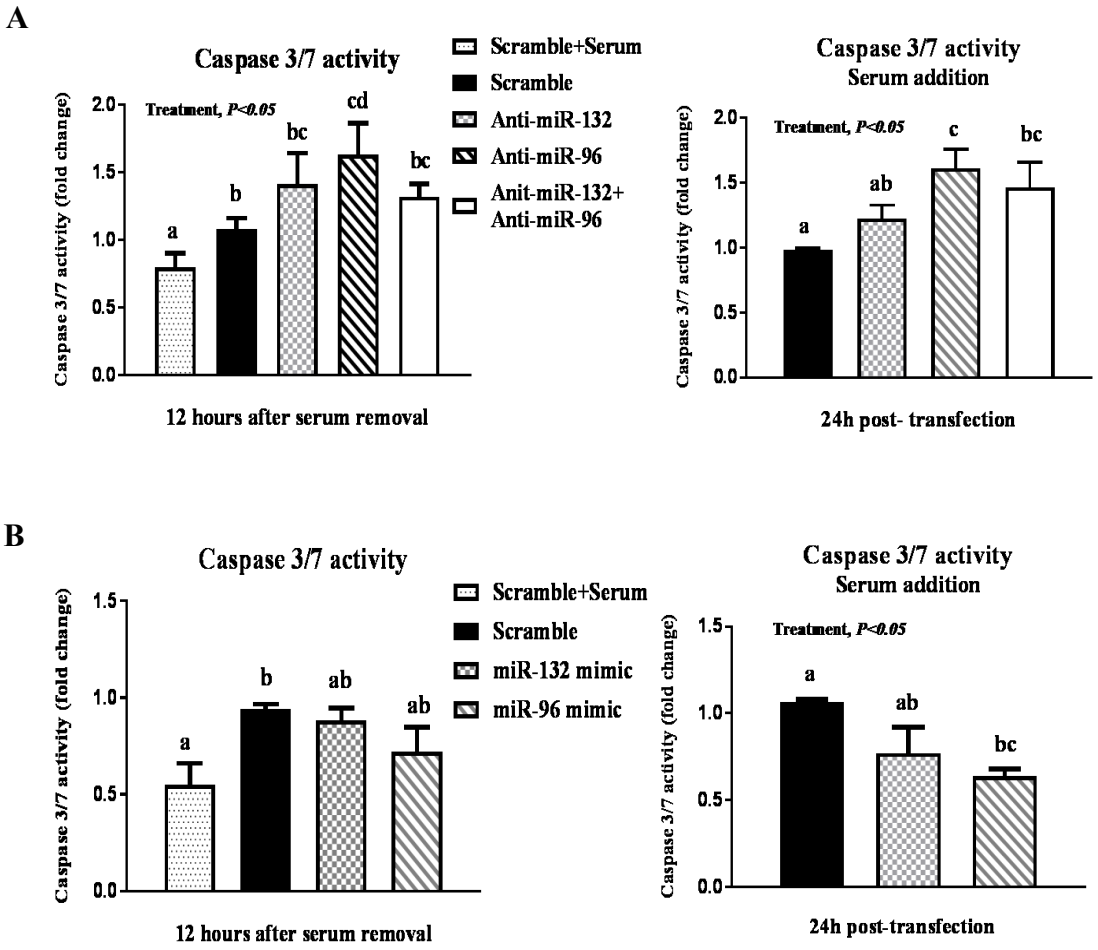


**Figure 3.22 Caspase 3/7 activity in cultured luteinised granulosa cells transfected with LNA inhibitors (A), mimics (B) (*n*=5 experiments). Values are presented as mean (± SEM) and were analysed using one-way ANOVA and Tukey's test. Significant differences are represented by different letters (a-b).**

### 3.4.1.2.2 Annexin-V/PI

To further confirm the effects of miR-96 inhibition on human luteinised granulosa cells apoptosis, Annexin-V/PI staining of cultured human LGCs was performed on the transfected cells with miR-96 inhibitor and scramble. Figure 3.23 illustrates the increase in cell apoptosis induced by miR-96 inhibitor (Figure 3.23.B) relative to scramble oligonucleotide (Figure 3.23.A).

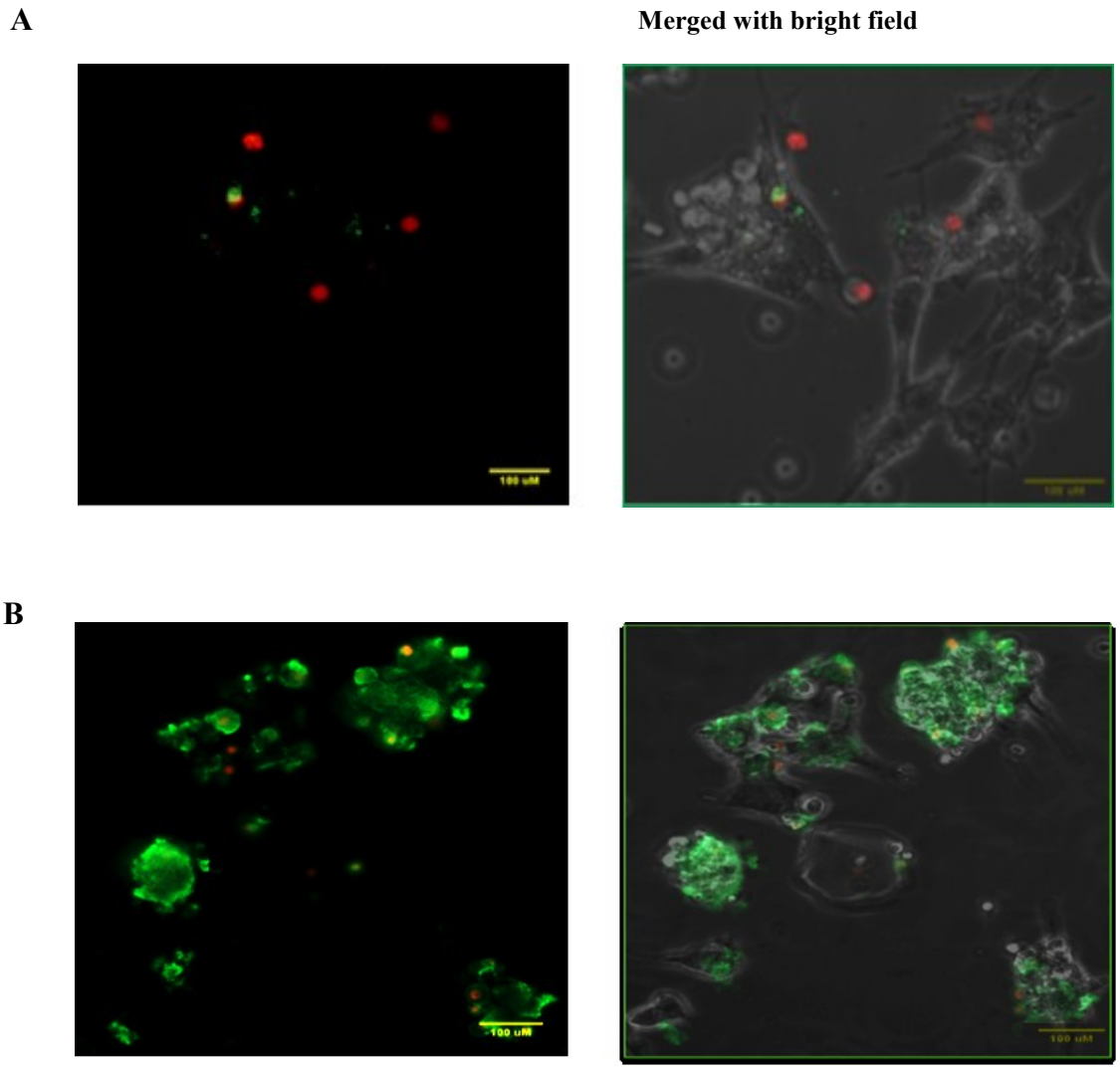


**Figure 3.23 Evaluation of cell apoptosis in human LGCs by staining with Annexin-V/PI. Cells were cultured in 2% FBS, transfected with control scramble oligonucleotide (A) or miR-96 inhibitor (B). Green=Annexin-V, Red=Propidium iodide. Scale 100 µm and magnification: ×20.**

### 3.4.1.2.3 Cell counting

Further confirmation of whether loss-of-function of miR-132 and miR-96 was associated with cell death was sought by using Trypan blue dye. hLGCs were transfected with miR-96 inhibitor or pooled inhibitors were significantly reduced in numbers compared with cells transfected with negative control (scramble) (Figure 3.24).

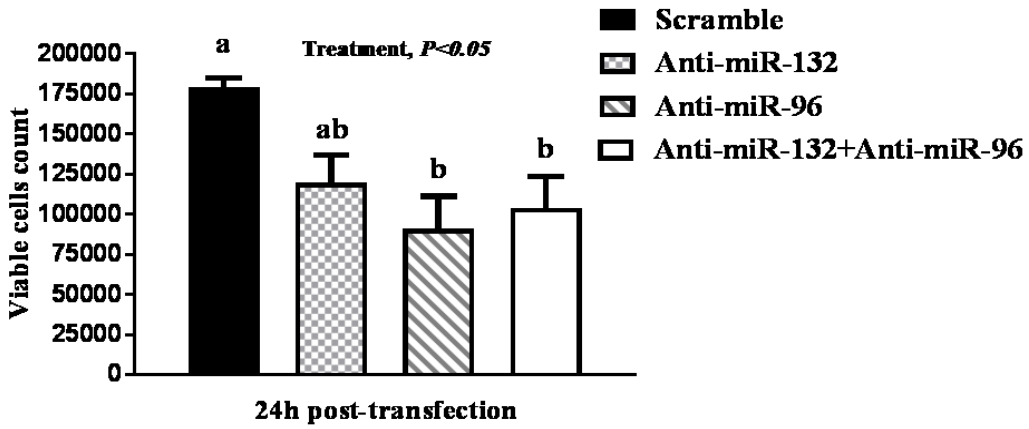


**Figure 3.24 Effects of miR-132 and miR-96 inhibition on cell numbers (*n*=3 experiments). Viable hLGCs were counted by trypan blue exclusion assay in triplicates at 24h post transfection. Values are presented as mean (± SEM) and were analysed using one-way ANOVA and Tukey's test. Significant differences are represented by different letters (a-b).**

### 3.4.1.2.4 Effect of FOXO1 downregulation on caspase 3/7 in response to miR-96 inhibition

To examine whether the effects of miR-96 inhibition on caspase 3/7 activity (Figure 3.25) were indeed mediated by the increase in FOXO1 protein (Figure 3.21) I simultaneously transfected cells with FOXO1 siRNA and with miR-96 inhibitor to determine whether a deficiency of FOXO1 changed the caspase 3/7 response to miRNA inhibition. I first tested the effects of FOXO siRNA on hLGCs and confirmed a reduction of FOXO1 protein levels beginning 24h after transfection with the siRNA (Figure 3.25. A).

Interestingly, in the presence of reduced FOXO1, miR-96 inhibition failed to induce an increase in Caspase 3/7 indicating the effects of the miRNA on apoptosis were mediated by FOXO1 (Figure 3.25.B).

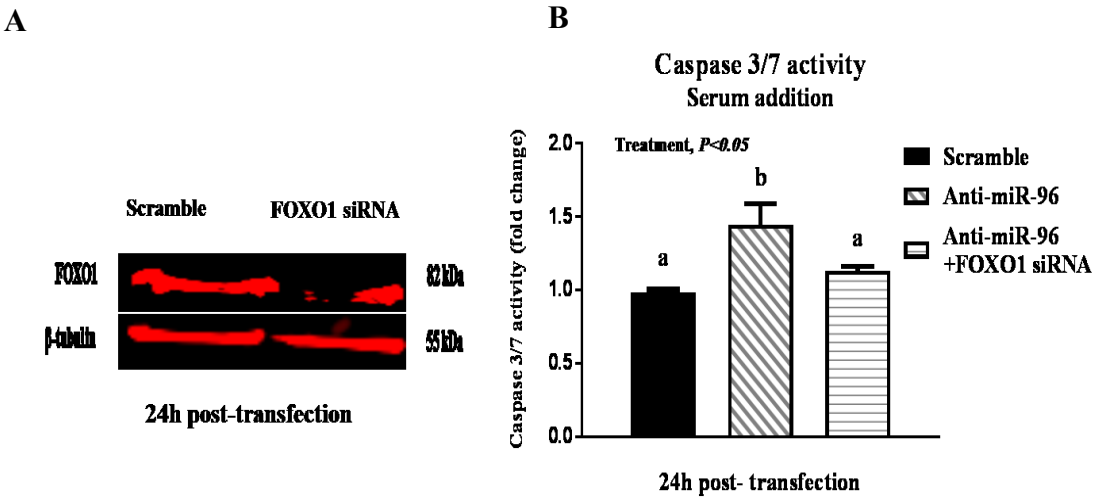


**Figure 3.25 Effects of miR-96 and FOXO1 siRNA depletions on hLGCs (*n*=5 experiments). A) Western blot showed a reduction in FOXO1 protein after transfection with FOXO1 siRNA. B) Effects of miR-96 and FOXO1 siRNA depletions on FOXO1 and caspase 3/7 activity. Values were presented as mean (± SEM) and were analysed using one-way ANOVA and Tukey's test. Significant differences are represented by different letters (a-b).**

### 3.4.1.3 Effect of inhibition of miR-132 and miR-96 on hormone production

To investigate whether manipulation of the miRNA levels might affect steroidogenesis of hLGCs. Measurement of steroid levels in spent cell culture media showed a significant reduction of progesterone levels at 24 h after transfection of cells with pooled miR-132 and miR-96 inhibitors (Figure 3.26.A). However, no effects of miRNA inhibition on oestrogen levels (Figure 3.26.B). Interestingly, in cells transfected with FOXO1 siRNA, inhibition of the two miRNAs failed to induce a decrease in progesterone levels (Figure 3.26. C), indicating that, as in the case of apoptosis, the effects of these miRNAs on progesterone production are mediated through targeting FOXO1.

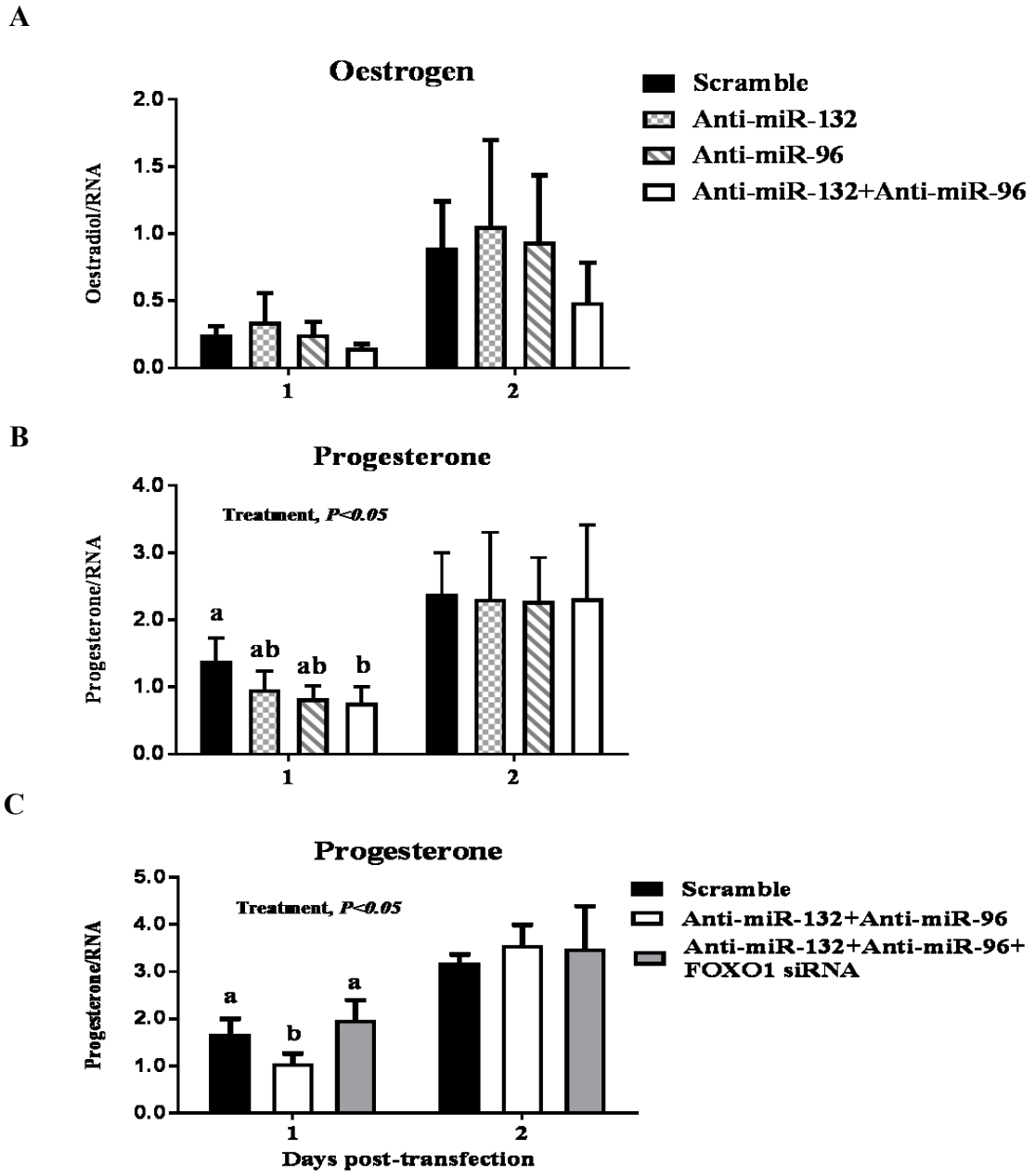


**Figure 3.26 Steroid concentrations after transfection of hLGCs cells with LNAs and FOXO1 siRNA (n=4 experiments). A) Oestrogen secretion after transfection of miRNA inhibitors. B) Progesterone level in transfected hLGCs. C) Progesterone level in response to pooled inhibitors and FOXO1 siRNA. Data were normalised to RNA level and to the corresponding value on the day of treatment (Day 0). Values are presented as mean (± SEM) and were analysed using one-way ANOVA and Tukey's test. Significant differences are represented by different letters (a-b).**

# Chapter 4

# Discussion and Conclusion

# Chapter 4: Discussion and Conclusion

## 4.1 Significance and the novel findings of this thesis

Surprisingly, most research on the follicle-luteal transition has focused on the transcriptional changes involved while little information is available on the post-transcriptional regulation of that process. Identification of miRNAs expressed in the bovine ovary may lead to a better understanding of the post-transcriptional regulation of ovarian function to improve the fertility in cattle and human. miRNAs have already been shown to be involved in the regulation of ovarian cell function in different species (reviewed in Donadeu et al., 2012, Maalouf et al., 2016b); however, limited studies have examined the role of miRNAs in the luteal tissue. The overall aim of this thesis was to gain novel insights into the physiological involvement of miR-212-132 and miR-183-96-182 clusters during luteinisation in the monovular ovary.

In this study, our laboratory has investigated the enrichment of miRNAs in bovine dominant follicles collected during the luteal phase of the oestrous cycle (day 5-17) and early CLs (day 1-4 of oestrous cycle). To examine the effect of these miRNAs during follicle-luteal transition. For this, we have generated miRNA microarray data from large healthy follicles (n=6) and early CLs (n=6). A total of 14 and 60 miRNAs were upregulated and down-regulated, respectively, in CLs relative to follicles. Top upregulated miRNAs in the CL were miR-212-132 and miR-183-96-182 which organised as cluster in the bovine genome. In contrast, a previous study in our laboratory and collaborator at the Roslin institute have identified a subset of miRNAs that up or downregulated in the preovulatory follicles (respond to LH and proceed to ovulation) that collected on the first day of oestrous and early CL (day 3 of oestrous cycle) in sheep (McBride et al., 2012). 17 out of 212 miRNAs with higher cloning frequencies were differentially expressed in the follicles and early CLs. Only three of the miRNAs decreased in the follicle including preovulatory follicle and increased in the early CLs, these are miR-503, miR-21 and miR-142-3p (McBride et al., 2012).

The expression of these miRNAs has been reported in different species during the earlier stage of luteinisation in response to LH/hGC (reviewed in Gebremedhn et al., 2016a).

In addition, different methodologies and experimental approaches have been used to profile the expression of miRNAs in sheep and bovine ovarian tissue. McBride et al. (2012) have performed miRNA cloning analysis to detect the expression of miRNAs and their abundance within ovarian tissues. After extraction of RNA from preovulatory follicles and early CLs then miRNAs libraries were prepared and cloned into small RNA fragments including miRNAs, tRNA and other small RNA. Only limited number of miRNA libraries were selected to be sequenced. The cloning of miRNAs was based on the ovine genome sequences which is poorly annotated. Novel miRNAs have been detected and majority of these miRNAs were identical to those from bovine. However, these novel miRNAs have been excluded from the study as they showed lower cloning counts. Northern blotting was used to validate the expression of miRNA. These methods are low-throughput, and require large amount of RNA for samples, this will affect the discovery of low abundant miRNAs in the cells or tissue (Koshiol et al., 2010, McBride et al., 2012) .

In this research, we have performed the miRCURY LNA™ microRNA Array 6th gen (Exiqon, Denmark), a high throughput mean that allow profiling thousands of specific mature miRNAs in bovine large healthy follicles and early CLs. A total of 1428 DNA probes were used which represent all miRNAs for human, mouse or rat registered in the miRBase 19.0. However, most of human miRNAs were highly conserved among species including bovine. Validation of bovine miRNAs was performed by qPCR, a specific and sensitive technique that can detect very small quantities of miRNAs, and the kits are widely available (Koshiol et al., 2010, Sontakke et al., 2014).

Given all the reason mentioned above and to use the cow as model to study human ovary, I have selected microarray data from bovine ovarian tissues for further study. Novelty lies in the fact that miR-212-132 and miR-183-96-182 clusters have an anti-apoptotic role, identified through targeting FOXO1 and their functions were determined through elimination of miR-96 and miR-132 in bovine and human luteinised granulosa cells. In the following discussion, I have presented the novel findings of our study, their implications for the bovine and human fertility research, and future studies that need to be performed.

## 4.2 Experimental approaches

In the present study, I investigated different approaches to better understand the complete role of miR-212-132 and miR-183-96-182 clusters during follicle-luteal development. In chapter 3.1 the initial stage of this study which involved the characterisation of miR-132 and miR-96 expression within luteal tissue using ISH and FACS approaches. Firstly, I optimised the ISH procedure in bovine paraffin embedded ovarian sections using a probe against RnU6, a constitutively-expressed small RNA, and then against miR-202, a gonad-specific miRNA and a scrambled oligonucleotide sequence was used as negative control (Donadeu et al., 2012, Sontakke et al., 2014). Significant work was required to optimise ISH and FACS procedures. Nile red was used to stain bovine luteal steroidogenic cells (Quirk et al., 2013), I have successfully used NR to sort bovine luteal steroidogenic cells by FACS. These approaches resulted in successful detection of miR-132 by ISH and the separation, using FACS, of steroidogenic and endothelial fractions in which the two miRNAs were profiled. Subsequently, to identify candidate miRNA targets I used miRTarBase and TarBase to obtain experimentally validated targets in human and mouse, and TargetScan to identify computationally predicted targets in bovine. Molecular and physiological functions related with the lists of targets of these miRNAs were identified using KEGG and GO enrichment analyses.

Chapter 3.2 we quantified the relative expression of miR-212-132 and miR-183-96-182 in bovine luteinised granulosa cell in vitro and determined the influential effect of these miRNAs on luteinisation. In chapter 3.2, 3.3 and 3.4 A useful approach to determine the function of miRNAs was to manipulate their expression in vitro. Overexpression and inhibition of miR-132 and miR-96 were achieved successfully using mimics and locked nucleic acid (LNA) inhibitors, respectively. LNAs contain a modification which locks the ribose ring in a conformation that results in increased sensitivity and specificity, as well as resistance to enzymatic degradation. Moreover, the transfection of bovine granulosa cells with miR-132 and miR-96 inhibitors led also to lower levels of miR-212 and miR-183, respectively. This may be due to identical or partial sequence homology of the miRNAs within each cluster.

Chapter 3.4 The aim of this study was to determine the role of the candidate miRNAs during luteinisation in cattle and human. In vivo and in vitro experiments with bovine tissues were used to initially candidate miRNAs and to begin to explore their functions. Cow ovaries can be easily obtained from the abattoir. The results obtained with bovine cells were then used for a more-in-depth exploration of miRNA roles using luteinised granulosa cells collected from IVF patients. When using this approach, consideration needs to be given to potential sources of variability from patient status including diet and potential disorders such as the cause of female and male infertility.

## 4.3 Relevant findings

### 4.3.1 Transcriptional regulation of miR-212-132 and miR-183-96-182 clusters

An increase in the levels of miR-212-132 and miR-183-96-182 in bovine CL relative to follicles as identified by preliminary work using microarray (Figure.1.7) is consistent with results from previous studies. A study in cattle using microarray identified 34 miRNAs which expression increased in pre-ovulatory follicle collected at oestrous (presumably in the process of luteinisation) compared to subordinate follicles including miR-212-132 and miR-183-96-182 (Gebremedhn et al., 2015). Other studies in horses (Schauer et al., 2013) and mice (Carletti et al., 2010, Fiedler et al., 2008) reported an up-regulation of miR-21, miR-132 and mR-212 in granulosa cells following administration of an ovulatory dose of hCG in live animals or LH/cAMP stimulation of granulosa cells (Fiedler et al., 2008). In addition, rat granulosa cells that were exposed to Bt2cAMP for 24 h showed a significant induction of miR-132, miR-212, miR-182 and miR-183 levels (Hu et al., 2013). These findings suggest a stimulatory effect of the LH surge, presumably through cAMP pathway, on the expression of the miR-212-132 and miR-183-96-182 clusters, consistent with my observation of an increase in the levels of all those miRNAs in bovine granulosa cells in response to Forskolin, an adenylate cyclase agonist (Figure 3.11). These observations also provide strong evidence of a conserved miRNA response to ovulation and luteinisation suggesting that these miRNAs play important roles during those processes.

In other cell types (neurons), miR-132 and miR-212 had already been reported to be transcriptionally-regulated by cAMP-response element binding (CREB) (Impey et al., 2004, Vo et al., 2005). In addition, miR-132 and miR-212 transcription is also regulated by Repressor Element 1 silencing transcription factor/neuron-restrictive silencer factor (REST/NRSF) in non-neuronal cells (Conaco et al., 2006).

In relation to miR-183-96-182, although their regulation by cAMP signalling has not been previously reported, several transcriptional factors including catenin/TCF/LEF, p53 and EVI1 can reportedly bind the promoter of hsa-miR-183 and regulate its expression (reviewed in Dambal et al., 2015, Tang et al., 2014).

### 4.3.2 Reported roles of miR-212-132 and miR-183-96-182 clusters in various tissues

Several studies have described the involvement of miR-212-132 and miR-183-96-182 clusters in development, maturation and function of different body organs as well as their association with numerous diseases (reviewed in Hornstein, 2012, Quinlan and Jimenez-Mateos, 2016, Sayed and Abdellatif, 2011).

High expression of miR-212-132 was detected in the brain and the pituitary gland. Upregulation of miR-132 and miR-212 stimulates morphogenesis of neurons through targeting p250GAP that is associated with neuronal differentiation (Wanet et al., 2012). miR-132 and miR-212 were shown to regulate plasticity in the visual cortex in response to light in mice (Tognini et al., 2011). Several studies have reported involvement of miR-212-132 in regulation of cardiovascular function. A study by Kumarswamy et al. (2014) showed that miR-212-132 cluster targets Gab1 and Sirt1 which have a stimulatory effect on angiogenesis. The authors indicated that knockdown of miR-212-132 in mice led to enhanced angiogenesis (Kumarswamy et al., 2014). In fibroblasts and myocytes from rat and mice, miR-212-132 expression was induced after addition of Angiotensin II (AngII) and overexpression of these miRNAs led to cardiac hypertrophy and eventually heart failure (Eskildsen et al., 2014, Ucar et al., 2012).

Ucar et al. (2010) have shown that miR-212-132 family is highly expressed in mice mammary stroma but not in epithelia and both target matrix metalloproteinase 9 (Mmp9) which is critically involved in tissue remodelling. miR-212-132 expression stimulated by cAMP in response to forskolin+IBMX or GLP-1 treatment resulted in an induction of insulin secretion through targeting cAMP-Regulated Transcriptional Co-activator-1 (CRTC1) in rat pancreatic β-cells (Malm et al., 2016).

A study have shown the inhibitory effect of miR-132-3p on osteogenic differentiation of the ligamentum flavum (Qu et al., 2016). These studies were consistent with ISH and FACS findings that showed the enrichment of miR-132 in different luteal cell types.

A role for miR-183-96-182 cluster has been described in craniofacial and sensory organ development in different species (Babak et al., 2004, Lumayag et al., 2013, Pierce et al., 2008, Xu et al., 2007). In addition, miR-96 was found to be expressed in human platelet and it targets VAMP8 protein (vesicle-associated membrane protein, also known as endobrevin) that regulate formation of platelet granules (Dangwal and Thum, 2012, Kondkar et al., 2010). Moreover, miR-96 contributes to suppression of neural differentiation by human embryonic stem cells through targeting paired box 6 (PAX6) (Du et al., 2013). Also, miR-96 is required for induction of osteoblast differentiation by targeting heparin-binding EGF-like growth factor (HB-EGF) (Papaioannou et al., 2015, Yang et al., 2014) and regulates vascular smooth muscle cell phenotype through partially inhibiting Tribbles-like protein 3 (Trb3) (Kim et al., 2014). A role of miR-96 was identified in human hepatocyte cholesterol uptake through directly repressing SR-BI which in turn supress HDL-C uptake (Wang et al., 2013).

In addition to their roles in non-transformed cells as described above, miR-212-132 and miR-183-96-182 clusters are involved in multiple types of cancer, where they may be pro-oncogenic or act as tumour suppressors. Indeed miR-132 exhibited an inhibitory effect on cell proliferation, migration and invasion of breast and ovarian cancer cells (Tian et al., 2016, Zhang et al., 2014b). In contrast, a study by Park et al. (2011) has shown the stimulatory effect of miR-132 on cell proliferation in pancreatic adenocarcinoma (PDAC). Furthermore miR-96 acts as oncogenic miRNA through promoting cellular growth and invasion in different cancers (Siu et al., 2015, Wang et al., 2016b, Xu et al., 2013). However, miR-96 may also reduce cancer pancreatic cell invasion and migration (Yu et al., 2010).

### 4.3.3 Identification of miRNA target genes in luteinising cells

Data from TargetScan, TarBase and miRTarBase were used to explore the miRNA target genes. In addition, the result of GO term analysis from predicted and validated miRNA target genes showed further significant biological and molecular processes (Figure 3.2). In this study GO annotation enrichment findings showed that these miRNAs are mostly associated with the regulation of cell cycle, cell adhesion, posttranscriptional regulation of gene expression and regulation of apoptosis. The KEGG analysis showed that FOXO signalling pathway was mostly enriched among the significantly abundant ones (Figure 3.2). In humans and/or rodents, FOXO1 and ADCY6 were previously validated experimentally as targets of ≥ 2 of the miRNAs in the miR-212-132 and miR-183-96-182 clusters (Table 3.2). Moreover, FOXO1 and ADCY6 were downregulated in bovine CL relative to pre-ovulatory-size follicles (Figure 3.4), consistent with these 2 genes being also targets of the two miRNA clusters during luteinisation in this species. FOXO transcription factors have pleiotropic roles involving regulation of cell cycle, apoptosis and metabolism. FOXO1 activity is in part regulated by phosphorylation through the PI3K/Akt signalling pathway (Martins et al., 2016). ADCY6 is a membrane associated enzyme that produces cAMP under stimulation by guanine nucleotide binding protein Gs, in turn activated by the LH receptor and other G-protein coupled receptors (reviewed in Stocco et al., 2007).

My attempts to implicate FOXO1 and ADCY6 in the effects of miR-132 and miR-96 during luteinisation using bovine in vitro luteinised granulosa cells were not successful as transcript levels for the two genes did not change after miRNA inhibition or overexpression. In retrospect, I could also have analysed FOXO1 and ADCY6 protein levels, however, an antibody recognising bovine ADCY6 was not available. Moreover, based on data comparing follicular and luteal tissues (Figure 3.4), I expected FOXO1 transcript levels to decrease during in vitro luteinisation; however, FOXO1 levels did not change (Figure 3.13), which I took as evidence that the in vitro granulosa cell model I was using did not faithfully replicate luteinisation and was therefore not suitable for my studies.

Based on this, I decided to use bovine luteal cell cultures, which did provide useful information on the involvement of FOXO1 (I did not pursue investigating ADCY6 because of the lack of antibodies) on miRNA effects during luteinisation.

Previous studies have shown that in the rodent ovary FOXO1 is mostly localised in follicular tissue but not in CL, and that it mediates granulosa cell apoptosis and proliferation (Shen et al., 2014, Shi and LaPolt, 2003) as well as regulating the expression of LH receptor and VEGF (Hunzicker-Dunn and Maizels, 2006, Liu et al., 2013). Also, FSH and LH suppress the expression of FOXO1 which in turn inhibits apoptosis of cultured granulosa cells (Herndon et al., 2016, Richards et al., 2002, Shen et al., 2014). In my study, an increase in FOXO1 protein level in response to anti-miR-96 in cultured bovine luteal and human luteinised granulosa cells was observed. A recent study showed that, similar to human FOXO1, bovine FOXO1 is a validated target of miR-183-96-182 cluster. In addition, FOXO1 showed a robust decline in the pre-ovulatory dominant follicle compared to subordinate follicle which was opposite to the expression pattern of miR-183-96-182 cluster (Gebremedhn et al., 2015). The same group has shown that inhibition of miR-183-96-182 resulted in an increase in FOXO1 level in bovine non luteinised granulosa cells cultured in DMEM/F-12 medium with 10% FBS. Based on expression of LHR and FSHR, the authors claimed that granulosa cells did not luteinise in their study. However, progesterone and HSD3B, which are strong indicators of luteinisation, were not measured to support their conclusions (Gebremedhn et al., 2016b). Another study showed that the miR-212-132 cluster controls GnRH induction of FSHB expression through targeting SIRT1 deacetylase which in turn promoted acetylation of FOXO1, a transcriptional repressor of FSHB in mouse LβT2 gonadotropes (Lannes et al., 2015).

### 4.3.4 The role of miR-132 and miR-96 in luteal steroidogenesis

In bovine luteinised granulosa cells, I observed a significant reduction in progesterone synthesis in response to miR-132 inhibitor but not to anti-miR-96 or both, while in human luteinised granulosa cells I obtained a significant decrease in progesterone level only after addition of inhibitors for both miRNAs. Sirotkin et al. (2009) showed that transfection of human granulosa cells with a subset of miRNAs including miR-132, miR-96 and miR-183 led to an inhibition of progesterone release while miR-182 promoted the release of progesterone; none of miR-132, miR-96, miR-183 and miR-182 had an effect on oestrogen secretion (Sirotkin et al., 2009). Another study reported that knockdown of miR-132 and miR-212 had no significant effects on progesterone or oestrogen production in mouse granulosa cells (Fiedler et al., 2008). Wu et al. (2015) showed that overexpression of miR-132 had a significant effect on induction of oestrogen synthesis through targeting Nurr1, a negative regulator of *CYP19A1*. Similarly, Sang et al. (2013) found that miR-132 promoted oestrogen production in KGN cell line. These findings were not consistent with my study as there was no significant difference in oestrogen production by transfected human luteinised granulosa cells. Overall, the different results among studies suggest that the effects of these two miRNAs on steroidogenesis may be dependent on the stage of cell differentiation, the species and the level of miRNAs in a cell. Nonetheless, the observation in my study that progesterone levels were effectively changed by these miRNAs in both human and bovine cells provide strong evidence of an involvement in luteal cell steroidogenesis.

Given the reported functions of FOXO1 in granulosa cells, I did not necessarily expect that an increase in FOXO1 levels after inhibition of miRNAs would led to a decrease in progesterone concentrations. Liu et al. (2009) showed that FOXO1 reduced the levels of many genes that are involved in steroid production as well as suppressing transcriptional factors that contribute to cholesterol biosynthesis and steroidogenesis. In contrast, FOXO1 promoted the expression of CYP27A1, a gene that is involved in degradation of cholesterol, in mouse granulosa cells (Liu et al., 2009).

However, these two genes (FOXO1 and CYP27A1) were significantly decreased after administration of FSH and LH in culture or in vivo. These findings suggest that FOXO1 might be involved in regulation of steroidogenesis in rat and mouse granulosa cells. However, I did not detect changes in any of the steroidogenic genes measured in bovine and human cells indicating that the effects of FOXO1 may have involved another mechanism that the one described in mice granulosa cells.

### 4.3.5 The role of miR-132 and miR-96 in proliferation and apoptosis of luteinising cells

Using the Xcelligence system, I observed no significant effects of inhibition or overexpression of miR-132 and miR-96 on bovine granulosa cell proliferation. Previous studies suggested that miR-132 stimulated proliferation of human granulosa cells while miR-183-96-182 cluster inhibited proliferation through targeting PCNA (Sirotkin et al., 2010). Gebremedhn et al. (2016b) showed that overexpression of miR-183-96-182 increased the proliferation of bovine granulosa cells while their inhibition led to a decrease in proliferation. However, a stimulatory effect of these miRNAs during luteinisation is counterintuitive as granulosa cells undergo cycle arrest during luteinisation (reviewed in Richards, 2007). The lack of agreement among studies highlights the need for further studies to clarify the effects, if any, of these miRNA clusters in cell cycle regulation during luteinisation.

The increase of caspase 3/7 activity in bovine luteal and human luteinised granulosa cells after inhibition of miR-96 revealed a novel role for miR-96 in preventing cell apoptosis. Although a previous study reported that up-regulation of miR-96 induced activity of caspase proteins which in turn resulted in a significant apoptosis in rat retinal ganglion cell line RGC-5 cells (Wang and Li, 2014), my results are in agreement with several reports of an involvement of miR-96 in inhibition of cell apoptosis in different cancers through targeting FOXO1 (reviewed in Urbánek and Klotz, 2016).

## 4.4 Proposed model of this study

We have shown that the levels of miR-212-132 and miR-183-96-182 increased dramatically during follicle-luteal transition. I postulated that LH/hGC/FSK mediated transcription of miR-212-132 and miR-183-96-182 clusters through PKA/CREB signalling (Figure 4.1). miR-212-132 and miR-183-96-182 suppress the level of FOXO1 in the luteal cells. Therefore, their inhibitions resulted in an increase in the cell apoptosis and a decrease in the progesterone secretion. However, further studies based on these data are required to fully understand how the progesterone production is controlled by these miRNAs. As gonadotropins in granulosa cells as well as progesterone in luteal cells act as pro-survival factors (Plant and Zeleznik, 2014), and my novel findings raise the possibility that miR-96 (perhaps with the contribution of miR-132) acts as an essential link between LH and progesterone to ensure luteal cell survival and therefore maintenance of the CL (Figure 4.1).

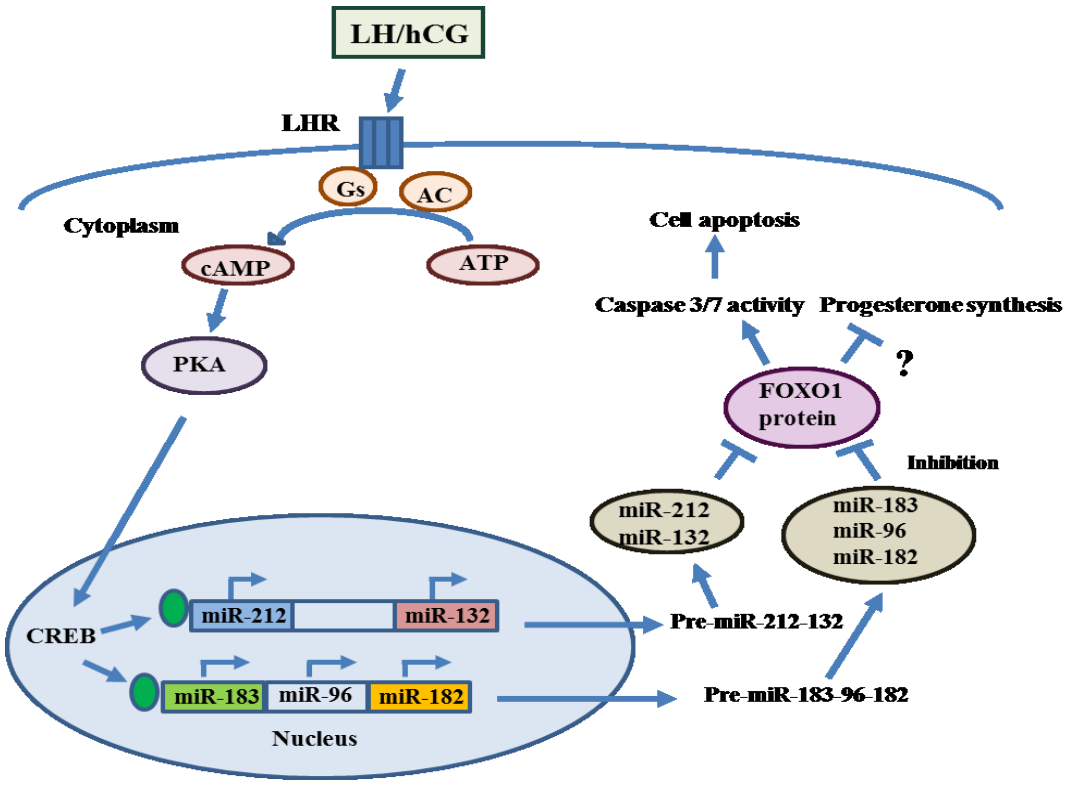


**Figure 4.1 Proposed model of miRNA regulation of granulosa-lutein/large luteal cell survival and steroidogenesis in bovine and women.**

## 4.5 Summary and Conclusion

My findings can be summarised as follows:

- Within the CL, miR-132 and miR-96 are expressed in several cell types, with miR-96 being enriched in the thelial cell fraction.

- miR-212-132 and miR-183-96-182 expression is induced by the adenylate cyclase agonist, Forskolin, consistent with the upregulation of these miRNA clusters by the LH surge in vivo

- The levels of miR-132 and miR-96 can be effectively and specifically down or up-regulated using LNA and mimics, respectively, in bovine and human ovarian cells.

- An in vitro model of bovine granulosa cell luteinisation did not replicate changes in FOXO1 expression occurring during luteinisation in vivo.

- Based on Caspase 3/7 activity, Annexin/PI staining and changes in cell numbers in response to miRNA inhibition, miR-96, possibly in synergy with miR-132, promotes luteal cell survival in both bovine and human. Moreover, results using FOXO siRNA in human cells indicate that those effects are mediated by these miRNAs targeting of FOXO1.

- In both bovine and human, luteinised granulosa cells showed reduced production of progesterone in response to inhibition of miR-132 and miR-96. The stimulatory effects of these miRNAs on progesterone are mediated, at least partially, by targeting of FOXO1.

In conclusion, my results show that the miR-212-132 and miR-183-96-182 clusters regulate important functions in the developing CL, including cellular survival and steroidogenesis, by targeting FOXO1. Moreover, I have shown that these mechanisms are conserved in both bovine and human. This novel information may help the design of new therapies to treat female reproductive disorders and infertility.

## 4.6 Future work

In order to identify further roles of miR-212-132 and miR-183-96-182 during luteinisation, additional target genes from those listed in Table 3.1 should be investigated in the future, for example, Activin A, a member of the transforming growth factor (TGF) superfamily that is expressed in granulosa cells of growing follicle but not luteal cells (Knight et al., 2012). In vitro studies have shown that Activin A suppressed luteinisation of human luteinised granulosa cells by decreasing the levels of LHCGR and StAR (Myers et al., 2008). The effect of inhibition and overexpression of miR-132 and miR-96 in luteinised granulosa cells could be explored in vitro using a similar methodology mentioned in this thesis.

Following from the encouraging results obtained by FACS that showed an increase in the level of miR-96 and miR-183 in endothelial cell of bovine CL. Angiogenesis is a critical process that maintains growth and development of the CL. Moreover, the optimal function of CL is highly related with the development of new blood vessels (Schams and Berisha, 2004), it would be interesting to investigate the function of these miRNAs in luteal angiogenesis through identification and functional analyses of miRNA target genes. A potential approach would be inhibition and overexpression of these miRNAs in endothelial cells followed by microarray or sequencing potential targets associated with luteal angiogenesis. This may provide new insights of the regulatory events that involved in luteal formation.

Recent studies in patients with ovarian disorders highlighted the potential effects of miRNAs on different reproductive disease phenotypes. Polycystic ovarian syndrome (PCOS) patients showed a decline in granulosa cell death. In addition, the level of many factors that inhibit apoptosis are increased in granulosa cells (Das et al., 2008, Dumesic and Richards, 2013, Salvetti et al., 2010). Since I have described herein that miR-96 is an anti-apoptotic factor, it would be interesting to investigate the expression and function of miR-96 in these cystic granulosa cells by examining the effect of suppressing the level of miRNAs through delivery of miRNA inhibitors or antagomiRNAs into ovarian tissue. Studies have shown that using these approaches have in ovarian cancer treatment (Gandhi et al., 2014).

These results may raise the prospect of using miRNAs as biomarkers of Cystic ovarian disease and develop miRNA therapeutic approaches to treat disease.

# Chapter 5

# Literature cited

# Chapter 5: Literature cited

Abd El Naby, W. S., Hagos, T. H., Hossain, M. M., Salilew-Wondim, D., Gad, A. Y., Rings, F., Cinar, M. U., Tholen, E., Looft, C., Schellander, K., Hoelker, M. & Tesfaye, D. 2013. Expression analysis of regulatory microRNAs in bovine cumulus oocyte complex and preimplantation embryos. *Zygote,* 21**,** 31-51.

Accialini, P., Hernandez, S. F., Bas, D., Pazos, M. C., Irusta, G., Abramovich, D. & Tesone, M. 2015. A link between Notch and progesterone maintains the functionality of the rat corpus luteum. *Reproduction,* 149**,** 1-10.

Adams, G. P. 1999. Comparative patterns of follicle development and selection in ruminants. *J Reprod Fertil Suppl,* 54**,** 17-32.

Agarwal, V., Bell, G. W., Nam, J.-W. & Bartel, D. P. 2015. Predicting effective microRNA target sites in mammalian mRNAs. *eLife,* 4**,** e05005.

Ahn, H. W., Morin, R. D., Zhao, H., Harris, R. A., Coarfa, C., Chen, Z.-J., Milosavljevic, A., Marra, M. A. & Rajkovic, A. 2010. MicroRNA transcriptome in the newborn mouse ovaries determined by massive parallel sequencing. *Molecular Human Reproduction,* 16**,** 463-471.

Alila, H. W., Dowd, J. P., Corradino, R. A., Harris, W. V. & Hansel, W. 1988. Control of progesterone production in small and large bovine luteal cells separated by flow cytometry. *Journal of Reproduction and Fertility,* 82**,** 645-655.

Alila, H. W. & Hansel, W. 1984. Origin of different cell types in the bovine corpus luteum as characterized by specific monoclonal antibodies. *Biol Reprod,* 31**,** 1015-25.

Altuvia, Y., Landgraf, P., Lithwick, G., Elefant, N., Pfeffer, S., Aravin, A., Brownstein, M. J., Tuschl, T. & Margalit, H. 2005. Clustering and conservation patterns of human microRNAs. *Nucleic Acids Research,* 33**,** 2697-2706.

Amselgruber, W. M., Schafer, M. & Sinowatz, F. 1999. Angiogenesis in the bovine corpus luteum: an immunocytochemical and ultrastructural study. *Anat Histol Embryol,* 28**,** 157-66.

Andrade, G., Silveira, J., Meirelles, F. & Perecin, F. 2016. Differentially expressed miRNAs in follicular cells and cell-secreted vesicles into the bovine ovarian follicular environment. *Animal Reproduction,* 13**,** 516-516.

Andreas, E., Hoelker, M., Neuhoff, C., Tholen, E., Schellander, K., Tesfaye, D. & Salilew-Wondim, D. 2016. MicroRNA 17-92 cluster regulates proliferation and differentiation of bovine granulosa cells by targeting PTEN and BMPR2 genes. *Cell Tissue Res,* 24**,** 24.

Armstrong, D. G. & Webb, R. 1997. Ovarian follicular dominance: the role of intraovarian growth factors and novel proteins. *Rev Reprod,* 2**,** 139-46.

Assou, S., Al-edani, T., Haouzi, D., Philippe, N., Lecellier, C.-H., Piquemal, D., Commes, T., Aït-Ahmed, O., Dechaud, H. & Hamamah, S. 2013.

MicroRNAs: new candidates for the regulation of the human cumulus–oocyte complex. *Hum Reprod*.

Augustin, H. G. 2001. *Vascular morphogenesis in the female reproductive system*, Springer Science & Business Media.

Babak, T., Zhang, W. E. N., Morris, Q., Blencowe, B. J. & Hughes, T. R. 2004. Probing microRNAs with microarrays: Tissue specificity and functional inference. *Rna-a Publication of the Rna Society,* 10**,** 1813-1819.

Baerwald, A. R., Adams, G. P. & Pierson, R. A. 2003. Characterization of Ovarian Follicular Wave Dynamics in Women. *Biology of Reproduction,* 69**,** 1023-1031.

Baerwald, A. R., Adams, G. P. & Pierson, R. A. 2012. Ovarian antral folliculogenesis during the human menstrual cycle: a review. *Hum Reprod Update,* 18**,** 73-91.

Bartel, D. P. 2009. MicroRNA Target Recognition and Regulatory Functions. *Cell,* 136**,** 215-233.

Batista, M., Torres, A., Diniz, P., Mateus, L. & Lopes-da-Costa, L. 2012. Development of a bovine luteal cell in vitro culture system suitable for co-culture with early embryos. *In Vitro Cellular & Developmental Biology - Animal,* 48**,** 583-592.

Berezikov, E. 2011. Evolution of microRNA diversity and regulation in animals. *Nat Rev Genet,* 12**,** 846-860.

Bertolin, K., Gossen, J., Schoonjans, K. & Murphy, B. D. 2014. The Orphan Nuclear Receptor Nr5a2 Is Essential for Luteinization in the Female Mouse Ovary. *Endocrinology,* 155**,** 1931-1943.

Brachova, P., Hung, W.-T., McGinnis, L. K. & Christenson, L. K. 2016. MicroRNA Regulation of Endocrine Functions in the Ovary. *In:* MENON, K. M. J. & GOLDSTROHM, C. A. (eds.) *Post-transcriptional Mechanisms in Endocrine Regulation.* Cham: Springer International Publishing.

Braw-Tal, R. & Yossefi, S. 1997. Studies in vivo and in vitro on the initiation of follicle growth in the bovine ovary. *J Reprod Fertil,* 109**,** 165-71.

Brown, H. M., Dunning, K. R., Robker, R. L., Boerboom, D., Pritchard, M., Lane, M. & Russell, D. L. 2010. ADAMTS1 Cleavage of Versican Mediates Essential Structural Remodeling of the Ovarian Follicle and Cumulus-Oocyte Matrix During Ovulation in Mice. *Biology of Reproduction,* 83**,** 549-557.

Calin, G., Sevignani, C., Dumitru, C., Hyslop, T., Noch, E., Yendamuri, S., Shimizu, M., Rattan, S., Bullrich, F. & Negrini, M. 2004. Human microRNA genes are frequently located at fragile sites and genomic regions involved in cancers. *Proceedings of the National Academy of Sciences USA,* 101**,** 2999 - 3004.

Campbell, B. K., Clinton, M. & Webb, R. 2012. The role of anti-Müllerian hormone (AMH) during follicle development in a monovulatory species (sheep). *Endocrinology,* 153**,** 4533-4543.

Campbell, B. K., Scaramuzzi, R. J. & Webb, R. 1996. Induction and maintenance of oestradiol and immunoreactive inhibin production with FSH by ovine granulosa cells cultured in serum-free media. *Journal of Reproduction and Fertility,* 106**,** 7-16.

Cao, R., Wu, W., Zhou, X., Liu, K., Li, B., Huang, X., Zhang, Y. & Liu, H. 2015. Let-7g induces granulosa cell apoptosis by targeting MAP3K1 in the porcine ovary. *Int J Biochem Cell Biol,* 68**,** 148-157.

Carletti, M., Fiedler, S. & Christenson, L. 2010. MicroRNA 21 blocks apoptosis in mouse periovulatory granulosa cells. *Biol Reprod,* 83**,** 286 - 95.

Castilho, A. C. S., Nogueira, M. F. G., Fontes, P. K., Machado, M. F., Satrapa, R. A., Razza, E. M. & Barros, C. M. 2014. Ovarian superstimulation using FSH combined with equine chorionic gonadotropin (eCG) upregulates mRNA-encoding proteins involved with LH receptor intracellular signaling in granulosa cells from Nelore cows. *Theriogenology,* 82**,** 1199-1205.

Chatterjee, R., Helal, M., Mobberley, M., Ryder, T. & Bajoria, R. 2014. Impaired steroidogenesis and apoptosis of granulosa-luteal cells in primary culture induced by cis-platinum. *American Journal of Obstetrics and Gynecology,* 210**,** 252.e1-252.e7.

Chi, S. W., Hannon, G. J. & Darnell, R. B. 2012. An alternative mode of microRNA target recognition. *Nat Struct Mol Biol,* 19**,** 321-7.

Chilvers, R. A., Bodenburg, Y. H., Denner, L. A. & Urban, R. J. 2012. Development of a novel protocol for isolation and purification of human granulosa cells. *Journal of Assisted Reproduction and Genetics,* 29**,** 547-556.

Choi, J. & Smitz, J. 2014. Luteinizing hormone and human chorionic gonadotropin: distinguishing unique physiologic roles. *Gynecological Endocrinology,* 30**,** 174-181.

Choudhary, E., Sen, A., Inskeep, E. K. & Flores, J. A. 2005. Developmental Sensitivity of the Bovine Corpus Luteum to Prostaglandin F2α (PGF2α) and Endothelin-1 (ET-1): Is ET-1 a Mediator of the Luteolytic Actions of PGF2α or a Tonic Inhibitor of Progesterone Secretion? *Biology of Reproduction,* 72**,** 633-642.

Conaco, C., Otto, S., Han, J. J. & Mandel, G. 2006. Reciprocal actions of REST and a microRNA promote neuronal identity. *Proc Natl Acad Sci U S A,* 103**,** 2422-7.

da Silveira, J. C., Veeramachaneni, D. N., Winger, Q. A., Carnevale, E. M. & Bouma, G. J. 2012. Cell-secreted vesicles in equine ovarian follicular fluid contain miRNAs and proteins: a possible new form of cell communication within the ovarian follicle. *Biol Reprod,* 86.

Dai, A., Sun, H., Fang, T., Zhang, Q., Wu, S., Jiang, Y., Ding, L., Yan, G. & Hu, Y. 2013. MicroRNA-133b stimulates ovarian estradiol synthesis by targeting Foxl2. *FEBS Lett,* 587**,** 2474-82.

Dambal, S., Shah, M., Mihelich, B. & Nonn, L. 2015. The microRNA-183 cluster: the family that plays together stays together. *Nucleic Acids Research*.

Dangwal, S. & Thum, T. 2012. MicroRNAs in platelet biogenesis and function. *Thrombosis and haemostasis,* 108**,** 599.

Das, M., Djahanbakhch, O., Hacihanefioglu, B., Saridogan, E., Ikram, M., Ghali, L., Raveendran, M. & Storey, A. 2008. Granulosa cell survival and proliferation are altered in polycystic ovary syndrome. *J Clin Endocrinol Metab,* 93**,** 881-7.

Davis, J. S., Rueda, B. R. & Spanel-Borowski, K. 2003. Microvascular endothelial cells of the corpus luteum. *Reprod Biol Endocrinol,* 1**,** 89-89.

de Mello Bianchi, P. H., Serafini, P., Monteiro da Rocha, A., Assad Hassun, P., Alves da Motta, E. L., Sampaio Baruselli, P. & Chada Baracat, E. 2010. Review: Follicular Waves in the Human Ovary: A New Physiological Paradigm for Novel Ovarian Stimulation Protocols. *Reproductive Sciences,* 17**,** 1067-1076.

Donadeu, F. X., Schauer, S. N. & Sontakke, S. D. 2012. Involvement of miRNAs in ovarian follicular and luteal development. *Journal of Endocrinology,* 215**,** 323-334.

Dong, J. C., Dong, H., Campana, A. & Bischof, P. 2002. Matrix metalloproteinases and their specific tissue inhibitors in menstruation. *Reproduction,* 123**,** 621-31.

Dongen, S. & Enright, A. 2014. Detecting MicroRNA Signatures Using Gene Expression Analysis. *In:* KASABOV, N. (ed.) *Springer Handbook of Bio-/Neuroinformatics*. Springer Berlin Heidelberg.

Doyle, L. K., Walker, C. A. & Donadeu, F. X. 2010. VEGF modulates the effects of gonadotropins in granulosa cells. *Domestic Animal Endocrinology,* 38**,** 127-137.

Du, X., Li, Q., Pan, Z. & Li, Q. 2016. AR and miRNA-126* axis controls FSHR expression in porcine ovarian granulosa cells. *Reproduction,* 24**,** 15-0517.

Du, Z.-W., Ma, L.-X., Phillips, C. & Zhang, S.-C. 2013. miR-200 and miR-96 families repress neural induction from human embryonic stem cells. *Development,* 140**,** 2611-2618.

Dumesic, D. A. & Richards, J. S. 2013. Ontogeny of the ovary in polycystic ovary syndrome. *Fertil Steril,* 100**,** 23-38.

Duncan, W., Myers, M., Dickinson, R., Van Den Driesche, S. & Fraser, H. 2009. Paracrine regulation of luteal development and luteolysis in the primate. *Anim Reprod,* 6**,** 34-46.

Duncan, W. C., Gay, E. & Maybin, J. A. 2005. The effect of human chorionic gonadotrophin on the expression of progesterone receptors in human luteal cells in vivo and in vitro. *Reproduction,* 130**,** 83-93.

Erickson, B. H. 1966. Development and Radio-Response of the Prenatal Bovine Ovary. *Reproduction,* 11**,** 97-105.

Eroschenko, V. P. & Di Fiore, M. S. 2013. *DiFiore's atlas of histology with functional correlations*, Lippincott Williams & Wilkins.

Eskildsen, T. V., Schneider, M., Sandberg, M. B., Skov, V., Brønnum, H., Thomassen, M., Kruse, T. A., Andersen, D. C. & Sheikh, S. P. 2014. The microRNA-132/212 family fine-tunes multiple targets in Angiotensin II signalling in cardiac fibroblasts. *Journal of Renin-Angiotensin-Aldosterone System*.

Fassl, A., Tagscherer, K. E., Richter, J., De-Castro Arce, J., Savini, C., Rosl, F. & Roth, W. 2015. Inhibition of Notch1 signaling overcomes resistance to the death ligand Trail by specificity protein 1-dependent upregulation of death receptor 5. *Cell Death Dis,* 6**,** e1921.

Feng, R., Sang, Q., Zhu, Y., Fu, W., Liu, M., Xu, Y., Shi, H., Xu, Y., Qu, R., Chai, R., Shao, R., Jin, L., He, L., Sun, X. & Wang, L. 2015. MiRNA-320 in the human follicular fluid is associated with embryo quality in vivo and affects mouse embryonic development in vitro. *Sci Rep,* 5.

Fiedler, S., Carletti, M., Hong, X. & Christenson, L. 2008. Hormonal regulation of MicroRNA expression in periovulatory mouse mural granulosa cells. *Biol Reprod,* 79**,** 1030 - 7.

Flemr, M., Malik, R., Franke, V., Nejepinska, J., Sedlacek, R., Vlahovicek, K. & Svoboda, P. 2013. A retrotransposon-driven dicer isoform directs endogenous small interfering RNA production in mouse oocytes. *Cell,* 155**,** 807-16.

Forabosco, A., Sforza, C., De Pol, A., Vizzotto, L., Marzona, L. & Ferrario, V. F. 1991. Morphometric study of the human neonatal ovary. *The Anatomical Record,* 231**,** 201-208.

Forde, N., Beltman, M. E., Lonergan, P., Diskin, M., Roche, J. F. & Crowe, M. A. 2011. Oestrous cycles in Bos taurus cattle. *Anim Reprod Sci,* 124**,** 163-9.

Fortune, J., Sirois, J., Turzillo, A. & Lavoir, M. 1990. Follicle selection in domestic ruminants. *Journal of reproduction and fertility. Supplement,* 43**,** 187-198.

Frandson, R. D., Wilke, W. L. & Fails, A. D. 2009. *Anatomy and physiology of farm animals*, John Wiley & Sons.

Fridén, B. E., Hagström, H.-G., Lindblom, B., Sjöblom, P., Wallin, A., Brännström, M. & Hahlin, M. 1999. Cell characteristics and function of two enriched fraction of human luteal cells prolonged culture. *Molecular Human Reproduction,* 5**,** 714-719.

Galv, #xe3, o, A., #xf3, M., n., Ferreira-Dias, G., #xe7 & Skarzynski, D. J. 2013. Cytokines and Angiogenesis in the Corpus Luteum. *Mediators of Inflammation,* 2013**,** 11.

Gandhi, N. S., Tekade, R. K. & Chougule, M. B. 2014. Nanocarrier mediated Delivery of siRNA/miRNA in Combination with Chemotherapeutic Agents for Cancer Therapy: Current Progress and Advances. *Journal of controlled release : official journal of the Controlled Release Society,* 0**,** 238-256.

Gaytán, F., Morales, C., García-Pardo, L., Reymundo, C., Bellido, C. & Sánchez-Criado, J. E. 1999. A Quantitative Study of Changes in the Human Corpus Luteum Microvasculature during the Menstrual Cycle. *Biology of Reproduction,* 60**,** 914-919.

Gebremedhn, S., Pandey, H., Salilew-Wondim, D., Hoelker, M., Schellander, K. & Tesfaye, D. 2016a. Dynamics and role of MicroRNAs during mammalian follicular development. *Anim. Reprod,* 13**,** 257-263.

Gebremedhn, S., Salilew-Wondim, D., Ahmad, I., Sahadevan, S., Hossain, M. M., Hoelker, M., Rings, F., Neuhoff, C., Tholen, E., Looft, C., Schellander, K. & Tesfaye, D. 2015. MicroRNA Expression Profile in Bovine Granulosa Cells of Preovulatory Dominant and Subordinate Follicles during the Late Follicular Phase of the Estrous Cycle. *PLoS One,* 10**,** e0125912.

Gebremedhn, S., Salilew-Wondim, D., Hoelker, M., Rings, F., Neuhoff, C., Tholen, E., Schellander, K. & Tesfaye, D. 2016b. MicroRNA-183~96~182 Cluster Regulate Bovine Granulosa Cell Proliferation and Cell Cycle Transition by Coordinately Targeting FOXO1. *Biology of Reproduction*.

Gilchrist, G., Tscherner, A., Nalpathamkalam, T., Merico, D. & LaMarre, J. 2016. MicroRNA Expression during Bovine Oocyte Maturation and Fertilization. *Int J Mol Sci,* 17**,** 396.

Ginther, O., Beg, M., Bergfelt, D., Donadeu, F. & Kot, K. 2001. Follicle selection in monovular species. *Biology of Reproduction,* 65**,** 638-647.

Ginther, O., Wiltbank, M., Fricke, P., Gibbons, J. & Kot, K. 1996. Selection of the dominant follicle in cattle. *Biology of Reproduction,* 55**,** 1187-1194.

Ginther, O. J., Gastal, E. L., Gastal, M. O., Bergfelt, D. R., Baerwald, A. R. & Pierson, R. A. 2004. Comparative Study of the Dynamics of Follicular Waves in Mares and Women. *Biology of Reproduction,* 71**,** 1195-1201.

Gutiérrez, C. G., Campbell, B. K. & Webb, R. 1997a. Development of a long-term bovine granulosa cell culture system: induction and maintenance of estradiol production, response to follicle-stimulating hormone, and morphological characteristics. *Biology of Reproduction,* 56**,** 608-616.

Gutiérrez, C. G., Oldham, J., Bramley, T. A., Gong, J. G., Campbell, B. K. & Webb, R. 1997b. The recruitment of ovarian follicles is enhanced by increased dietary intake in heifers. *J Anim Sci,* 75**,** 1876-1884.

Ha, M. & Kim, V. N. 2014. Regulation of microRNA biogenesis. *Nature reviews Molecular cell biology,* 15**,** 509-524.

Hafner, M., Landthaler, M., Burger, L., Khorshid, M., Hausser, J., Berninger, P., Rothballer, A., Ascano, M., Jr., Jungkamp, A. C., Munschauer, M., Ulrich, A., Wardle, G. S., Dewell, S., Zavolan, M. & Tuschl, T. 2010. Transcriptome-wide identification of RNA-binding protein and microRNA target sites by PAR-CLIP. *Cell,* 141**,** 129-41.

Helwak, A., Kudla, G., Dudnakova, T. & Tollervey, D. 2013. Mapping the human miRNA interactome by CLASH reveals frequent noncanonical binding. *Cell,* 153**,** 654-65.

Helwak, A. & Tollervey, D. 2014. Mapping the miRNA interactome by cross-linking ligation and sequencing of hybrids (CLASH). *Nat Protoc,* 9**,** 711-28.

Herndon, M. K., Law, N. C., Donaubauer, E. M., Kyriss, B. & Hunzicker-Dunn, M. 2016. Forkhead box O member FOXO1 regulates the majority of follicle-stimulating hormone responsive genes in ovarian granulosa cells. *Molecular and Cellular Endocrinology,* 434**,** 116-126.

Hornstein, E. 2012. *MicroRNAs in development*, Academic Press.

Hossain, M. M., Ghanem, N., Hoelker, M., Rings, F., Phatsara, C., Tholen, E., Schellander, K. & Tesfaye, D. 2009. Identification and characterization of miRNAs expressed in the bovine ovary. *BMC genomics,* 10**,** 1.

Hu, X., Pokharel, K., Peippo, J., Ghanem, N., Zhaboyev, I., Kantanen, J. & Li, M. H. 2016. Identification and characterization of miRNAs in the ovaries of a highly prolific sheep breed. *Anim Genet,* 47**,** 234-9.

Hu, Z., Shen, W.-J., Kraemer, F. B. & Azhar, S. 2012. MicroRNAs 125a and 455 Repress Lipoprotein-Supported Steroidogenesis by Targeting Scavenger Receptor Class B Type I in Steroidogenic Cells. *Molecular and Cellular Biology,* 32**,** 5035-5045.

Hu, Z., Shen, W., Cortez, Y., Tang, X., Liu, L. & Kraemer, F. 2013. Hormonal regulation of microRNA expression in steroid producing cells of the ovary, testis and adrenal gland. *PLoS One,* 8**,** e78040.

Huang, J., Ju, Z., Li, Q., Hou, Q., Wang, C., Li, J., Li, R., Wang, L., Sun, T., Hang, S., Gao, Y., Hou, M. & Zhong, J. 2011. Solexa sequencing of novel and differentially expressed microRNAs in testicular and ovarian tissues in Holstein cattle. *Int J Biol Sci,* 7**,** 1016-26.

Hunzicker-Dunn, M. & Maizels, E. T. 2006. FSH signaling pathways in immature granulosa cells that regulate target gene expression: Branching out from protein kinase A. *Cellular signalling,* 18**,** 1351-1359.

Impey, S., McCorkle, S. R., Cha-Molstad, H., Dwyer, J. M., Yochum, G. S., Boss, J. M., McWeeney, S., Dunn, J. J., Mandel, G. & Goodman, R. H. 2004. Defining the CREB regulon: a genome-wide analysis of transcription factor regulatory regions. *Cell,* 119**,** 1041-54.

Ireland, J. J., Murphee, R. L. & Coulson, P. B. 1980. Accuracy of Predicting Stages of Bovine Estrous Cycle by Gross Appearance of the Corpus Luteum1. *Journal of Dairy Science,* 63**,** 155-160.

Irving-Rodgers, H. F., van Wezel, I. L., Mussard, M. L., Kinder, J. E. & Rodgers, R. J. 2001. Atresia revisited: two basic patterns of atresia of bovine antral follicles. *Reproduction,* 122**,** 761-75.

Jaffe, L. A. & Norris, R. P. 2010. Initiation of the meiotic prophase-to-metaphase transition in mammalian oocytes. *Oogenesis: The universal process (ed. Verlhac MH, Villenuve A)***,** 181-198.

Jones, L. S., Ottobre, J. S. & Pate, J. L. 1992. Progesterone regulation of luteinizing hormone receptors on cultured bovine luteal cells. *Mol Cell Endocrinol,* 85**,** 33-9.

Jones, P. B., Welsh, T. H., Jr. & Hsueh, A. J. 1982. Regulation of ovarian progestin production by epidermal growth factor in cultured rat granulosa cells. *J Biol Chem,* 257**,** 11268-73.

Juengel, J. L., Sawyer, H. R., Smith, P. R., Quirke, L. D., Heath, D. A., Lun, S., Wakefield, S. J. & McNatty, K. P. 2002. Origins of follicular cells and ontogeny of steroidogenesis in ovine fetal ovaries. *Mol Cell Endocrinol,* 191**,** 1-10.

Kim, S., Hata, A. & Kang, H. 2014. Down-regulation of miR-96 by bone morphogenetic protein signaling is critical for vascular smooth muscle cell phenotype modulation. *J Cell Biochem,* 115**,** 889-95.

Kitahara, Y., Nakamura, K., Kogure, K. & Minegishi, T. 2013. Role of microRNA-136-3p on the expression of luteinizing hormone-human chorionic gonadotropin receptor mRNA in rat ovaries. *Biol Reprod,* 89.

Knight, P. G., Satchell, L. & Glister, C. 2012. Intra-ovarian roles of activins and inhibins. *Mol Cell Endocrinol,* 359**,** 53-65.

Kondkar, A. A., Bray, M. S., Leal, S. M., Nagalla, S., Liu, D. J., Jin, Y., Dong, J. F., Ren, Q., Whiteheart, S. W., Shaw, C. & Bray, P. F. 2010. VAMP8/endobrevin is overexpressed in hyperreactive human platelets: suggested role for platelet microRNA. *J Thromb Haemost,* 8**,** 369-78.

Koshiol, J., Wang, E., Zhao, Y., Marincola, F. & Landi, M. T. 2010. Strengths and limitations of laboratory procedures for microRNA detection. *Cancer Epidemiology Biomarkers & Prevention,* 19**,** 907-911.

Kühnel, W. & Kuhnel, W. 2003. *Color atlas of cytology, histology, and microscopic anatomy*, Stuttgart; New York: Thieme.

Kumarswamy, R., Volkmann, I., Beermann, J., Napp, L. C., Jabs, O., Bhayadia, R., Melk, A., Ucar, A., Chowdhury, K., Lorenzen, J. M., Gupta, S. K., Batkai, S. & Thum, T. 2014. Vascular importance of the miR-212/132 cluster. *Eur Heart J,* 35**,** 3224-3231.

Landgraf, P., Rusu, M., Sheridan, R., Sewer, A., Iovino, N., Aravin, A., Pfeffer, S., Rice, A., Kamphorst, A. O., Landthaler, M., Lin, C., Socci, N. D., Hermida, L., Fulci, V., Chiaretti, S., Foà, R., Schliwka, J., Fuchs, U., Novosel, A., Müller, R.-U., Schermer, B., Bissels, U., Inman, J., Phan, Q., Chien, M., Weir, D. B., Choksi, R., De Vita, G., Frezzetti, D., Trompeter, H.-I., Hornung, V., Teng, G., Hartmann, G., Palkovits, M., Di Lauro, R., Wernet, P., Macino, G., Rogler, C. E., Nagle, J. W., Ju, J., Papavasiliou, F. N., Benzing, T., Lichter, P., Tam, W., Brownstein, M. J., Bosio, A., Borkhardt, A., Russo, J. J., Sander, C., Zavolan, M. & Tuschl, T. 2007. A Mammalian microRNA Expression Atlas Based on Small RNA Library Sequencing. *Cell,* 129**,** 1401-1414.

Lannes, J., L'Hôte, D., Garrel, G., Laverrière, J.-N., Cohen-Tannoudji, J. & Quérat, B. 2015. Rapid Communication: A MicroRNA-132/212 Pathway Mediates GnRH Activation of FSH Expression. *Molecular Endocrinology,* 29**,** 364-372.

Lee, Y., Jeon, K., Lee, J., Kim, S. & Kim, V. 2002. MicroRNA maturation: stepwise processing and subcellular localization. *EMBO J,* 21**,** 4663 - 4670.

Lei, L., Jin, S., Gonzalez, G., Behringer, R. R. & Woodruff, T. K. 2010. The regulatory role of Dicer in folliculogenesis in mice. *Molecular and Cellular Endocrinology,* 315**,** 63-73.

Lei, Z. M., Chegini, N. & Rao, C. V. 1991. Quantitative cell composition of human and bovine corpora lutea from various reproductive states. *Biology of Reproduction,* 44**,** 1148-1156.

Li, C., Chen, C., Chen, L., Chen, S., Li, H., Zhao, Y., Rao, J. & Zhou, X. 2016. BDNF-induced expansion of cumulus oocyte complexes in pigs was mediated by microRNA-205. *Theriogenology*.

Li, M., Liu, Y., Wang, T., Guan, J., Luo, Z., Chen, H., Wang, X., Chen, L., Ma, J., Mu, Z., Jiang, A. A., Zhu, L., Lang, Q., Zhou, X., Wang, J., Zeng, W., Li, N., Li, K., Gao, X. & Li, X. 2011. Repertoire of porcine microRNAs in adult ovary and testis by deep sequencing. *Int J Biol Sci,* 7**,** 1045-55.

Libri, V., Helwak, A., Miesen, P., Santhakumar, D., Borger, J. G., Kudla, G., Grey, F., Tollervey, D. & Buck, A. H. 2012. Murine cytomegalovirus encodes a miR-27 inhibitor disguised as a target. *Proceedings of the National Academy of Sciences of the United States of America,* 109**,** 279-284.

Lim, H., Paria, B. C., Das, S. K., Dinchuk, J. E., Langenbach, R., Trzaskos, J. M. & Dey, S. K. 1997. Multiple Female Reproductive Failures in Cyclooxygenase 2–Deficient Mice. *Cell,* 91**,** 197-208.

Lin, F., Li, R., Pan, Z. X., Zhou, B., Yu de, B., Wang, X. G., Ma, X. S., Han, J., Shen, M. & Liu, H. L. 2012. miR-26b promotes granulosa cell apoptosis by targeting ATM during follicular atresia in porcine ovary. *PLoS ONE,* 7**,** 21.

Lingenfelter, B. M., Tripurani, S. K., Tejomurtula, J., Smith, G. W. & Yao, J. 2011. Molecular cloning and expression of bovine nucleoplasmin 2 (NPM2): a maternal effect gene regulated by miR-181a. *Reprod Biol Endocrinol,* 9**,** 40-40.

Liu, J., Tu, F., Yao, W., Li, X., Xie, Z., Liu, H., Li, Q. & Pan, Z. 2016. Conserved miR-26b enhances ovarian granulosa cell apoptosis through HAS2-HA-CD44-Caspase-3 pathway by targeting HAS2. *Sci Rep,* 6.

Liu, J., Yao, W., Yao, Y., Du, X., Zhou, J., Ma, B., Liu, H., Li, Q. & Pan, Z. 2014. MiR-92a inhibits porcine ovarian granulosa cell apoptosis by targeting Smad7 gene. *FEBS Lett,* 588**,** 4497-4503.

Liu, Y. X. 1999. Regulation of the plasminogen activator system in the ovary. *Biol Signals Recept,* 8**,** 160-77.

Liu, Z., Castrillon, D. H., Zhou, W. & Richards, J. S. 2013. FOXO1/3 depletion in granulosa cells alters follicle growth, death and regulation of pituitary FSH. *Mol Endocrinol,* 27**,** 238-52.

Liu, Z., Rudd, M. D., Hernandez-Gonzalez, I., Gonzalez-Robayna, I., Fan, H.-Y., Zeleznik, A. J. & Richards, J. S. 2009. FSH and FOXO1 Regulate Genes in the Sterol/Steroid and Lipid Biosynthetic Pathways in Granulosa Cells. *Molecular Endocrinology,* 23**,** 649-661.

Lonergan, P. & Forde, N. 2015. The Role of Progesterone in Maternal Recognition of Pregnancy in Domestic Ruminants. *Adv Anat Embryol Cell Biol,* 216**,** 87-104.

Lucy, M. C. 2007. The bovine dominant ovarian follicle. *Journal of Animal Science,* 85**,** E89-E99.

Lumayag, S., Haldin, C. E., Corbett, N. J., Wahlin, K. J., Cowan, C., Turturro, S., Larsen, P. E., Kovacs, B., Witmer, P. D., Valle, D., Zack, D. J., Nicholson, D. A. & Xu, S. 2013. Inactivation of the microRNA-183/96/182 cluster results in syndromic retinal degeneration. *Proc Natl Acad Sci U S A,* 110**,** 22.

Lussier, J. G., Matton, P. & Dufour, J. J. 1987. Growth rates of follicles in the ovary of the cow. *J Reprod Fertil,* 81**,** 301-7.

Ma, T., Jiang, H., Gao, Y., Zhao, Y., Dai, L., Xiong, Q., Xu, Y., Zhao, Z. & Zhang, J. 2011. Microarray analysis of differentially expressed microRNAs in non-regressed and regressed bovine corpus luteum tissue; microRNA-378 may suppress luteal cell apoptosis by targeting the interferon gamma receptor 1 gene. *J Appl Genet,* 52**,** 481-6.

Maalouf, S., Smith, C. & Pate, J. L. 2016a. Changes in MicroRNA Expression During Maturation of the Bovine Corpus Luteum: Regulation of Luteal Cell Proliferation and Function by MicroRNA-34a. *Biol Reprod,* 10**,** 135053.

Maalouf, S. W., Liu, W.-S., Albert, I. & Pate, J. L. 2014. Regulating life or death: Potential role of microRNA in rescue of the corpus luteum. *Mol Cell Endocrinol,* 398**,** 78-88.

Maalouf, S. W., Liu, W. S. & Pate, J. L. 2016b. MicroRNA in ovarian function. *Cell Tissue Res,* 363**,** 7-18.

Mahdipour, M., van Tol, H. T. A., Stout, T. A. E. & Roelen, B. A. J. 2015. Validating reference microRNAs for normalizing qRT-PCR data in bovine oocytes and preimplantation embryos. *BMC Dev Biol,* 15**,** 1-10.

Malm, H. A., Mollet, I. G., Berggreen, C., Orho-Melander, M., Esguerra, J. L., Goransson, O. & Eliasson, L. 2016. Transcriptional regulation of the miR-212/miR-132 cluster in insulin-secreting beta-cells by cAMP-regulated transcriptional co-activator 1 and salt-inducible kinases. *Mol Cell Endocrinol,* 424**,** 23-33.

Maroni, D. & Davis, J. S. 2011. TGFB1 disrupts the angiogenic potential of microvascular endothelial cells of the corpus luteum. *Journal of Cell Science,* 124**,** 2501-2510.

Martins, R., Lithgow, G. J. & Link, W. 2016. Long live FOXO: unraveling the role of FOXO proteins in aging and longevity. *Aging Cell,* 15**,** 196-207.

Mathelier, A. & Carbone, A. 2013. Large scale chromosomal mapping of human microRNA structural clusters. *Nucleic Acids Research,* 41**,** 4392-4408.

Mayes, M. 2002. The meiotic arrest of bovine oocytes.

McBride, D., Carré, W., Sontakke, S. D., Hogg, C. O., Law, A., Donadeu, F. X. & Clinton, M. 2012. Identification of miRNAs associated with the follicular–luteal transition in the ruminant ovary. *Reproduction,* 144**,** 221-233.

McGee, E. A. & Hsueh, A. J. W. 2000. Initial and Cyclic Recruitment of Ovarian Follicles. *Endocrine Reviews,* 21**,** 200-214.

Mehlmann, L. M. 2005. Oocyte-specific expression of Gpr3 is required for the maintenance of meiotic arrest in mouse oocytes. *Developmental Biology,* 288**,** 397-404.

Meidan, R., Girsh, E., Blum, O. & Aberdam, E. 1990. In vitro differentiation of bovine theca and granulosa cells into small and large luteal-like cells: morphological and functional characteristics. *Biology of Reproduction,* 43**,** 913-921.

Meidan, R., Levy, N., Kisliouk, T., Podlovny, L., Rusiansky, M. & Klipper, E. 2005. The yin and yang of corpus luteum-derived endothelial cells: balancing life and death. *Domest Anim Endocrinol,* 29**,** 318-28.

Menon, B., Gulappa, T. & Menon, K. M. 2015. miR-122 Regulates LH Receptor Expression by Activating Sterol Response Element Binding Protein in Rat Ovaries. *Endocrinology,* 156**,** 3370-80.

Menon, B., Sinden, J., Franzo-Romain, M., Botta, R. B. & Menon, K. M. J. 2013. Regulation of LH Receptor mRNA Binding Protein by miR-122 in Rat Ovaries. *Endocrinology,* 154**,** 4826-4834.

Mihm, M., Gangooly, S. & Muttukrishna, S. 2011. The normal menstrual cycle in women. *Anim Reprod Sci,* 124**,** 229-36.

Miles, J., McDaneld, T., Wiedmann, R., Cushman, R., Echternkamp, S., Vallet, J. & Smith, T. 2012. MicroRNA expression profile in bovine cumulus–oocyte complexes: Possible role of let-7 and miR-106a in the development of bovine oocytes. *Anim Reprod Sci,* 130**,** 16-26.

Miranda, L. 2010. Regulation of cholesterol intake by the corpus luteum.

Mishima, T., Takizawa, T., Luo, S.-S., Ishibashi, O., Kawahigashi, Y., Mizuguchi, Y., Ishikawa, T., Mori, M., Kanda, T., Goto, T. & Takizawa, T. 2008. MicroRNA (miRNA) cloning analysis reveals sex differences in miRNA expression profiles between adult mouse testis and ovary. *Reproduction,* 136**,** 811-822.

Moreno, J. M., Núñez, M. J., Quiñonero, A., Martínez, S., de la Orden, M., Simón, C., Pellicer, A., Díaz-García, C. & Domínguez, F. Follicular fluid and mural granulosa cells microRNA profiles vary in in vitro fertilization patients depending on their age and oocyte maturation stage. *Fertil Steril,* 104**,** 1037-1046.e1.

Murchison, E. P., Stein, P., Xuan, Z., Pan, H., Zhang, M. Q., Schultz, R. M. & Hannon, G. J. 2007. Critical roles for Dicer in the female germline. *Genes & Development,* 21**,** 682-693.

Myers, M., van den Driesche, S., McNeilly, A. S. & Duncan, W. C. 2008. Activin A reduces luteinisation of human luteinised granulosa cells and has opposing effects to human chorionic gonadotropin in vitro. *J Endocrinol,* 199**,** 201-12.

Nagaraja, A. K., Andreu-Vieyra, C., Franco, H. L., Ma, L., Chen, R., Han, D. Y., Zhu, H., Agno, J. E., Gunaratne, P. H., DeMayo, F. J. & Matzuk, M. M. 2008. Deletion of Dicer in Somatic Cells of the Female Reproductive Tract Causes Sterility. *Molecular Endocrinology,* 22**,** 2336-2352.

Nam, J. W., Rissland, O. S., Koppstein, D., Abreu-Goodger, C., Jan, C. H., Agarwal, V., Yildirim, M. A., Rodriguez, A. & Bartel, D. P. 2014. Global analyses of the effect of different cellular contexts on microRNA targeting. *Mol Cell,* 53**,** 1031-43.

Nie, M., Yu, S., Peng, S., Fang, Y., Wang, H. & Yang, X. 2015. miR-23a and miR-27a Promote Human Granulosa Cell Apoptosis by Targeting SMAD5. *Biology of Reproduction,* 93**,** 98, 1-10.

Nielsen, B. S. 2012. MicroRNA in situ hybridization. *Methods Mol Biol,* 822**,** 67-84.

Niswender, G. D., Juengel, J. L., McGuire, W. J., Belfiore, C. J. & Wiltbank, M. C. 1994. Luteal function: the estrous cycle and early pregnancy. *Biol Reprod,* 50**,** 239-47.

O'Shea, J. D., Rodgers, R. J. & D'Occhio, M. J. 1989. Cellular composition of the cyclic corpus luteum of the cow. *Journal of Reproduction and Fertility,* 85**,** 483-487.

Okuda, K., Miyamoto, A., Sauerwein, H., Schweigert, F. J. & Schams, D. 1992. Evidence for oxytocin receptors in cultured bovine luteal cells. *Biol Reprod,* 46**,** 1001-6.

Otsuka, M., Zheng, M., Hayashi, M., Lee, J. D., Yoshino, O., Lin, S. & Han, J. 2008. Impaired microRNA processing causes corpus luteum insufficiency and infertility in mice. *J Clin Invest,* 118**,** 1944-54.

Pan, B., Toms, D., Shen, W. & Li, J. 2015. MicroRNA-378 regulates oocyte maturation via the suppression of aromatase in porcine cumulus cells. *American Journal of Physiology - Endocrinology and Metabolism*.

Papaioannou, G., Lisse, T. & Kobayashi, T. 2015. Chapter 14 - miRNAs in Bone Formation and Homeostasis A2 - Sen, Chandan K. *MicroRNA in Regenerative Medicine.* Oxford: Academic Press.

Park, J.-K., Henry, J. C., Jiang, J., Esau, C., Gusev, Y., Lerner, M. R., Postier, R. G., Brackett, D. J. & Schmittgen, T. D. 2011. miR-132 and miR-212 are increased in pancreatic cancer and target the retinoblastoma tumor suppressor. *Biochem Biophys Res Commun,* 406**,** 518-523.

Pate, J. L. & Condon, W. A. 1982. Effects of serum and lipoproteins on steroidogenesis in cultured bovine luteal cells. *Molecular and Cellular Endocrinology,* 28**,** 551-562.

Pate, J. L. & Landis Keyes, P. 2001. Immune cells in the corpus luteum: friends or foes? *Reproduction,* 122**,** 665-76.

Pelletier, G., Li, S., Luu-The, V., Tremblay, Y., Belanger, A. & Labrie, F. 2001. Immunoelectron microscopic localization of three key steroidogenic enzymes (cytochrome P450(scc), 3 beta-hydroxysteroid dehydrogenase and cytochrome P450(c17)) in rat adrenal cortex and gonads. *Journal of Endocrinology,* 171**,** 373-383.

Peng, J. Y., An, X. P., Fang, F., Gao, K. X., Xin, H. Y., Han, P., Bao, L. J., Ma, H. D. & Cao, B. Y. 2016. MicroRNA-10b suppresses goat granulosa cell proliferation by targeting brain-derived neurotropic factor. *Domest Anim Endocrinol,* 54**,** 60-67.

Peters, H. 1969. The development of the mouse ovary from birth to maturity. *Acta Endocrinol,* 62**,** 98-116.

Pierce, M. L., Weston, M. D., Fritzsch, B., Gabel, H. W., Ruvkun, G. & Soukup, G. A. 2008. MicroRNA-183 family conservation and ciliated neurosensory organ expression. *Evol Dev,* 10**,** 106-13.

Plant, T. M. & Zeleznik, A. J. 2014. *Knobil and Neill's Physiology of Reproduction: Two-Volume Set*, Academic Press.

Pritchard, C. C., Cheng, H. H. & Tewari, M. 2012. MicroRNA profiling: approaches and considerations. *Nat Rev Genet,* 13**,** 358-369.

Qu, X., Chen, Z., Fan, D., Sun, C. & Zeng, Y. 2016. MiR-132-3p Regulates the Osteogenic Differentiation of Thoracic Ligamentum Flavum Cells by Inhibiting Multiple Osteogenesis-Related Genes. *International Journal of Molecular Sciences,* 17**,** 1370.

Quezada, M., Wang, J., Hoang, V. & McGee, E. A. 2012. Smad7 is a transforming growth factor-beta-inducible mediator of apoptosis in granulosa cells. *Fertil Steril,* 97**,** 1452-9.

Quinlan, S. & Jimenez-Mateos, E. M. 2016. Can we protect the brain via preconditioning? Role of microRNAs in neuroprotection. *Neural Regeneration Research,* 11**,** 388-389.

Quirk, S. M., Cowan, R. G. & Harman, R. M. 2013. Role of the cell cycle in regression of the corpus luteum. *Reproduction,* 145**,** 161-175.

Redmer, D., Doraiswamy, V., Bortnem, B., Fisher, K., Jablonka-Shariff, A., Grazul-Bilska, A. & Reynolds, L. 2001. Evidence for a role of capillary pericytes in vascular growth of the developing ovine corpus luteum. *Biol Reprod,* 65**,** 879 - 89.

Rekawiecki, R., Kowalik, M. K., Slonina, D. & Kotwica, J. 2008. Regulation of progesterone synthesis and action in bovine corpus luteum. *J Physiol Pharmacol,* 9**,** 75-89.

Richards, J. S. 2007. Genetics of ovulation. *Semin Reprod Med,* 25**,** 235-42.

Richards, J. S., Sharma, S. C., Falender, A. E. & Lo, Y. H. 2002. Expression of FKHR, FKHRL1, and AFX genes in the rodent ovary: evidence for regulation by IGF-I, estrogen, and the gonadotropins. *Mol Endocrinol,* 16**,** 580-99.

Robker, R. L. & Richards, J. S. 1998. Hormone-induced proliferation and differentiation of granulosa cells: a coordinated balance of the cell cycle regulators cyclin D2 and p27Kip1. *Mol Endocrinol,* 12**,** 924-40.

Robker, R. L., Russell, D. L., Espey, L. L., Lydon, J. P., O'Malley, B. W. & Richards, J. S. 2000. Progesterone-regulated genes in the ovulation process: ADAMTS-1 and cathepsin L proteases. *Proceedings of the National Academy of Sciences,* 97**,** 4689-4694.

Rodgers, R. J. & Irving-Rodgers, H. F. 2010. Morphological classification of bovine ovarian follicles. *Reproduction,* 139**,** 309-18.

Roy, S. K. & Greenwald, G. S. 1990. Immunohistochemical localization of epidermal growth factor-like activity in the hamster ovary with a polyclonal antibody. *Endocrinology,* 126**,** 1309-17.

Russell, D. L., Brown, H. M. & Dunning, K. R. 2015. ADAMTS proteases in fertility. *Matrix Biology,* 44–46**,** 54-63.

Russell, D. L. & Robker, R. L. 2007. Molecular mechanisms of ovulation: co-ordination through the cumulus complex. *Hum Reprod Update,* 13**,** 289-312.

Sagata, N. 1996. Meiotic metaphase arrest in animal oocytes: its mechanisms and biological significance. *Trends Cell Biol,* 6**,** 22-8.

Salustri, A., Camaioni, A., Di Giacomo, M., Fulop, C. & Hascall, V. C. 1999. Hyaluronan and proteoglycans in ovarian follicles. *Hum Reprod Update,* 5**,** 293-301.

Salvetti, N. R., Stangaferro, M. L., Palomar, M. M., Alfaro, N. S., Rey, F., Gimeno, E. J. & Ortega, H. H. 2010. Cell proliferation and survival mechanisms underlying the abnormal persistence of follicular cysts in bovines with cystic ovarian disease induced by ACTH. *Anim Reprod Sci,* 122**,** 98-110.

Sang, Q., Yao, Z., Wang, H., Feng, R., Wang, H. & Zhao, X. 2013. Identification of microRNAs in human follicular fluid: characterization of microRNAs that govern steroidogenesis in vitro and are associated with polycystic ovary syndrome in vivo. *J Clin Endocrinol Metab,* 98**,** 3068 - 79.

Santonocito, M., Vento, M., Guglielmino, M. R., Battaglia, R., Wahlgren, J., Ragusa, M., Barbagallo, D., Borzi, P., Rizzari, S., Maugeri, M., Scollo, P., Tatone, C., Valadi, H., Purrello, M. & Di Pietro, C. 2014. Molecular characterization of exosomes and their microRNA cargo in human follicular fluid: bioinformatic analysis reveals that exosomal microRNAs control pathways involved in follicular maturation. *Fertil Steril,* 102**,** 1751-61.

Sayed, D. & Abdellatif, M. 2011. MicroRNAs in Development and Disease. *Physiological Reviews,* 91**,** 827-887.

Scaramuzzi, R., Baird, D., Campbell, B., Driancourt, M.-A., Dupont, J., Fortune, J., Gilchrist, R., Martin, G., McNatty, K. & McNeilly, A. 2011. Regulation of folliculogenesis and the determination of ovulation rate in ruminants. *Reproduction, Fertility and Development,* 23**,** 444-467.

Schams, D. & Berisha, B. 2004. Regulation of Corpus Luteum Function in Cattle – an Overview. *Reproduction in Domestic Animals,* 39**,** 241-251.

Schauer, S., Sontakke, S., Watson, E., Esteves, C. & Donadeu, F. 2013. Involvement of miRNAs in equine follicle development. *Reproduction,* 146**,** 273 - 82.

Schirle, N. T. & MacRae, I. J. 2012. The Crystal Structure of Human Argonaute2. *Science,* 336**,** 1037-1040.

Sen, A., Prizant, H., Light, A., Biswas, A., Hayes, E., Lee, H.-J., Barad, D., Gleicher, N. & Hammes, S. R. 2014. Androgens regulate ovarian follicular development by increasing follicle stimulating hormone receptor and microRNA-125b expression. *Proceedings of the National Academy of Sciences,* 111**,** 3008-3013.

Shah, D. & Nagarajan, N. 2013. Luteal insufficiency in first trimester. *Indian Journal of Endocrinology and Metabolism,* 17**,** 44-49.

Shen, M., Liu, Z., Li, B., Teng, Y., Zhang, J., Tang, Y., Sun, S. C. & Liu, H. 2014. Involvement of FoxO1 in the effects of follicle-stimulating hormone on inhibition of apoptosis in mouse granulosa cells. *Cell Death Dis,* 16**,** 400.

Shi, F. & LaPolt, P. S. 2003. Relationship between FoxO1 protein levels and follicular development, atresia, and luteinization in the rat ovary. *J Endocrinol,* 179**,** 195-203.

Shirasuna, K., Nitta, A., Sineenard, J., Shimizu, T., Bollwein, H. & Miyamoto, A. 2012. Vascular and immune regulation of corpus luteum development, maintenance, and regression in the cow. *Domest Anim Endocrinol,* 43**,** 198-211.

Siomi, H. & Siomi, M. C. 2010. Posttranscriptional Regulation of MicroRNA Biogenesis in Animals. *Mol Cell,* 38**,** 323-332.

Sirois, J., Sayasith, K., Brown, K. A., Stock, A. E., Bouchard, N. & Doré, M. 2004. Cyclooxygenase-2 and its role in ovulation: a 2004 account. *Hum Reprod Update,* 10**,** 373-385.

Sirotkin, A. V., Laukova, M., Ovcharenko, D., Brenaut, P. & Mlyncek, M. 2010. Identification of microRNAs controlling human ovarian cell proliferation and apoptosis. *J Cell Physiol,* 223**,** 49-56.

Sirotkin, A. V., Ovcharenko, D., Grossmann, R., Laukova, M. & Mlyncek, M. 2009. Identification of microRNAs controlling human ovarian cell steroidogenesis via a genome-scale screen. *J Cell Physiol,* 219**,** 415-20.

Siu, M. K., Tsai, Y. C., Chang, Y. S., Yin, J. J., Suau, F., Chen, W. Y. & Liu, Y. N. 2015. Transforming growth factor-beta promotes prostate bone metastasis through induction of microRNA-96 and activation of the mTOR pathway. *Oncogene,* 34**,** 4767-76.

Sjaastad, O. V., Hove, K. & Sand, O. 2010. *Physiology of domestic animals*, Scan. Vet. Press.

Skarzynski, D. J., Piotrowska-Tomala, K. K., Lukasik, K., Galvão, A., Farberov, S., Zalman, Y. & Meidan, R. 2013. Growth and Regression in Bovine Corpora Lutea: Regulation by Local Survival and Death Pathways. *Reproduction in Domestic Animals,* 48**,** 25-37.

Smith, M., McIntush, E., Ricke, W., Kojima, F. & Smith, G. 1998. Regulation of ovarian extracellular matrix remodelling by metalloproteinases and their tissue inhibitors: effects on follicular development, ovulation and luteal function. *Journal of reproduction and fertility. Supplement,* 54**,** 367-381.

Smith, M. F., McIntush, E. W. & Smith, G. W. 1994. Mechanisms associated with corpus luteum development. *J Anim Sci,* 72**,** 1857-72.

Sohel, M. M., Hoelker, M., Noferesti, S. S., Salilew-Wondim, D., Tholen, E., Looft, C., Rings, F., Uddin, M. J., Spencer, T. E., Schellander, K. & Tesfaye, D. 2013. Exosomal and Non-Exosomal Transport of Extra-Cellular microRNAs in Follicular Fluid: Implications for Bovine Oocyte Developmental Competence. *PLoS One,* 8.

Sontakke, S. D., Mohammed, B. T., McNeilly, A. S. & Donadeu, F. X. 2014. Characterization of microRNAs differentially expressed during bovine follicle development. *Reproduction,* 148**,** 271-283.

Stocco, C., Telleria, C. & Gibori, G. 2007. The Molecular Control of Corpus Luteum Formation, Function, and Regression. *Endocrine Reviews,* 28**,** 117-149.

Stormshak, F. 2003. Biochemical and endocrine aspects of oxytocin production by the mammalian corpus luteum. *Reprod Biol Endocrinol,* 1**,** 92-92.

Tanaka, N., Espey, L. L. & Okamura, H. 1989. Increase in ovarian blood volume during ovulation in the gonadotropin-primed immature rat. *Biol Reprod,* 40**,** 762-8.

Tang, F., Kaneda, M., O'Carroll, D., Hajkova, P., Barton, S. C., Sun, Y. A., Lee, C., Tarakhovsky, A., Lao, K. & Surani, M. A. 2007. Maternal microRNAs are essential for mouse zygotic development. *Genes & Development,* 21**,** 644-648.

Tang, X., Zheng, D., Hu, P., Zeng, Z., Li, M., Tucker, L., Monahan, R., Resnick, M. B., Liu, M. & Ramratnam, B. 2014. Glycogen synthase kinase 3 beta inhibits microRNA-183-96-182 cluster via the beta-Catenin/TCF/LEF-1 pathway in gastric cancer cells. *Nucleic Acids Res,* 42**,** 2988-98.

Tesfaye, D., Worku, D., Rings, F., Phatsara, C., Tholen, E., Schellander, K. & Hoelker, M. 2009. Identification and expression profiling of microRNAs during bovine oocyte maturation using heterologous approach. *Mol Reprod Dev,* 76**,** 665-77.

Thomas, M., Lieberman, J. & Lal, A. 2010. Desperately seeking microRNA targets. *Nat Struct Mol Biol,* 17**,** 1169-74.

Tian, H., Hou, L., Xiong, Y.-M., Huang, J.-X., Zhang, W.-H., Pan, Y.-Y. & Song, X.-R. 2016. miR-132 targeting E2F5 suppresses cell proliferation, invasion, migration in ovarian cancer cells. *American Journal of Translational Research,* 8.

Tognini, P., Putignano, E., Coatti, A. & Pizzorusso, T. 2011. Experience-dependent expression of miR-132 regulates ocular dominance plasticity. *Nat Neurosci,* 14**,** 1237-1239.

Toms, D., Xu, S., Pan, B., Wu, D. & Li, J. 2015. Progesterone receptor expression in granulosa cells is suppressed by microRNA-378-3p. *Mol Cell Endocrinol,* 399**,** 95-102.

Tong, X.-H., Xu, B., Zhang, Y.-W., Liu, Y.-S. & Ma, C.-H. 2014. Research Resources: Comparative MicroRNA Profiles in Human Corona Radiata Cells and Cumulus Oophorus Cells Detected by Next-Generation Small RNA Sequencing. *PLoS One,* 9**,** e106706.

Tripurani, S. K., Lee, K. B., Wee, G., Smith, G. W. & Yao, J. 2011. MicroRNA-196a regulates bovine newborn ovary homeobox gene (NOBOX) expression during early embryogenesis. *BMC Dev Biol,* 11**,** 11-25.

Tripurani, S. K., Wee, G., Lee, K.-B., Smith, G. W., Wang, L. & JianboYao 2013. MicroRNA-212 Post-Transcriptionally Regulates Oocyte-Specific Basic-Helix-Loop-Helix Transcription Factor, Factor in the Germline Alpha (FIGLA), during Bovine Early Embryogenesis. *PLoS One,* 8**,** e76114.

Tripurani, S. K., Xiao, C., Salem, M. & Yao, J. 2010. Cloning and analysis of fetal ovary microRNAs in cattle. *Anim Reprod Sci,* 120**,** 16-22.

Troppmann, B., Kossack, N., Nordhoff, V., Schuring, A. N. & Gromoll, J. 2014. MicroRNA miR-513a-3p acts as a co-regulator of luteinizing hormone/chorionic gonadotropin receptor gene expression in human granulosa cells. *Mol Cell Endocrinol,* 390**,** 65-72.

Trzeciak, P., Rapala, L., Starzynski, R., Dabrowski, S. & Duszewska, A. M. 2012. [TSG-6 protein and its role during maturation of ovarian follicles]. *Postepy Hig Med Dosw,* 66**,** 543-8.

Tscherner, A., Gilchrist, G., Smith, N., Blondin, P., Gillis, D. & LaMarre, J. 2014. MicroRNA-34 family expression in bovine gametes and preimplantation embryos. *Reproductive Biology and Endocrinology,* 12**,** 1-9.

Tu, F., Pan, Z. X., Yao, Y., Liu, H. L., Liu, S. R., Xie, Z. & Li, Q. F. 2014. miR-34a targets the inhibin beta B gene, promoting granulosa cell apoptosis in the porcine ovary. *Genet Mol Res,* 13**,** 2504-12.

Ucar, A., Gupta, S. K., Fiedler, J., Erikci, E., Kardasinski, M., Batkai, S., Dangwal, S., Kumarswamy, R., Bang, C. & Holzmann, A. 2012. The miRNA-212/132 family regulates both cardiac hypertrophy and cardiomyocyte autophagy. *Nature Communications,* 3**,** 1078.

Ucar, A., Vafaizadeh, V., Jarry, H., Fiedler, J., Klemmt, P. A. B., Thum, T., Groner, B. & Chowdhury, K. 2010. miR-212 and miR-132 are required for epithelial stromal interactions necessary for mouse mammary gland development. *Nat Genet,* 42**,** 1101-1108.

Urbánek, P. & Klotz, L. O. 2016. Posttranscriptional regulation of FOXO expression: microRNAs and beyond. *British Journal of Pharmacology***,** n/a-n/a.

Vlachos, I. S., Zagganas, K., Paraskevopoulou, M. D., Georgakilas, G., Karagkouni, D., Vergoulis, T., Dalamagas, T. & Hatzigeorgiou, A. G. 2015. DIANA-miRPath v3.0: deciphering microRNA function with experimental support. *Nucleic Acids Research*.

Vo, N., Klein, M. E., Varlamova, O., Keller, D. M., Yamamoto, T., Goodman, R. H. & Impey, S. 2005. A cAMP-response element binding protein-induced microRNA regulates neuronal morphogenesis. *Proceedings of the National Academy of Sciences of the United States of America,* 102**,** 16426-16431.

Wanet, A., Tacheny, A., Arnould, T. & Renard, P. 2012. miR-212/132 expression and functions: within and beyond the neuronal compartment. *Nucleic Acids Research*.

Wang, L., Jia, X. J., Jiang, H. J., Du, Y., Yang, F., Si, S. Y. & Hong, B. 2013. MicroRNAs 185, 96, and 223 repress selective high-density lipoprotein cholesterol uptake through posttranscriptional inhibition. *Mol Cell Biol,* 33**,** 1956-64.

Wang, S. & Li, K. 2014. MicroRNA-96 regulates RGC-5 cell growth through caspase-dependent apoptosis. *Int J Clin Exp Med,* 7**,** 3694-702.

Wang, S., Liu, J., Li, X., Ji, X., Zhang, J., Wang, Y. & Cui, S. 2016a. MiR-125b Regulates Primordial Follicle Assembly by Targeting Activin Receptor Type 2a in Neonatal Mouse Ovary. *Biol Reprod,* 9**,** 131128.

Wang, T. H., Yeh, C. T., Ho, J. Y., Ng, K. F. & Chen, T. C. 2016b. OncomiR miR-96 and miR-182 promote cell proliferation and invasion through targeting ephrinA5 in hepatocellular carcinoma. *Mol Carcinog,* 55**,** 366-75.

Webb, R., Campbell, B. K., Garverick, H. A., Gong, J. G., Gutierrez, C. G. & Armstrong, D. G. 1999. Molecular mechanisms regulating follicular recruitment and selection. *J Reprod Fertil Suppl,* 54**,** 33-48.

Weigel, P. H., Hascall, V. C. & Tammi, M. 1997. Hyaluronan synthases. *J Biol Chem,* 272**,** 13997-4000.

Wiles, J. R., Katchko, R. A., Benavides, E. A., O'Gorman, C. W., Escudero, J. M., Keisler, D. H., Stanko, R. L. & Garcia, M. R. 2014. The effect of leptin on luteal angiogenic factors during the luteal phase of the estrous cycle in goats. *Anim Reprod Sci,* 148**,** 121-9.

Wiltbank, M., Salih, S., Atli, M., Luo, W., Bormann, C., Ottobre, J., Vezina, C., Mehta, V., Diaz, F. & Tsai, S. 2012. Comparison of endocrine and cellular mechanisms regulating the corpus luteum of primates and ruminants. *Animal reproduction/Colegio Brasileiro de Reproducao Animal,* 9**,** 242.

Wu, S., Sun, H., Zhang, Q., Jiang, Y., Fang, T., Cui, I., Yan, G. & Hu, Y. 2015. MicroRNA-132 promotes estradiol synthesis in ovarian granulosa cells via translational repression of Nurr1. *Reproductive Biology and Endocrinology,* 13**,** 94.

Wulff, C., Dickson, S. E., Duncan, W. C. & Fraser, H. M. 2001. Angiogenesis in the human corpus luteum: simulated early pregnancy by HCG treatment is associated with both angiogenesis and vessel stabilization. *Hum Reprod,* 16**,** 2515-2524.

Xiao, G., Xia, C., Yang, J., Liu, J., Du, H., Kang, X., Lin, Y., Guan, R., Yan, P. & Tang, S. 2014. MiR-133b regulates the expression of the Actin protein TAGLN2 during oocyte growth and maturation: a potential target for infertility therapy. *PLoS One,* 9**,** e100751.

Xiong, F., Hu, L., Zhang, Y., Xiao, X. & Xiao, J. 2016. miR-22 inhibits mouse ovarian granulosa cell apoptosis by targeting SIRT1. *Biology Open*.

Xu, D., He, X., Chang, Y., Xu, C., Jiang, X., Sun, S. & Lin, J. 2013. Inhibition of miR-96 expression reduces cell proliferation and clonogenicity of HepG2 hepatoma cells. *Oncol Rep,* 29**,** 653-61.

Xu, S., Linher-Melville, K., Yang, B., Wu, D. & Li, J. 2011a. Micro-RNA378 (miR-378) regulates ovarian estradiol production by targeting aromatase. *Endocrinology,* 152**,** 3941 - 51.

Xu, S., Witmer, P. D., Lumayag, S., Kovacs, B. & Valle, D. 2007. MicroRNA (miRNA) transcriptome of mouse retina and identification of a sensory organ-specific miRNA cluster. *J Biol Chem,* 282**,** 25053-66.

Xu, Y.-W., Wang, B., Ding, C.-H., Li, T., Gu, F. & Zhou, C. 2011b. Differentially expressed micoRNAs in human oocytes. *Journal of Assisted Reproduction and Genetics,* 28**,** 559-566.

Yan, G., Zhang, L., Fang, T., Zhang, Q., Wu, S. & Jiang, Y. 2012. MicroRNA-145 suppresses mouse granulosa cell proliferation by targeting activin receptor IB. *FEBS Lett,* 586**,** 3263 - 70.

Yang, D. Z., Yang, W., Li, Y. & He, Z. 2013a. Progress in understanding human ovarian folliculogenesis and its implications in assisted reproduction. *Journal of Assisted Reproduction and Genetics,* 30**,** 213-219.

Yang, M., Pan, Y. & Zhou, Y. 2014. miR-96 promotes osteogenic differentiation by suppressing HBEGF-EGFR signaling in osteoblastic cells. *FEBS Lett,* 588**,** 4761-8.

Yang, S., Wang, S., Luo, A., Ding, T., Lai, Z., Shen, W., Ma, X., Cao, C., Shi, L., Jiang, J., Rong, F., Ma, L., Tian, Y., Du, X., Lu, Y., Li, Y. & Wang, S. 2013b. Expression patterns and regulatory functions of microRNAs during

the initiation of primordial follicle development in the neonatal mouse ovary. *Biol Reprod,* 89.

Yao, G., Liang, M., Liang, N., Yin, M., Lu, M., Lian, J., Wang, Y. & Sun, F. 2014. MicroRNA-224 is involved in the regulation of mouse cumulus expansion by targeting Ptx3. *Mol Cell Endocrinol,* 382**,** 244-53.

Yao, G., Yin, M., Lian, J., Tian, H., Liu, L., Li, X. & Sun, F. 2010. MicroRNA-224 Is Involved in Transforming Growth Factor-β-Mediated Mouse Granulosa Cell Proliferation and Granulosa Cell Function by Targeting Smad4. *Molecular Endocrinology,* 24**,** 540-551.

Yin, M., Lu, M., Yao, G., Tian, H., Lian, J. & Liu, L. 2012. Transactivation of microRNA-383 by steroidogenic factor-1 promotes estradiol release from mouse ovarian granulosa cells by targeting RBMS1. *Mol Endocrinol,* 26**,** 1129 - 43.

Yin, M., Wang, X., Yao, G., Lü, M., Liang, M., Sun, Y. & Sun, F. 2014. Transactivation of MicroRNA-320 by MicroRNA-383 Regulates Granulosa Cell Functions by Targeting E2F1 and SF-1 Proteins. *J Biol Chem,* 289**,** 18239-18257.

Yu, S., Lu, Z., Liu, C., Meng, Y., Ma, Y., Zhao, W., Liu, J., Yu, J. & Chen, J. 2010. miRNA-96 suppresses KRAS and functions as a tumor suppressor gene in pancreatic cancer. *Cancer Research,* 70**,** 6015-6025.

Yuan, S., Ortogero, N., Wu, Q., Zheng, H. & Yan, W. 2014. Murine Follicular Development Requires Oocyte DICER, but Not DROSHA. *Biology of Reproduction,* 91**,** 39, 1-8.

Zhang, H., Jiang, X., Zhang, Y., Xu, B., Hua, J., Ma, T., Zheng, W., Sun, R., Shen, W., Cooke, H. J., Hao, Q., Qiao, J. & Shi, Q. 2014a. microRNA 376a regulates follicle assembly by targeting Pcna in fetal and neonatal mouse ovaries. *Reproduction,* 148**,** 43-54.

Zhang, J.-Q., Gao, B.-W., Wang, J., Ren, Q.-L., Chen, J.-F., Ma, Q., Zhang, Z.-J. & Xing, B.-S. 2016. Critical Role of FoxO1 in Granulosa Cell Apoptosis Caused by Oxidative Stress and Protective Effects of Grape Seed Procyanidin B2. *Oxidative Medicine and Cellular Longevity,* 2016**,** 16.

Zhang, J., Ji, X., Zhou, D., Li, Y., Lin, J., Liu, J., Luo, H. & Cui, S. 2013a. miR-143 is critical for the formation of primordial follicles in mice. *Frontiers in bioscience (Landmark edition)* [Online], 18. Available: http://europepmc.org/abstract/MED/23276944

http://dx.doi.org/10.2741/4122 [Accessed 2013].

Zhang, Q., Sun, H., Jiang, Y., Ding, L., Wu, S. & Fang, T. 2013b. MicroRNA-181a suppresses mouse granulosa cell proliferation by targeting activin receptor IIA. *PLoS One,* 8**,** e59667.

Zhang, Z. G., Chen, W. X., Wu, Y. H., Liang, H. F. & Zhang, B. X. 2014b. MiR-132 prohibits proliferation, invasion, migration, and metastasis in breast cancer by targeting HN1. *Biochem Biophys Res Commun,* 454**,** 109-14.

Zhou, J., Liu, J., Pan, Z., Du, X., Li, X., Ma, B., Yao, W., Li, Q. & Liu, H. 2015. The let-7g microRNA promotes follicular granulosa cell apoptosis by targeting transforming growth factor-β type 1 receptor. *Mol Cell Endocrinol,* 409**,** 103-112.

# Appendix I

# Appendix I

## Reagents and cell culture media

### Reagents

**Washing Buffer**

0.1% TWEEN®20 (v/v) (BP337-100; Fisher Scientific) in tris-buffered saline (BP2471-1; Fisher Scientific) (TBST).

**PBS-G**

0.1% swine skin gelatine (w/v) (G1890; Sigma-Aldrich) in phosphate-buffered saline.

**Blocking Buffer**

2% BSA (w/v) (Sigma A-2153) in TBS for immunochemistry.

**0.1% DEPC water**

For 1 L: 1 ml of Diethyl pyrocarbonate DEPC (D5758; Sigma-Aldrich) was added to 1 L of $dH_2O$, keep overnight at room temperature in the dark then autoclave for 20 minutes.

**4% Paraformaldehyde Solution**

4 g paraformaldehyde (P6148; Sigma) was dissolved in 0.1 M phosphate buffer. Heat to 60-65ºC on magnetic stirrer. 1M NaOH added dropwise until solution clears. Cool and filter.

**Imidazole Buffer**

(0.13 M 1–methylimidazole(, 8.05852.0100; VWR International Ltd). 1.6 ml of 1-methylimidazole was added to 130 ml $dH_2O$, pH 8.0 adjusted by 12 M HCl, then 16 ml 3 M NaCl and $dH_2O$ added to a final volume of 160 ml.

**EDC Solution**

(0.16 M l–ethyl–3– (3–dimethylaminopropyl) carbodiimide (EDC) (39391; Sigma). 176 µl EDC was added to 10 ml of imidazole buffer, and then pH adjusted to 8.0 by adding about 100 µl 12 M HCl.

**Pre-hybridisation**

50% formamide (47671; Sigma), 5x SSC (15557-044; Life Technologies) in DEPC-water.

**Hybridisation Buffer**

50% formamide (47671; Sigma), 5x SSC (15557-044; Life Technologies), 10 % Dextran Sulphate Sodium (D-8906; Sigma), 1x Denhardt's solution (30915; Sigma) and 200 μg/ml yeast tRNA (7120G; Ambion).

**Post-hybridisation**

0.2x SSC + 2% BSA in DEPC water.

**Blocking Solution for ISH**

1% Sheep serum (S3772; Sigma) and 2 % BSA (A-2153; Sigma) in TBS.

**Antibody Solution for ISH**

Anti-DIG-AP Fab fragment antibody (11093274910; Roche) in 10 % sheep serum in TBST.

**NBT/BCIP Solution**

Mix one tablet of NBT/BCIP (B5655; Sigma) in 10 ml Milli-Q water.

**Nuclear Fast Red**

Aluminium sulphate 5 g (368458; Sigma) was dissolved in 100 ml $dH_2O$ then 0.1 g Nuclear fast red (60700; Fluka) was added and slowly heated to boil and then allowed to cool.

**Nile Red stock**

Nile red (N3013; Sigma-Aldrich) was dissolved in absolute Ethanol to make up (1 mg/ml).

**Western Blot**

12% SDS-PAGE gels were prepared with Bis-acrylamide, Tris and SDS (Sigma-Aldrich). Ammonium persulphate and TEMED were then added to induce the acrylamide to polymerise. Four percent stacking solution was overlaid then 10 wells comb was inserted and left for 30 mins to set before using the gel.

**2x Sample Buffer**

4% SDS, 20% glycerol, 10% 2-mercaptoethanol, 0.004% bromphenol blue and 0.125 M Tris HCl, pH approx. 6.8 (S3401; Sigma-Aldrich). 1x sample buffer was used to extract total protein after dilution with $dH_2O$.

**5x Running Buffer**

For 1 L: 15 g Tris (BP152-1; Fisher Scientific), 72 g of Glycine (G7126; Sigma-Aldrich) and 5 g Dodecyl sulfate sodium salt (S/5200/53; Fisher Scientific) were added to $dH_2O$ and filtered.

**Transfer Buffer**

For 1L: 2.42 g Tris (BP152-1; Fisher Scientific), 11.54 g of Glycine (G7126; Sigma-Aldrich) and 200 ml of methanol (M/4000/17; Fisher Scientific) were added to $dH_2O$ and filtered.

**Blocking Solution**

5% BSA in 1x TBS-T.

## Bovine granulosa cell culture

McCoy's 5a medium (500 ml, M8403; Sigma) was prepared by adding 3 mM L-Glutamine (Sigma G7513), 20 mM HEPES(Sigma H0887), 1% Pen-Strep (15140-122; Life technologies), 0.1% BSA (Sigma A9418), $10^{-7}$ M androstenedione, 10 ng/ml bovine Insulin (I1882; Sigma-Aldrich), 2.5 µg/ml Transferrin (T1428; Sigma-Aldrich) and 4 ng/ml sodium selenite (S9133; Sigma-Aldrich). Luteinisation was induced by treating GCs with Forskolin cocktail 10 µM FSK, 1% Fetal Bovine Serum (v/v) (10500-064; Life Technologies) and 1µg/ml Bovine Insulin.

## Bovine luteal and human luteinised granulosa cells cultures

DMEM/F-12 (31330-095; Life Technologies) containing 2.5 mM L-Glutamine, 15 mM HEPES, 1% Pen-Strep, Fetal Bovine Serum (v/v) and ITS (bovine Insulin (5 µg/ml), Transferrin (5 µg/ml) and sodium selenite (5 ng/ml) and Fungizone (2.5 µg/ml) (15290, Invitrogen, Paisley, UK).

## Dissociation solution

DMEM/F-12 (31330-095; Life Technologies) was supplemented with 1%Pen-Strep (15140-122; Life technologies), 2 mg/ml collagenase Type II (C6885; Sigma-Aldrich) and 5 mg/ml of BSA and 0.025 mg/ml of DNase I (D5025; Sigma-Aldrich).